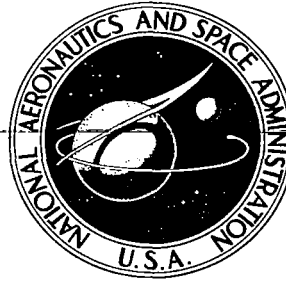


NASA CONTRACTOR REPORT

NASA CR-1375



NASA CR-1375

0060531



TECH LIBRARY KAFB, NM

LOAN COPY: RETURN TO
AFWL (W10L-2)
KIRTLAND AFB, N MEX

ANALYTICAL STUDY OF CONTAMINANT AND ATMOSPHERIC SENSOR

PHASE I

Prepared by

PERKIN - ELMER CORPORATION

Pomona, Calif.

for Langley Research Center

NATIONAL AERONAUTICS AND SPACE ADMINISTRATION • WASHINGTON, D. C. • SEPTEMBER 1969



0060531

NASA CR-1375

ANALYTICAL STUDY OF CONTAMINANT
AND ATMOSPHERIC SENSOR
PHASE I

Distribution of this report is provided in the interest of information exchange. Responsibility for the contents resides in the author or organization that prepared it.

Issued by Originator as Perkin-Elmer SPO No. 20224

Prepared under Contract No. NAS 1-7260 by
PERKIN - ELMER CORPORATION
Pomona, Calif.

for Langley Research Center

NATIONAL AERONAUTICS AND SPACE ADMINISTRATION

For sale by the Clearinghouse for Federal Scientific and Technical Information
Springfield, Virginia 22151 - CFSTI price \$3.00

TABLE OF CONTENTS

INTRODUCTION	1
DESIGN ANALYSIS.	3
THE MEASUREMENT OF CO.	21
DIRECT SOLUTIONS TO CO MEASUREMENT PROBLEMS.	27
CARBON MONOXIDE DETERMINATION BY THE ACCUMULATOR CELL METHOD	32
DESIGN CONSIDERATIONS FOR A CARBON MONOXIDE DETERMINATION USING AN ACCUMULATOR CELL.	33
SUMMARY OF SOLUTIONS TO CO PROBLEM	36
ANALYZER LAYOUT.	37
SUPPORT ELECTRONICS SUBSYSTEM.	37
POWER SUMMARY.	47
PUMPING.	50
ANALYZER SUBSYSTEM CONSIDERATIONS.	56
SAMPLE INLET	61
ACCUMULATOR CELL AND VALVES.	62
ION SOURCE	66
MECHANICAL DESIGN AND PACKAGING.	70
CONCLUSIONS.	80
APPENDIX A - Resolution and Sensitivity Needed for the Measurement of Total Hydrocarbons and CO	83
APPENDIX B - Crosstalk and Organic Fragment Interference at Mass 28. . .	101
APPENDIX C - Evaluation of the Effect of Lowering the Electron Energy on Fragmentation and Sensitivity.	103
APPENDIX D - New Magnet Design	123
APPENDIX E - Ion Source Construction Materials	133

ANALYTICAL STUDY OF A
CONTAMINANT AND ATMOSPHERIC SENSOR

THE PERKIN-ELMER CORPORATION

INTRODUCTION

As the projected duration of manned spacecraft missions has increased, a need to measure more accurately the parameters influencing man in his closed ecological system has evolved. In the early stages of the program it was necessary to monitor only the major atmospheric components. As man's exposure to these closed environments has increased, so has the complexity of his environment. The result of this evolution has been the need for the development of a front line atmospheric monitor capable of indicating the general condition of a spacecraft cabin atmosphere. It is the purpose of this study to define an instrument capable of meeting the needs of present and future extended mission manned spacecraft.

The proposed design of the instrumentation described in this report is based on an existing analytical instrument. Under NASA Contract NAS 1-5679, Development of a Two Gas Atmosphere Sensor System (Mass Spectrometer), Perkin Elmer Aerospace Systems studied the use of a mass spectrometer sensor system to measure the partial pressures of oxygen, nitrogen, carbon dioxide and water vapor within a space vehicle cabin environment. The contract called for this sensor system to be compatible with the Apollo cabin environment (as well as possible extensions of the Apollo mission) and to be capable of presenting electrical voltage outputs which were suitable for input to existing types of atmosphere control devices as well as probable control systems on vehicles of longer duration, and for telemetry and visual display. The final report under this contract presented the results of this study, and recommended the use of a single-focusing magnetic sector type of mass spectrometer. The study included an examination of weight, electrical power requirements, complexity, and compatibility with system performance goals. A detailed analysis of this magnetic sector instrument led to a design, which was documented in the final report under this contract. Expected performance of this system was given and no fundamental problems were anticipated in the attainment of these goals in the fabrication and testing of a flight prototype instrument.

The fabrication of units based on this design was undertaken under Langley Research Center contract NAS 1-6387. One engineering test model and four flight prototype units will result from this effort.

The flight prototype hardware design embodies inherent ruggedness, operational simplicity, reliability, minimum power requirements, optimum size and weight compatible with flight environments. The major requirements of NPC 200-2, 200-4, and 250-1 such as reliability analysis, certified soldering personnel and drawing change control were implemented as agreed to with LRC.

For electronic subsystems, established reliability parts and components were used where possible, and in general, electronic parts were stressed to no more than 50% of rating. Electronic parts received 100% screening for known types of defects. The reliability and quality assurance effort for the development of the sensor system was flexible enough for the changes required by the developmental nature of the task, but they will assure that, for the deliverable items all major reliability and quality assurance requirements have been met. These efforts provide assurance that, for possible future flight articles, the imposition of the full reliability and quality assurance provisions for manned flight will result in minimum discrepancies in the design and manufacturing procedures, and at the same time, the limited application of this technology will result in a delivered sensor that shows improved reliability and quality without the expenditure of the time and effort that would be required if the sensor system were to be designed and constructed under the complete application of these documents.

The Two Gas Atmosphere Sensor System

The Two Gas Atmosphere Sensor System consists of a small single focusing 90° magnetic sector-type mass spectrometer. Ions are supplied to the analyzer from a non-magnetic dual electron gun, high differential pumping ion source with a parallel electrode ionizing region, and a thermal imaging type of ion focusing. The ionizing beam of electrons is obtained from one of two 0.003-inch diameter tungsten-rhenium alloy wire filaments. The object slit plate of the ion source also forms the mounting plate for the ion source components on one side and the z-axis focus lens elements on the other side. This assembly is mounted in a thin-walled housing which is an integral part of the analyzer envelope and collector flange assembly. The mass resolution is accomplished by the action of the magnetic field (from an Alnico V permanent magnet) as the ions pass through the envelope section of the analyzers. The four gases of interest are separated and sampling collectors which are mounted on the collector flange. These gases are H₂O, N₂, O₂, and CO which correspond to ion mass-to-charge ratios of m/e 18, m/e 28, m/e 32, and m/e 44.

The cabin atmosphere is admitted to the ion source through a viscous pressure divider inlet system. This consists of a single capillary line and a pump out line with a platinum aperture molecular leak at their juncture. This system can sample at various points in the cabin or be attached to a suit loop or calibration source.

The internal vacuum necessary for operation of the analyzer can be maintained by pumping to outer space through a pump out tube or by accessory pumps.

Each of the collected ion currents is amplified to the required output level by an all solid-state electrometer amplifier. Each amplifier is set for the sensitivity commensurate with the expected sample range of that atmospheric component.

These amplifiers have a high input impedance and utilize 100% current feedback to obtain an output which is essentially independent of any active devices which is equal to the input current multiplied by the feedback resistance.

In addition to the four ion amplifiers the sensor system support electronics subsystem consists of three modules which provide the electronic functions necessary for the operation of the analyzer. First, there is a filament supply and emission regulator which supplies an ac voltage to the filament. This supply is a closed loop control system which senses on the ionizing current collected at the anode of the ion source and uses this feedback current to control the filament current so that the ionizing current remains constant. System considerations also require that this module be floated above ground at the anode potential. An inverter is used for this and its pulse width modulated output drives the filament.

The electrode bias supply provides the voltages to the various focusing electrodes in the ion source. It consists of a single inverter with a multiple winding output. Series voltage regulators operate off of two of the rectified outputs and these are used to compensate for variations in two of the other outputs. The result is three stacked high voltage outputs two of which are regulated and the third is unregulated. These outputs are loaded by a voltage divider resistance network with potentiometers which are cabled to the ion source headers.

The detector power supply consists of a single free running inverter which drives B⁺ and B⁻ series regulators. These regulators operate using a common zener diode reference and supply +10 and -10 volts to the detectors.

DESIGN ANALYSIS

Statement of the Problem

In order that the performance of an environmental control system may be subjected to a first order evaluation, it is required that an instrument be devised which is capable of providing information relating to the concentrations of hydrogen, helium or nitrogen, oxygen, carbon dioxide, water vapor, carbon monoxide, methane and total hydrocarbons. The basis for the selection of these atmospheric constituents is not within the scope of this report. The concentration ranges associated with the selected gases are shown in Table 1.

TABLE 1

Hydrogen	0 to 16 torr (0 to 40,000 PPM)
Helium	0 to 200 torr (0 to 500,000 PPM)
Oxygen	0 to 200 torr (0 to 500,000 PPM)
Carbon Dioxide	0 to 20 torr (0 to 50,000 PPM)
Water Vapor	0 to 20 torr (0 to 50,000 PPM)
Carbon Monoxide	0 to 30 mg/m ³ (0 to 48 PPM)
Methane	0 to 650 mg/m ³ (0 to 1,950 PPM)
Total Hydrocarbons	0 to 1,000 PPM

Analytical Discussion.— The major atmospheric constituents have been monitored using the basic Two Gas Atmosphere Sensor System. With minor modification, analysis has been provided for both nitrogen-oxygen and helium-oxygen atmospheres. There is no reason to believe that extending the analytical capability of the basic system would result in any determined influence on the measurement of these constituents.

The basic Two Gas Atmosphere Sensor System is capable of a resolving power of 18. This is sufficient to separate the four gases monitored from their nearest neighbors. The required resolution to separate each gas from its nearest neighbor of magnitude sufficiently large to cause interference is:

Resolving Power Required	
H ₂ O	18
O ₂	10
N ₂	10
CO ₂	15

In previous Two Gas Atmosphere Sensor Systems these values were readily obtained. No serious interference or crosstalk problems have previously occurred in the monitoring of H₂O, O₂, N₂, and CO₂. There is no reason to anticipate that new interference problems will occur.

Measurement of H₂ and He.

H₂ and He form low-mass ions which reach their focal point inside the magnets field. Unlike the other ions, m/e 2 and m/e 4 require collectors in the gap of the magnet.

The sensitivities needed for measurement of He and H₂ were determined from the concentration limits specified in the work statement. Using the 1% full-scale rule, a lower limit is determined. The concentration limits become:

H ₂	400 to 40,000 PPM
He	5,000 to 500,000 PPM

These concentration limits fall well within the detectable limits of which the Two Gas Atmosphere Sensor System is capable. The lower limit value can be lowered if desired. The sensitivity of the Two Gas Atmosphere Sensor System can permit a detectable limit in the 10 PPM range for H₂ and in the 50 PPM range for He. An analysis of the lower detectable limits of which the Two Gas Sensor is capable is found in Appendix A.

Resolution requirements can be very low for a He and H₂ measurement. A resolution of 2 is required to separate He (m/e 4) from H₂ (m/e 2). This resolution is about 1/9th of the maximum resolution of the Two Gas Sensor. No resolution problem should occur.

The only possible interference of any magnitude is due to He⁺⁺ being collected at m/e 2. By examining mass spectra of He, it was found that the m/e 2 peak (He⁺⁺) due to He was 0.12% of the m/e 4 (He) peak. If a maximum He concentration of 500,000 PPM is expected, a m/e 2 current of $(0.12 \times 10^{-2}) (5 \times 10^5) = 600$ PPM due to He is calculated. This contribution is greater than the minimum required measurement for H₂ of 400 PPM. A subtraction circuit will be required.

An investigation of the z-axis focusing for m/e 2 and 4 is required to determine if a portion of the ion beam will be lost due to collisions with the analyzer wall. A degradation of the beam intensity by losses caused by collisions with the analyzer wall lowers the sensitivity of the mass spectrometer and gives a current reading not truly indicative of the partial pressure of the ion species.

The z-axis focusing of the Two Gas Sensor consists primarily of two parts. They are:

- (1) Focusing due to the ion source
- (2) Focusing due to fringe field of the magnet

Focusing due to the z-axis electrodes is independent of the mass of the ion. An analysis of this effect is found in NASA Final Report, "Two Gas Atmosphere Sensor System", Phase 2B.

Z-axis focusing due to the magnetic fringe field is mass dependent. The z-axis focusing for m/e 2 and 4 acts to spread (defocus) the ion beams. Whether z-axis focusing is focusing, or defocusing, is dependent on the angle the ion beam makes with the pole face (see Figures 1 and 2).

Focusing occurs when ϵ is positive, that is, increasing towards the center of curvature. Defocusing occurs when ϵ is negative. Analyzing the computer trajectories for m/e 2 and 4 shows that ϵ for m/e 2 and 4 is negative, defocusing. A derivation of the angle of deflection in z-axis focusing follows:

The force acting on an ion in a magnetic field can be expressed in terms of force components.

$$\frac{e}{m} (v_y B_z - v_z B_y) = \ddot{x}$$

$$\frac{e}{m} (v_x B_z - v_z B_x) = -\ddot{y}$$

$$\frac{e}{m} (v_x B_y - v_y B_x) = \ddot{z}$$

$$B_x = 0$$

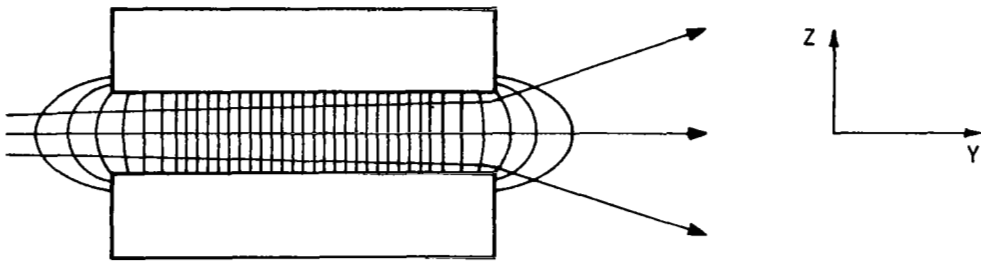
therefore,

$$\ddot{z} = v_x B_y \left(\frac{e}{m} \right)$$

$$v_x = \dot{y} \tan \epsilon$$

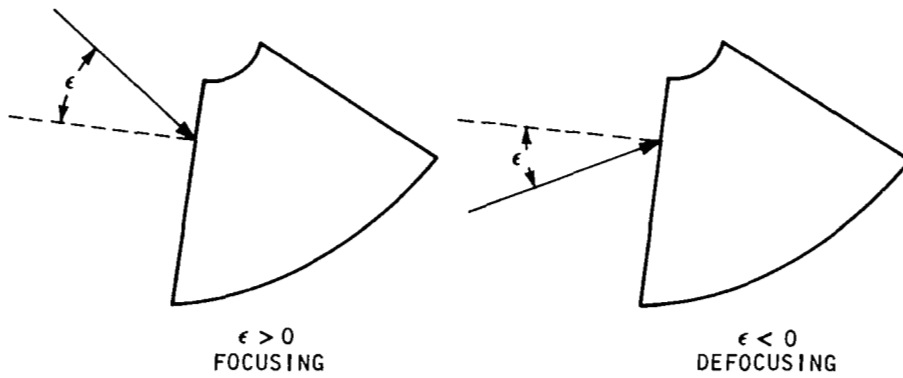
$$v_x = \frac{dy}{dt} \tan \epsilon$$

$$\ddot{z} = \frac{dy}{dt} \tan \epsilon B_y \frac{e}{m}$$



A-254C

FIGURE 1
Z-Axis Focusing



A-255C

FIGURE 2
Z-Axis Focusing and Defocusing

$$\int_0^t \left(\frac{d^2 z}{dt^2} \right) dt = \tan \epsilon \frac{e}{m} \int_{-\infty}^0 B_y dy$$

$$\dot{z} = \frac{e}{m} \tan \epsilon \int_{-\infty}^0 B_y dy$$

In order to calculate $\int_{-\infty}^0 B_y dy$, use $\oint \mathbf{B} \cdot d\mathbf{s} = 0$ along the path shown in Figure 3.

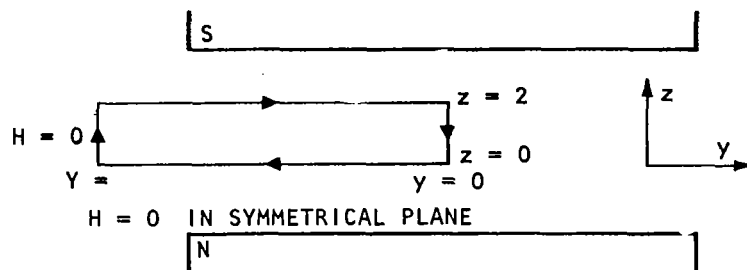


FIGURE 3
Ampere's Circuital Law Diagram

$$\oint \mathbf{B} \cdot d\mathbf{s} = 0$$

$$\oint \mathbf{B} \cdot d\mathbf{s} = \int_{-\infty}^0 B_y dy + \int_z^0 B_z dz = \int_0^{\infty} B_y dy + \int_0^z B_z dz$$

$z = Z \quad y = 0 \quad z = z \quad y = \infty$

$$0 = \int_z^0 B_y dy + B_z \int_z^0 dz + \int_0^{\infty} 0 \cdot dy + \int_0^z 0 \cdot dz$$

therefore,

$$\int_0^{\infty} B_y dy = B_z \int_z^0 dz$$

$$\int_{-\infty}^0 B_y dy = B_z Z$$

Using the solution for $\int_{-\infty}^0 B_y dy$

$$\text{and obtain } \dot{z} = \frac{e}{m} \tan \epsilon Bz$$

The angle of defection is given by \dot{z}/v_o

$$v_o = \frac{reB}{m}$$

$$\text{therefore, } \alpha = \frac{z \tan \epsilon}{r}$$

where z is the half-height of the beam entering the field and r is radius of the ion. For a length path of c in the field a change in z of

$$c \sin \alpha \doteq c\alpha = \frac{cz \tan \epsilon}{r}$$

is obtained.

There is a similar deflection of the beam when it exits the field. But m/e 4 is collected inside the field and consideration of the exit defocusing is not required (see Figure 4).

Next evaluate α and αc

$$r = 1.08 \text{ cm}, c = (0.75) (2.54) \text{ cm}$$

$$c \cong 8^\circ \rightarrow 15^\circ, c = 1.93 \text{ cm}$$

(ϵ is determined from plots of computer data)

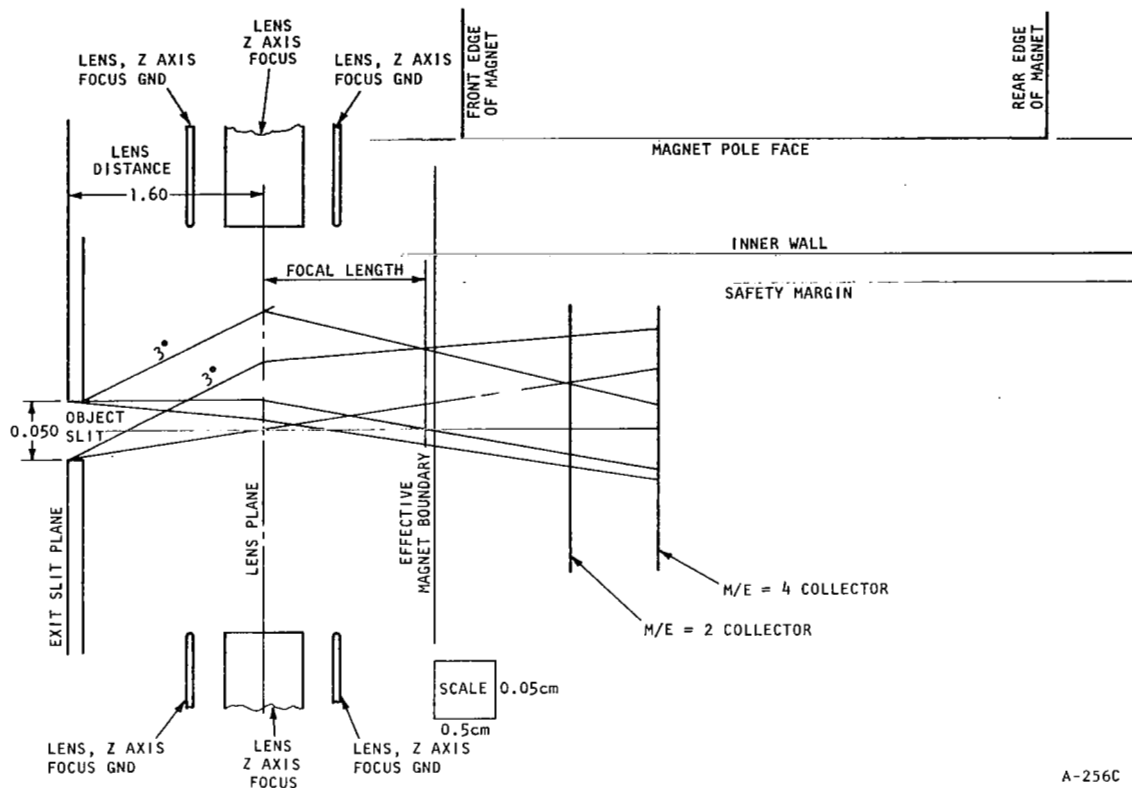
$$\alpha = \frac{z \tan \epsilon}{r}$$

$$\text{for } \alpha = 8^\circ$$

$$\alpha = \frac{(0.075) (0.104)}{1.08} = 0.00725 \quad \alpha = 0.423^\circ$$

$$\text{for } \epsilon = 15^\circ$$

$$\alpha = \frac{(0.075) (0.267)}{1.08} = 0.0193 \quad \alpha = 1.1^\circ$$



A-256C

FIGURE 4
Z-Axis Focus Design Schematic With Trajectory Construction

for $\epsilon = 8^\circ$

$$dc = 0.014 \text{ cm}$$

for $\epsilon = 15^\circ$

$$\alpha c = 0.0376 \text{ cm}$$

The m/e 4 collector is found to be 1.93 cm from the magnet boundary and has a half height of 1.35 cm in the z direction. By adding the c value to the deflection of the worst case shown in Figure 4, the effects of the electrode and fringe field are found. Figure 4 shows that focusing effects of the lens. Noting that the worst case is approximately 0.035 cm from the safety margin line and about 0.05 cm from the end of the collector. Therefore, z-axis defocusing does not cause loss of ions, at least within the accuracy of the derivation and measurement of

The values of interest for m/e 2 are

$$r = 0.765$$

$$z = 0.075$$

$$\alpha = 15^\circ - 25^\circ$$

for $\alpha = 15^\circ$

$$\begin{aligned}\alpha &= \frac{Z \tan \epsilon}{r} \\ &= \frac{(0.075) (267)}{0.765} \\ &= 0.0259\end{aligned}$$

$$\therefore \alpha c = (0.0259) (1.14) = 0.0296$$

for $\alpha = 25^\circ$

$$\begin{aligned}\alpha &= \frac{(0.075) (0.450)}{0.765} = 0.044 \\ \alpha c &= (0.0442) (1.14) = 0.050\end{aligned}$$

Therefore, it is noted that m/e 2 also falls within the safety margin. A further analysis for the other masses is not needed since m/e 2 and m/e 4 are the worse cases.

Measurement of Methane and Total Hydrocarbons

It has been determined that it would be of great value to measure independently the concentration of methane and the total concentration of other hydrocarbons. With separate measurement, the sensitivity ranges of the two outputs can be adjusted to provide a more adequate and meaningful assay of the environmental control system performance.

Sensitivities needed for measurement of methane and total hydrocarbons.-

Methane has a molecular weight of 16, but the fact that the atmosphere to be sampled is 50% oxygen, which was a 10% peak at m/e 16, forbids the use of m/e 16 to detect methane. The m/e 15 peak from methane is almost as large as the parent m/e 16 peak. Mass spectral data gives the m/e 15 to m/e 16 ratio as about 0.9. Therefore, the m/e 15 collector would be used as an indicator of the amount of methane present.

The hydrocarbons to be monitored are generally organics with molecular weights above 50 A.M.U. It is envisioned that a large bucket could be used to collect m/e in the 47 to 120 ranges as an indication of the hydrocarbons present. The lower limit of 47 was chosen primarily for two reasons. The first is that few organics have substantial contributions in the 44-46 range. Second, no increase in resolution of the Two Gas Atmosphere Sensor System is required to separate m/e 44 from m/e 47.

The expected range of concentrations for methane is 0 to 650 mg/m³ (0 to 1,950 PPM). Since the measurement of a zero quantity of methane is an impossibility, a lower limit of 1% of the full-scale reading (2,000 PPM) was taken as being sufficient. This sets the lower limit to be 20 PPM. The sensitivity of the present Two Gas Atmosphere Sensor System is about 1×10^{-6} amps/torr for nitrogen. The sensitivities for nitrogen and CH₄ are within approximately 10% of each other. The sensitivities for nitrogen and CH₄ will be considered to 1×10^{-6} amps/torr. The Two Gas Sensor is designed to operate at a pressure of 2×10^{-4} torr. Therefore, a methane atmosphere would give an ion current of 2×10^{-10} amps. Amplifier noise and drift can be reduced to the 1×10^{-15} amp level. Taking a signal-to-noise ratio of 2 to be sufficient for this application, we find a minimum detectable concentration of 10 PPM methane. Therefore, it is noted that the present Two Gas Sensor has adequate sensitivity for the detection of methane.

The sensitivity needed for the monitoring of total hydrocarbons was determined by two methods. The first method utilized the procedure used for methane. One percent of the maximum or full-scale reading was taken as the lower limit. This value is 10 PPM. Assuming a sensitivity of the same value as for nitrogen, this Two Gas Sensor was found capable of a detectable limit of 10 PPM assuming a signal to noise ratio of 2.

The second method used to determine the needed sensitivity required the formation of an atmosphere. MOL documents specify an expected contaminant range of 50 mg/m³ to 500 mg/m³. Fifty contaminants were selected to form an atmosphere in the concentration range specified. This data was reduced to determine the expected m/e 47-120 concentration in PPM. The results for the fifty contaminants, each occupying 1/50th of the atmosphere by weight were:

PPM m/e 47-120	
50 mg/m ³	39 PPM
500 mg/m ³	390 PPM

For concentration levels even down to 12.5 mg/m³, the sensitivity of the Two Gas Sensor is sufficient. A detailed analysis of the calculations performed is found in Appendix A.

Interference in measuring THC.- The primary interference with the measurement of THC at m/e 47/120 is due to the isotopes carbon and oxygen from CO₂.

The natural percentage abundancies of the isotopes of carbon and oxygen are:

$$C^{12} \quad \sim 100\%$$

$$O^{16} \quad \sim 100\%$$

$$C^{13} \quad = 1.11\%$$

$$O^{17} \quad = 0.037\%$$

$$O^{18} \quad = 0.204\%$$

From the percentage abundancies it can be determined the 45, 46, and 47 ion currents due to isotopes of carbon and oxygen from CO₂.

m/e 45,

$$C^{13} (O^{16})_2 = \frac{1.11}{100} = 1.11 \times 10^{-2}$$

$$C^{12} O^{17} O^{16} = 2 \frac{(0.037)}{100} = 7.4 \times 10^{-4}$$

m/e 46,

$$C^{13} O^{17} O^{16} = 2 \frac{(1.11)}{100} \frac{(0.037)}{100} = 8.2 \times 10^{-6}$$

$$C^{12} O^{17} O^{17} = \frac{0.037}{100} \left(\frac{0.037}{100} \right) = 13.7 \times 10^{-8}$$

$$C^{12} O^{18} O^{16} = \frac{2(0.204)}{100} = 0.40 \times 10^{-2}$$

$$= 4 \times 10^{-3}$$

m/e 47,

$$C^{13} O^{18} O^{16} = 2 \left(\frac{1.11}{100} \right) \left(\frac{0.204}{100} \right) = 0.44 \times 10^{-4}$$

$$C^{12} O^{18} O^{17} = 2 \left(\frac{0.204}{100} \right) \left(\frac{0.037}{100} \right) = 1.5 \times 10^{-6}$$

$$C^{13} O^{17} O^{17} = \left(\frac{1.111}{100} \right) \left(\frac{0.037}{100} \right) = 14 \times 10^{-10}$$

Totals

$$\text{Mass 45} = 1.18 \times 10^{-2}$$

$$\text{Mass 46} = 4.0 \times 10^{-3}$$

$$\text{Mass 47} = 4.4 \times 10^{-5}$$

The values are calculated for masses 45, 46, and 47. The fraction becomes even smaller for masses 48 and 49.

A CO₂ concentration of 20 torr corresponds to 50,000 PPM. The 45 peak due to isotopes is a little over 1% of this value, approximately 500 PPM. Since the resolution of the instrument is only about 12-16 at m/e 44, m/e 45 will not be separated from 47. The expected hydrocarbon level is less than 500 PPM. Therefore, most of the ion current at m/e 47-120 is due to CO₂. This can be easily corrected by placing the total hydrocarbon collector in position for collection of m/e 49-120. This minor adjustment will enable m/e 45 and 46 not to be collected in the total hydrocarbon collector. Also, it should be remembered that the worse case CO₂ value, 20 torr, was used in this discussion. It is probable is that the actual CO₂ concentration will be considerably lower. Because the resolution is only about 15, hydrocarbons of mass 47-120 and CO₂ isotopes of mass 47, 48, and 49 will still be collected. The CO₂ contribution at masses 47, 48, and 49 is very small and can be neglected.

Interferences on the methane measurement.— The interference problem for methane is different for each of the two atmospheres. In the oxygen-helium atmosphere, interference at m/e 15 is due primarily to O₂⁺₁₆ tail from O₂. The atmosphere is one-half O₂. O₂⁺₁₆ is about 10% in abundance with respect to O₂⁺₂ for 70 e.v. electrons. Therefore, we can expect a current of about 50,000 PPM at m/e 16 due to O₂⁺₁₆. This is a value of about 50 times the expected methane contribution of m/e 15. Since one peak is so much larger than the other, the possibility exists that the tail from m/e 16 could washout m/e 15.

The Johnson-Nier Equation¹ gives the expression for the displacement of a ray from the central ray due to small variations in initial displacement, velocity, mass, or angle:

$$g = d \left\{ \cos \phi - n_i \sin \phi \right\} + r_o \delta \left\{ 1 - \cos \phi + n_i \sin \phi \right\} \\ + r_o \alpha \left\{ (1 - n_o n_i) \sin \phi + (n_o + n_i) \cos \phi \right\} \\ - 1/2 r_o \alpha^2 \left\{ g^2 + \frac{1}{g} \right\}$$

and

$$\delta = \beta + \gamma$$

where:

ϕ = angle of deflection in the magnetic field

d = initial displacement from the central ray

r_o = radius of curvature in the magnetic field

β = velocity dispersion = $\Delta v/v$

γ = mass dispersion = $\Delta m/m$

$$n_o = \frac{l_o}{r_o}$$

$$n_i = \frac{x}{r_o}$$

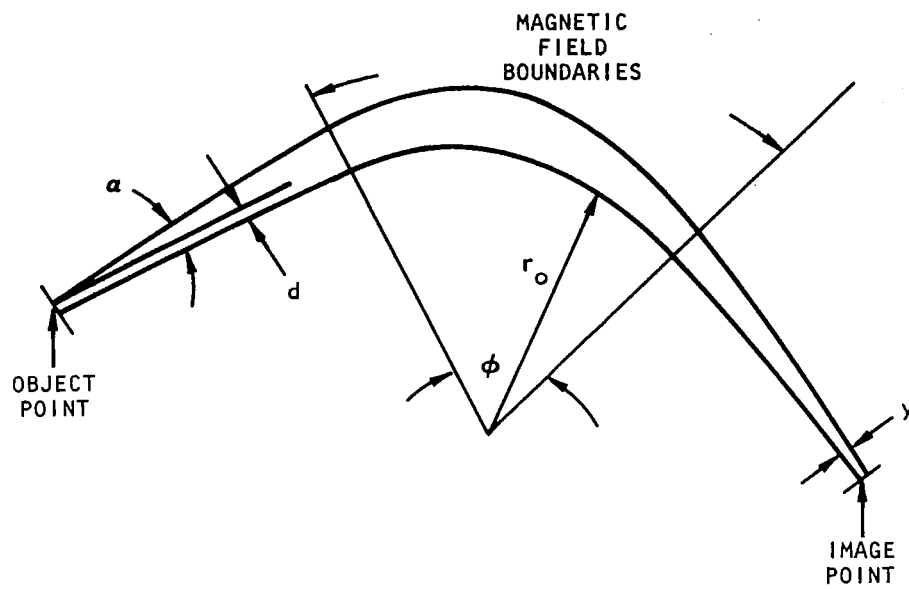
l_o = object-magnet boundary distance

x = image magnet boundary distance

$$g = \cos (\tan^{-1} n_i) / \cos (\tan^{-1} n_o)$$

These relationships are found in Figure 5. It can be shown that the biggest aberration is the α aberration and therefore, the first step in order to reduce overlap is to make the first order alpha focus as close to zero as possible.

¹ "Angular Aberrations in Sector-Shaped Electromagnetic Lenses for Focusing Beams of Charged Particles", Physical Review Vol. 91, No. 1, July 1, 1953 by E. G. Johnson and A. O. Nier.



A-287C

FIGURE 5
Magnetic Focusing Relations

The only negative term in the equation is α^2 term

$$\left(-1/2 r_o \alpha^2 \left\{ g^2 + \frac{1}{g} \right\} \right)$$

Negative terms refer to spreading (or tails) on the low mass side while the positive terms refer to spreading and tails on the high mass side. As can be shown, the largest tail is on the high mass side of the peak.

One group of ions which contribute to tails are the ions which leave the source at a large angle α . By far the greatest ion density is found in the center of the ion beam. The density decreases sharply as one moves from the center of the beam. Proper baffling can be designed that will eliminate most of these ions which cause the tails and yet not severely effect the intensity of the ion beam. It is expected that the problem of interference at m/e 15 due to the low mass side of m/e 16 can be solved by the use of such baffling and stops.

When operation in a nitrogen-oxygen atmosphere is considered, a number of problems occur at m/e 15. Interference due to

(1) O_{16} tail

(2) N_{15}^+ isotope

(3) N_{14}^+ tail

need be considered. The problem due to O_{16}^+ in an nitrogen-oxygen atmosphere is essentially the same as in the helium-oxygen atmosphere previously discussed.

Interference will occur at m/e 15 due to the m/e 15 isotope of nitrogen. The natural abundance of N_{15} is 0.37%.

Calculating the fraction of m/e 28 to be found at m/e 15 due to the N^{15} isotope we obtain

$$\begin{aligned} (N^{15})_2 &= \left(\frac{0.37}{100} \right) \left(\frac{0.37}{100} \right) \\ N^{15} N^{14} &= 2 \frac{0.37}{100} \\ &\sim \frac{0.74}{100} + \frac{(0.37)^2}{10^4} \\ &\approx 0.74 \times 10^{-2} \\ &= 7.4 \times 10^{-3} \end{aligned}$$

as the fraction of N_2 molecules having an N^{15} atom.

Half of the atmosphere in the nitrogen-oxygen atmosphere case is nitrogen. Therefore, 500,000 PPM N_2 is present. About 14% of the N_2 (m/e 28 peak intensity is found at m/e 14, about 70,000 PPM. Due to the N^{15} isotope about 500 PPM of N^{15} will be collected in the m/e 15 collector. This is about 1/4 the maximum methane current. This isotopic interference can be subtracted out of the signal by means of differential amplifiers. The m/e 28 peak will be due almost entirely to N_2^+ . The amount of N_2^{15} can be determined if the amount of N_2^+ is known. This ratio is a definite number at a given temperature for a given mass spectrometer. The number 7.4×10^{-3} is an estimate of the N_2^{15}/N_2^+ ratio. This ratio can be determined accurately on the mass spectrometer to be used. The problem of isotopic interference at m/e 15 is not a difficult one to overcome.

The most difficult problem of interference in a nitrogen-oxygen atmosphere at mass 15 is due to the N^{14} tails. The N^{14} concentration is about 50 times larger than the expected methane concentration. This time the high mass tail causes the problem. The tail on the high mass side of the 14 peak is due primarily to two factors. These factors are:

(1) The thermal energy of the ions

(2) The kinetic energy of the dissociative fragments.

(There is also a $\alpha\beta$ and a β^2 term but these terms are small.)

In order to obtain an estimate of the affect of the m/e 14 (N^+) tail on m/e 15, consideration of the Maxwellian distribution of velocities was necessary. The energy aberration term is given by

$$= \frac{K_2}{2} r_o \frac{\Delta V}{V} =$$

where

$$V = 225$$

$$K_2 \approx 1.50$$

$$r_o = 2.0$$

and

ΔV is to be determined for the case considered

A voltage of 225 volts corresponds to a velocity given by

$$v = 1.30 \times 10^6 \sqrt{\frac{V}{M}} \left(\frac{\text{cm}}{\text{Sec}} \right)$$

where

V is volts, M is molecular weight in A.M.U.

$$= 1.39 \times 10^6 \cdot \sqrt{\frac{225}{14}}$$

$$= 5.6 \times 10^4 \text{ m/sec}$$

At a source temperature of 500°K, the most probable thermal velocity of an N⁺ ion is given by

$$v_m = \sqrt{\frac{2KT}{m}}$$

where

K is Boltzman's constant

T is Kelvin Temperature

m is the mass in Kg

$$v = \sqrt{\frac{(2) (1.38) (10^{-23}) 500}{(14) (1.67) (10)^{-27}}}$$

$$v = 7.7 \times 10^2 \frac{\text{m}}{\text{sec}}$$

The error function ²

$$\text{erf}(x) e = \frac{2}{\sqrt{\pi}} \int_0^x e^{-x^2} dx$$

gives the number of ions with velocities less than a given value. X is defined as

$$X = \frac{v_x}{v_m} \quad (v_x \text{ is the upper velocity limit})$$

Error function is shown in Table 2. For an X value of 2.8 only 1 particle out of 10,000 is not considered. This function is used to calculate the energy aberration shift which contains 9,999 out of 10,000 of the particles.

$$= \frac{k_2}{2} r_o \frac{\Delta v}{v} = K_2 r_o \frac{\Delta v}{v}$$

²Sears, F. W., Thermodynamics, Addison & Wesley (1953) Cambridge, Mass. Page 236

TABLE 2.- ERROR FUNCTION

Values of the error function $\text{erf}(x) = \frac{2}{\sqrt{\pi}} \int_0^x e^{-x^2} dx$.

x	erf(x)	x	erf(x)
0.0	0.0	1.6	0.9763
0.2	0.2227	1.8	0.9891
0.4	0.4284	2.0	0.9953
0.6	0.6039	2.2	0.9981
0.8	0.7421	2.4	0.9993
1.0	0.8427	2.6	0.9998
1.2	0.9103	2.8	0.9999
1.4	0.9523	--	----

For values of x larger than those given in the table, erf(x) can be computed from the semiconvergent series

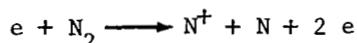
$$\text{erf}(x) = 1 - \frac{e^{-x^2}}{\sqrt{\pi} x} \left(1 - \frac{1}{2x^2} + \frac{1 \cdot 3}{(2x^2)^2} - \frac{1 \cdot 3 \cdot 5}{(2x^2)^3} + \dots \right)$$

but

$$\begin{aligned} \therefore &= \frac{k_2}{2} r_o \frac{(2.8) (7.7 \times 10^2)}{(5.60 \times 10^4)} \\ &= \frac{1.5}{2.0} \frac{(2.8) (7.7 \times 10^2)}{(5.52 \times 10^4)} \\ &\approx .11 \text{ cm} \end{aligned}$$

This means that due to thermal energy only 1 particle out of 10,000 will be displaced towards the 15 collector more than .11 cm. Therefore, the thermal contribution to the m/e 14 tail can be neglected.

Next, we shall determine the effect of the dissociative kinetic energy. The kinetic energy of dissociation is a function of electron energy. Tate and Lozier³ have presented data which gives the energy of dissociation of N₂ as a function of electron energy. At an electron energy of 70 e.v., the dissociative kinetic energy is about 12 e.v. since the reaction described is



it is seen that the N⁺ ion takes away 1/2 the dissociation kinetic energy. Assuming that the ions have a Maxwellian distribution with 6 volts as the most probable energy allows the use of the energy aberration relation

$$= \frac{k_2}{2} r_o \frac{\Delta v}{v}$$

A 6 volt energy corresponds to a velocity of

$$\begin{aligned} v &= 1.39 \times 10^6 \sqrt{\frac{V}{M}} \frac{\text{cm}}{\text{sec}} \\ &= 1.30 \times 10^6 \sqrt{\frac{6}{14}} \\ &= 0.66 \times 10^4 \frac{\text{m}}{\text{sec}} \end{aligned}$$

This time demanding that X = 2.0 in order to achieve 1 part in 200 condition calculate the energy aberration shift to be

³ Tate, J. T., and Lozier, W. W., Phys. Rev. 39, 254 (1932).

$$= \frac{K_2}{r_o} \frac{(2.0) (0.66) (10^4)}{(5.52 \times 10^4)}$$

$$= 0.72 \text{ cm}$$

The separation of the midpoints of the ion beams for m/e 14 and m/e 15 is about 00.2 cm; therefore, the tail from m/e 14 does cause interference at m/e 15. A precise theoretical determination of contribution of m/e 14 to m/e 15 is a complex problem. By far the simplest and most exact determination of the effect of the m/e 14 tail can be performed experimentally. The percentage of the m/e 14 peak overlapping into the m/e 15 collector could be determined. The determination of this value would allow the tail to be subtracted from the m/e 15 measurement and give the correct methane measurement.

THE MEASUREMENT OF CO

Sensitivity requirement for measurement of CO. - The Two Gas Sensor can be operated with an ion source sensitivity of 2×10^{-6} amps/torr for CO. Laboratory values obtained are 1×10^{-6} to 1.4×10^{-6} amps/torr. The 2×10^{-6} amp/torr value is given as an upper sensitivity limit which provides an indication of the detectable limit of the Two Gas Sensor. This sensitivity with an ion source operating pressure of 2×10^{-4} torr would produce an ion current of 4×10^{-10} amps in a 100% CO atmosphere. Detector noise of 1×10^{-15} amps with a one second 0 to 90% rise time has been obtained in laboratory tests. 1×10^{-15} amps can be achieved for flight application with a longer rise time.

A flight detector system would require additional capabilities and modifications because laboratory use and flight applications are quite different. For a detailed description of the detector system see Support Electronics Subsystem section below.

A signal to noise ratio of 3 will provide a good signal for this application. An ion current of 3×10^{-15} amps corresponds to a CO concentration of 7.5 PPM. A reduction of the signal to noise ratio to 2 will permit concentrations as small as 5 PPM to be detected. PPM and mg/m^3 (milligrams per cu. meter) are related in a 380 torr atmosphere by

$$1 \frac{\text{mg}}{\text{m}^3} = \frac{44.8}{\text{MW}} \text{ PPM}$$

where MW is the molecular weight in grams. Therefore, for CO

$$5 \text{ PPM} = 3.15 \frac{\text{mg}}{\text{m}^3}$$

The limits on the CO concentration to be measured as specified in the contract work statement, are given as 0 to 30 mg/m³. Of course, the zero values can not be measured. The lower limit using the instrument detector noise and ion source sensitivity previously given becomes 5 PPM or 3.15 mg/m³, while 30 mg/m³ converted to PPM is 48 PPM. Therefore, the Two Gas Sensor is capable of detecting concentrations from 5 to 48 PPM assuming that no interference is encountered. Unfortunately, interferences are encountered from a number of directions. These interferences are discussed in the next section.

Interferences.- The three contributors to interference of mass 28 due to the sample mixture can be broken down as follows:

- (1) Interference due to hydrocarbon fragmentation
- (2) Interference due to N₂
- (3) Interference due to CO₂

An atmosphere sufficiently detailed to allow an estimation of the spectral pattern formed due to hydrocarbon and contaminants was not furnished with the contract. This data is important because interferences, their magnitudes, and their locations, play a major part in determining possible instrument modifications and overall job feasibility. Since no atmosphere was furnished, atmospheres representing possible situations were constructed. Atmosphere number one was formed by taking 50 contaminants which spectra data was available from the laboratory contaminant sensor contract, NAS-1-8258. These compounds have a high probability of being present in a helium-oxygen atmosphere. Spectra data for these compounds was reduced to give data in PPM for the following cases:

- (1) As if each contaminant occupied the atmosphere by itself (this was done for concentrations of 50 mg/m³ and 500 mg/m³).
- (2) As to form a composite atmosphere in which each compound appeared in equal concentration as to weight.

Appendix A explains the details of this analysis. Results of 50 compounds taken individually is also found in the Appendix. Results of the composite atmosphere follows:

	m/e 15	m/e 27	m/e 28	m/e 29	m/e 47-120
50 mg/m ³	6.78	8.20	4.62	13.33	39.40
500 mg/m ³	67.8	82.0	46.2	133.5	394.0

Atmosphere Number 2 was formed from the 10 compounds with the highest m/e 27 + m/e 28 + m/e 29 contribution. This data provided the worse case interference situation. Which yielded:

	m/e 15	m/e 27	m/e 28	m/e 29	m/e 47-120
50 mg/m ³	6.14	23.29	15.79	48.43	22.34
500 mg/m ³	61.4	232.9	157.9	484.3	223.4

Also, the 10 compounds with the smallest 27 + 28 + 29 were examined. These 10 compounds had no m/e 27, 28, or 29 contribution and formed too favorable a situation to be seriously considered.

Interference of m/e 15 is quite small when compared to the expected methane concentration of about 2000 PPM. No interference problem at mass 15 is expected.

Mass 28 interference provides the largest problem. Mass 27 and 29 had to be considered because the resolution of the present Two Gas Sensor is only 18; therefore, the instrument is not able to separate 27 or 29 from mass 28. An ion current reading taken at m/e 28 collector would be the sum of the 27, 28, and 29 ions.

For the 50 contaminants at the low concentration of 50 mg/m³, some interference at m/e 28 is observed. The summation of m/e 27, m/e 28, and m/e 29 for the 50 contaminants yields 26.17 PPM. This is a significant amount when compared to the maximum amount of CO expected, 48 PPM. For concentrations greater than 50 mg/m³ and for atmospheres composed of a less favorable mixture of contaminants, such as the 10 contaminants with the highest 27, 28, and 29 contribution, the situation rapidly deteriorates. Solutions to this problem such as increasing the resolution and scrubbing will be discussed in a later section.

An evaluation of a probable method, utilizing low-energy electrons as a means to decrease fragmentation, has been completed. Unfortunately, the results were unfavorable. The decrease in fragmentation of masses 27, 28, and 29 was quite small when compared to the large decrease in CO sensitivity when low energy electrons were contemplated. A detailed study appears in Appendix C.

Interferences due to large concentrations of N₂ and CO₂ can completely destroy a CO measurement. Both CO₂ and N₂ have a 28 contribution. For a method of measuring CO to be successful limits must be put on the CO₂ and N₂ concentrations. If the atmosphere to be monitored is a helium-oxygen atmosphere, CO₂ and N₂ levels are expected to be low.

Subtracting out both the contributions of nitrogen and carbon dioxide in an oxygen-helium atmosphere at m/e 28 is possible since their concentrations can be determined at other mass-to-charge ratios. In an nitrogen-oxygen atmosphere, a subtraction method can not be used. Carbon dioxide has its parent peak at m/e 44 and only approximately an 11% contribution at m/e 28. Nitrogen on the other hand is a parent peak at m/e 28 but has a fragment peak of approximately

15% at m/e 14. By making measurements at m/e 44 and m/e 14, and appropriately ratioing the outputs subtracting out the contributions of carbon dioxide and nitrogen at m/e 28 is possible. This can be accomplished automatically by the use of operational amplifiers and the appropriate logic connections. This is shown schematically in Figure 6.

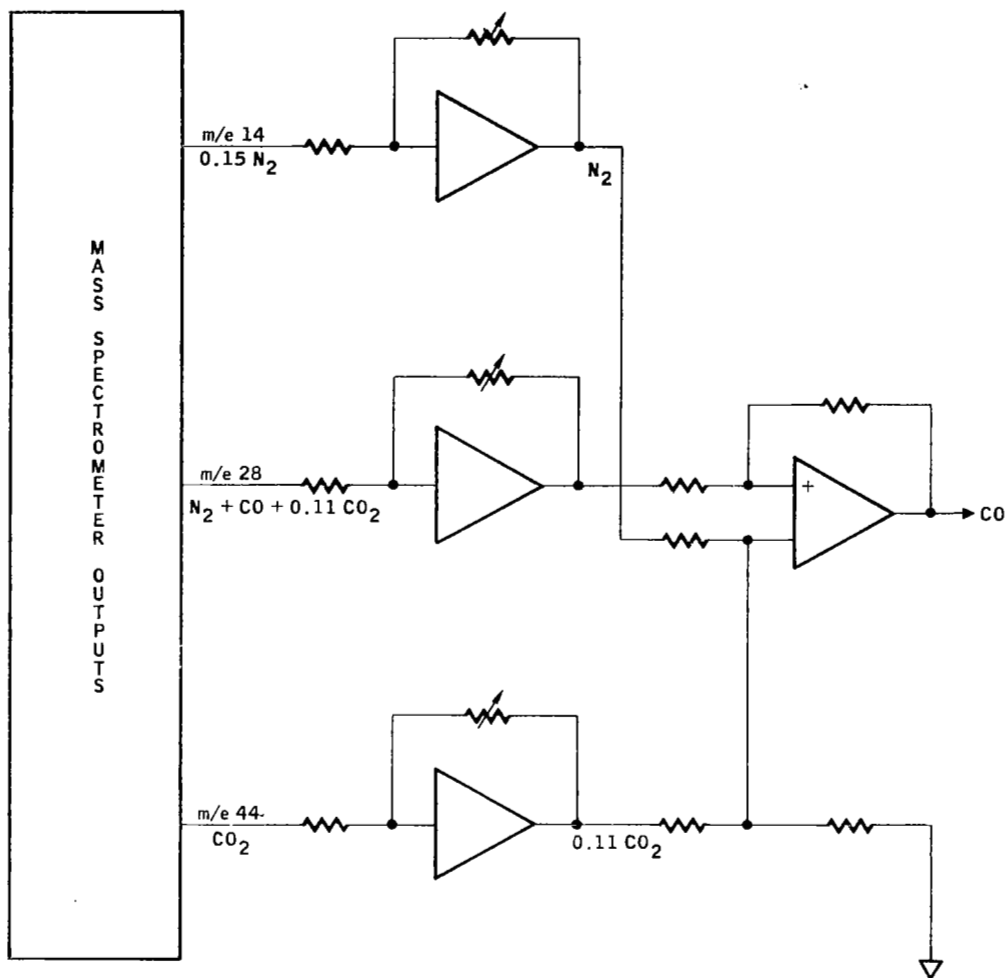
The limitations in applying this approach becomes the accuracy with which the required outputs can be measured and ratioed. By controlling the temperature of the ion source maintaining the stability of the parent to fragment peak ratios within 0.1% is possible even though the absolute errors of the instrument might be on the order of 10 times larger than this. Most of the variations which cause changes in the mass spectrometer outputs affect all of the mass peaks equally.

Assume that the atmosphere has 1% contributions from nitrogen and carbon dioxide and an 18 part per million carbon monoxide level. For simplicity, assume that the mass spectrometer has an equal sensitivity for all three constituents. This is approximately true. Further, assume that the fragmentation pattern has been adjusted so that carbon dioxide is a 10% fragment at m/e 28. By using the ratio technique described above, measurements made at m/e 14 and m/e 44 will then be used to subtract out the nitrogen and carbon dioxide contributions. This can only be done with a 0.1% accuracy; therefore, there will be errors in the carbon monoxide output equivalent to 10 PPM for nitrogen and 1 PPM for carbon dioxide for a total possible error of 11 PPM. This compares to the expected signal level corresponding to 18 PPM for carbon monoxide. It represents a little over 50 percent error in the reading. The situation will improve as a lower concentration of nitrogen is assumed. Careful attention to the control of the stability of the ion source and other circuits will lead to improved results. The method is valuable for atmospheres of 1% or less CO₂ and N₂.

Due to the large concentration of nitrogen, about 500,000 PPM, this subtraction method can not be applied. Therefore, if the Two Gas Sensor is to be used in nitrogen-oxygen atmospheres, an indirect method must be used. Possible solutions to this problem are examined in the Direct Solutions to CO Measurement Problem discussion below.

A second factor is the possibility of an additional error which will be introduced by the noise level of the electrometer amplifier outputs. A 1% nitrogen level will induce a 0.3% error in the m/e 14 output. Therefore, the electrometer amplifier noise levels must be reduced. This error can be reduced by an additional filtering at the electrometer output with some sacrificing in time response. An acceptable level will be obtained; however, while still achieving a 0 to 90% response time of less than 30 seconds. Amplifier drift will be controlled by the use of a rezero circuit which is standard practice for low-level electrometer amplifiers and has been successfully employed on flyable electrometer amplifiers with detectable limits in the 10⁻¹⁶ amp range.

Reactions in the ion source. - The possibility of reactions on the ion source walls may be considered briefly. The composition of the gas in the ion source is roughly comparable to that of the sample and is given in Table 3.



A-U26A

FIGURE 6
Schematic Diagram for Obtaining Carbon Monoxide From
 $m/e\ 14$, $m/e\ 28$ and $m/e\ 44$ Outputs

TABLE 3.- ION SOURCE GAS

O_2	Bulk
H	Bulk
H_2O	----
CO	10-100 PPM
CO_25%
CH_4	500-2000 PPM
Organics500 PPM

The ion source pressure is low, 2×10^{-4} torr, and since the flow pattern is molecular, wall collisions are much more frequent than intermolecular collisions. Under these conditions, the most probable reactions are those which take place on the walls of the ion source and which involve one of the major constituents of the mixtures, in this case oxygen or possibly water. Reactions involving two minor constituents are relatively improbable.

Surface adsorbed films are expected to consist mainly of oxygen and water and the amount of adsorbed material is expected to be low. The principal reactions which can be expected are those which can occur between oxygen or water and the constituents of the mixtures. Oxidation of carbon monoxide or organics appear to be the most probable reactions. Either water or carbon monoxide can serve as the oxidizing agent for carbon monoxide. Susceptibility of organics to oxidation depends on the nature of the compounds; aldehydes, for example, may be particularly prone to oxidation.

The ion source temperature (400°K) is relatively high from the point of view of absorption. Most absorption studies of metal films are carried out at lower temperatures in order to obtain measurable amount of gas sorbed. Extrapolation of data obtained under these conditions to those existing in the ion source is questionable. On the other hand, reaction rates of oxygen with carbon monoxide or methane are relatively slow at the ion source temperature. Rate measurements are typically made at temperatures starting from about 400°C. Reaction rates of catalyzed reactions are also difficult to estimate. Gold is not a particularly good catalyst, and is therefore not expected that

catalytic effects are important in potential ion source reactions. Since gold is inert, chemisorbed films (oxide film, for example) are not expected to be formed in baking out the system or that chemisorbed films would play an important part in ion source reactions.

Reactions with the tungsten filament are not considered as ion source reactions. However, these reactions are important and can affect the analytical results. Water vapor reacts with tungsten to form tungsten oxides which lower the emissivity of the filament. Reactions of tungsten with organics results in the formation of tungsten carbides, which can in turn react with oxygen to produce carbon monoxide and carbon dioxide. If these products re-enter the ion source, they will contribute to the observed signal at mass 28 and 44. This source of sample distortion is dependent on the organic concentrations in the gas stream and is not eliminated by background measurements in the absence of organics. Any ion source design must, therefore, consider the filament positions carefully in order to minimize re-entry of filament reaction products into the ionization region.

Resolution requirement. - As previously stated, the Two Gas Sensor has a resolution of 18 and is not able to separate 27 and 29 from 28. Increasing the resolution from 18 to 28 would decrease the interference at mass 28, but the decrease in interference would not solve all the interference problems at mass 28 due to hydrocarbons. A decrease in interference at 28 by about a factor of 5 would be obtained. For high concentrations of organics and low CO levels, the interference is still troublesome. A more effective way of decreasing interference or increasing the CO signal, then increasing the resolution to 28 is required.

DIRECT SOLUTIONS TO CO MEASUREMENT PROBLEMS

The preceding section demonstrates that a number of complex problems exists when an attempt is made to measure CO at mass 28 on the Two Gas Sensor.

Modifications and/or additions are needed to solve these specific problems:

- (1) Interference due to hydrocarbons
- (2) Interference due to N₂
- (3) Interference due to CO₂

(4) Interference due to background CO

(5) Difficulty in detecting CO concentrations below 10 PPM

Solutions that would decrease the interference to a very small percentage of the CO concentration or increase the CO signal to a level far above the interference would be of value. Such solutions are discussed in the following sections.

Increasing the resolution. - A decrease in interference at m/e 28 is accomplished by increasing the resolution. If the resolution of the instrument is increased from 18 to 28, the interference due to hydrocarbons as previously mentioned, drops by about a factor of five. But for high concentrations of organics and low CO levels, even in a helium-oxygen atmosphere, the interference still can destroy the CO measurement. In a nitrogen-oxygen atmosphere increasing the resolution to 28 does not produce a noticeable effect at m/e 28, since the N₂ contribution at m/e 28 is about 1000 times greater than any other contribution.

Increasing the resolution to 3000 would offer a solution, but the problem of obtaining this resolution in a flight mass spectrometer is too great to be overcome at this time without sacrificing sensitivity and adding tremendously to the size and weight. Increasing the resolution to 3000 essentially eliminates all interference at m/e 28 because only ions with mass differences of less than one part in 3000 would be collected at m/e 28. In an oxygen-helium atmosphere this may be sufficient to separate CO from the N₂ present, assuming the amount of N₂ is quite small. Even if the mass difference between CO and N₂ is greater than one part in 3000, if the N₂ peak is much larger than the CO peak the N₂ tail may possibly wash out the CO peak. Therefore, it is noted that increasing the resolution within the limits that can be tolerated by size and sensitivity requirements is not the answer.

Low energy mass spectrometry. - Low Energy Mass Spectrometry refers to mass spectrometry in which low-energy electrons are used to cause fragmentation. In most cases, the energy of the bombarding electrons is chosen to be less than 4 volts above the ionization potential of the substance to be studied. Low Energy Mass Spectrometry is used primarily to decrease the fragmentation patterns of complex compounds or mixtures of compounds. Therefore, the probability exists that a possible solution to the problem of interference due to organics at m/e 28 may be found by utilizing a low energy electron method. The evaluation of the positive characteristics of a low energy electron method was necessary, a possible decrease in fragmentation against the negative aspect of a considerable decrease in sensitivity. A detailed report of this investigation is found in Appendix C. A summary of the points of interest determined in this study follows.

Modifications and/or additions are needed to solve these specific problems:

- (1) Interference due to hydrocarbons
- (2) Interference due to N_2
- (3) Interference due to CO_2
- (4) Interference due to background CO
- (5) Difficulty in detecting CO concentrations below 10 PPM

Solutions that would decrease the interference to a very small percentage of the CO concentration or increase the CO signal to a level far above the interference would be of value. Such solutions are discussed in the following sections.

Increasing the resolution.- A decrease in interference at $m/e 28$ is accomplished by increasing the resolution. If the resolution of the instrument is increased from 18 to 28, the interference due to hydrocarbons as previously mentioned, drops by about a factor of five. But for high concentrations of organics and low CO levels, even in a helium-oxygen atmosphere, the interference still can destroy the CO measurement. In an nitrogen-oxygen atmosphere increasing the resolution to 28 does not produce a noticeable effect at $m/e 28$, since the N_2 contribution at $m/e 28$ is about 1000 times greater than any other contribution.

Increasing the resolution to 3000 would offer a solution, but the problem of obtaining this resolution in a flight mass spectrometer is too great to be overcome at this time without sacrificing sensitivity and adding tremendously to the size and weight. Increasing the resolution to 3000 essentially eliminates all interference at $m/e 28$ because only ions with mass differences of less than one part in 3000 would be collected at $m/e 28$. In an oxygen-helium atmosphere this may be sufficient to separate CO from the N_2 present, assuming the amount of N_2 is quite small. Even if the mass difference between CO and N_2 is greater than one part in 3000, if the N_2 peak is much larger than the CO peak the N_2 tail may possibly wash out the CO peak. Therefore, it is noted that increasing the resolution within the limits that can be tolerated by size and sensitivity requirements is not the answer.

Low energy mass spectrometry.- Low Energy Mass Spectrometry refers to mass spectrometry in which low-energy electrons are used to cause fragmentation. In most cases, the energy of the bombarding electrons is chosen to be less than 4 volts above the ionization potential of the substance to be studied. Low Energy Mass Spectrometry is used primarily to decrease the fragmentation patterns of complex compounds or mixtures of compounds. Therefore, the probability exists that a possible solution to the problem of interference due to organics at $m/e 28$ may be found by utilizing a low energy electron method. Therefore, the evaluation of the

- (1) Fragmentation does not always decrease when low electron energies are used. In fact, in some cases, fragmentation decreases.
- (2) Most organics have ionization potentials between 8 and 12 e.v. Operating 4 volts above 12 e.v. gives an electron energy of 16 volts.
- (3) The I.P. of CO is 14.1 volts. The CO current at 16 e.v. is about 3% of the CO ion current at 70 e.v.

The decisive factor in determining the value of the low energy electron method is that at the highest electron energy acceptable to give a decrease in fragmentation in the favorable cases (no decreases is realized in the unfavorable cases) the CO ion current is 3% of its value at 70 e.v. The maximum value of CO expected is 48 PPM, 3% of 48 PPM is 1.6 PPM. This signal falls well within the noise of the Two Gas Sensor and is not detectable. Therefore, note that a small decrease in fragmentation around m/e 28 is offset by a large decrease in sensitivity. Low voltage mass spectrometry is not the solution to the interference problem.

Hydrocarbon scrubber.- Direct determination of carbon monoxide in the atmosphere requires the removal of organics from the gas sample since many of these compounds can fragment to yield ions in the mass range 27-29. This can be accomplished by passing the gas through a sorbent such as charcoal or molecular sieve 5A. The choice of sorbent depends on the relative sorptive capacity for carbon monoxide and the organics which may be present in the atmosphere. If the maximum anticipated concentration of organics is 1000 mg/m³ and the required detectable limit for carbon monoxide is about 10 mg/m³, the sorbent must be capable of reducing the organic concentration in the gas sample by a factor of at least 100 without adsorbing significant amounts of the carbon monoxide. Charcoal is probably the best adsorbent for this purpose although it may prove worthwhile to investigate other adsorbents as well. Charcoal has a high sorption capacity for most organics and a relatively low capacity for carbon monoxide and nitrogen and oxygen at room temperature.

Two considerations are involved in selection of the amount of charcoal to be used. The use of as much charcoal as possible is advantageous in order to be sure of removing organics to a very low concentration level. However, the more charcoal used, the longer will be the response time of the system to changes in the carbon monoxide concentration. A certain volume of sample must be passed through the charcoal in order for the sorbed carbon monoxide to be in equilibrium with the partial pressure of carbon monoxide in the gas phase. In the case where the adsorbent does not adsorb carbon monoxide, this volume is simply the free gas volume of the packed charcoal. The number of analyses that can be performed before organics will begin to interfere will depend on the ratio of the breakthrough volume for organics to this equilibration volume for carbon monoxide.

The breakthrough volume for organics in this case is taken as that volume of gas containing organics at 1000 mg/m³ which pass through charcoal before the organic concentration in the exit gas reaches a concentration of 10 mg/m³. This ratio depends only on the relative adsorption constraints for the organics and carbon monoxide for the particular charcoal used and is independent of the amount of charcoal used.

Accordingly, the maximum amount of sorbent should be used which will permit analyses to be performed for carbon monoxide at the desired frequency for the available gas flow rate or pumping speed. For example, if the desired time to sample for CO is once a minute and the available pumping speed is 50 cc/minute, the amount of a adsorbent can not exceed that which will equilibrate with 50 cc of sample. The sorbent should be packed in a relatively long, narrow channel rather than a short, flat bed in order to eliminate the possibility of premature breakthrough of organics due to packing irregularities.

Most organic compounds are strongly adsorbed on charcoal. In general, the adsorption capacity of charcoal increases with the boiling point of the organic. Low boiling, low molecular weight compounds such as methane, ethane, etc., are not strongly adsorbed and may cause interference with the carbon monoxide determination. Low molecular weight polar compounds are usually adsorbed fairly strongly particularly in the presence of oxygen. The composition of the gas mixture also is a factor in determining the adsorptive capacity of charcoal for organics; the adsorptive characteristics may change somewhat if the water content of the sample gas changes significantly. This factor plus the normal differences in charcoals and the fact that most adsorption data are obtained for pure components makes it difficult to predict the effective on stream time for the charcoal adsorbent. The one percent breakthrough volume for butene-1 on charcoal has been shown to be about 32 liters/gm for 1000 PPM butene-1. The adsorption of carbon monoxide on this sorbent could not be detected. This implies that only 10 analyses could be performed before the sorbent would be passing organics. Assuming for example, that the volume of gas required for the carbon monoxide to come to equilibrium is 500 cc/gm, 34 analyses could be performed before organics would begin to interfere. These factors should be determined experimentally for the particular charcoal and anticipated gas mixtures in actual usage.

The scrubber does offer a solution to the problems encountered under certain conditions. These conditions are:

- (1) Helium-oxygen atmosphere with small CO₂ and N₂ content
- (2) When the CO concentration is greater than 10 PPM
- (3) Background CO formed is very small, considerably smaller than 10 PPM

The helium-oxygen atmosphere restriction is made because the scrubber does not scrub nitrogen and CO₂. The allowable concentrations of N₂ and CO must be small or the contributions from CO₂ and N₂ at m/e 28 will dwarf the CO contribution. The temperature of the ion source must be controlled

because the fragmentation ratio can change with temperature. A method of accurately subtracting out the N_2 and CO_2 contribution to m/e 28 would require a closely regulated ion source temperature or a constant measurement of the temperature to be mated with a knowledge of how the ratios vary with temperature.

If all the interference at mass 28 is eliminated, the Two Gas Sensor equipped with scrubber, is still only capable of detecting CO at, and above, the 10 PPM level.

Considerable difficulty in determining how much of the CO detected is indicative of the composition of the atmosphere and how much comes from the filament or walls of the ion source is still present. If the CO from the atmosphere is smaller, or near the same magnitude as the CO from the filament and walls of the ion source, the determination of the CO concentration under these conditions becomes unclear.

CARBON MONOXIDE DETERMINATION BY THE ACCUMULATOR CELL METHOD

While the direct determination of carbon monoxide with the mass spectrometer is theoretically possible in practical application, the difficulties in making accurate difference measurements, and the relatively high and variable signal from carbon monoxide generated at the filament, make this measurement unacceptable except for relatively high concentrations of carbon monoxide. An alternate method for determination of carbon monoxide is the use of the accumulation technique developed on NASA CONTRACT NAS 1-7266, Laboratory Contaminant Sensor Development Program.

The essential elements of this technique are the extraction of carbon monoxide from an air sample on a suitable sorbent, and desorption of the concentrated carbon monoxide by heating the sorbent. Air is removed from the sorbent before the carbon monoxide is desorbed so that interference due to nitrogen is eliminated. Heating the cell rapidly removes the carbon monoxide in a concentrated burst so that the signal is effectively enhanced.

The sorbent used for extraction of carbon monoxide is a palladium-coated charcoal. This sorbent will also be expected to sorb organic contaminants some of which may fragment in the mass spectrometer to yield a 28 peak which will invalidate the carbon monoxide measurement. This interference can be eliminated by removing organics prior to sorption of carbon monoxide. This can be accomplished by inserting a sorbent cell for organics in front of the palladium-charcoal accumulator cell. Tentatively assume that charcoal will be a suitable sorbent for this purpose, although other sorbents should be investigated. The prime requirements for this prescrubbing sorbent are high sorptive capacity for organics and very low capacity for carbon monoxide.

An alternate approach is an investigation of other adsorbents for carbon monoxide. In the original Laboratory Contaminant Sensor Development Program, several sorbents were tested for retention of carbon monoxide at room temperature but were found to be unsatisfactory. These include charcoal, Molecular Sieve 5A,

silica gel and some other specially prepared sorbents. However, since the palladium-coated charcoal appeared to work satisfactorily, it might prove worthwhile to investigate other palladium sorbents. Pure palladium might be considered, as well as palladium supported on glass beads, porous silica beads, or other types of support. The degree of inertness in the support may affect both the retention of carbon monoxide and organics. If the capacity for carbon monoxide can be enhanced, while that for organics is reduced, eliminating the prescrubber cell may prove possible. A study of palladium sorbents for carbon monoxide could prove worthwhile both from the point of view of enhancing our present understanding of the sorption characteristics, and from the point of view of developing an optimum CO monitoring system.

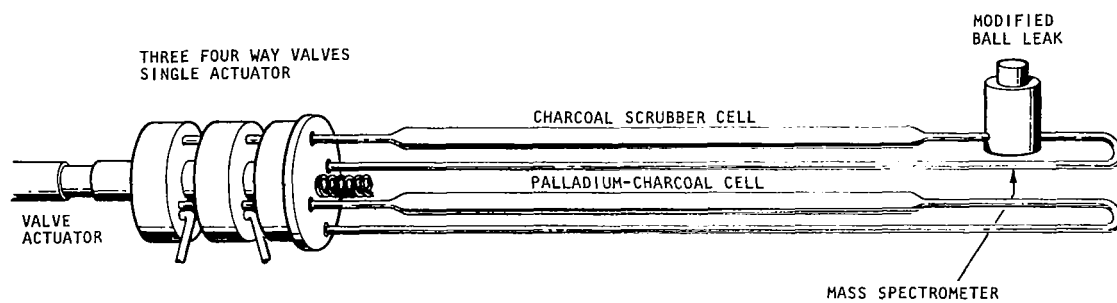
At present, assume that a prescrubber for organics will be used. A simple system for carbon monoxide analysis on an intermittent basis is described in the following section.

DESIGN CONSIDERATIONS FOR A CARBON MONOXIDE DETERMINATION USING AN ACCUMULATOR CELL

The basic instrument of the Contaminant Atmosphere Sensor is the Two Gas Analyzer with the ball leak inlet system. The instrument is operated continuously monitoring water, nitrogen, oxygen, and carbon dioxide on four fixed collectors. For the total hydrocarbon measurement, a collector for m/e 47-120 is added and, for helium oxygen atmospheres, a mass 4 collector is added. With the accumulation techniques, carbon monoxide is determined on an intermittent basis. The normal sample gas flow pattern is interrupted to permit Two Gas Sensor to monitor CO at m/e 28 as it is desorbed from the accumulator cell.

Some modifications to the inlet system are required to accommodate the carbon monoxide measurement. Those include modification of the ball leak to permit the gas flow to be channeled to the leak, and valving to switch from the total atmosphere monitoring to carbon monoxide determination. A relatively simple system proposed for this purpose is shown in Figure 7. The flow switching is accomplished by a simple switching valve. In normal atmosphere, monitoring the sample flow past the ball leak, through a charcoal scrubber, through the valve and out of the palladium charcoal cell, back through the valve and out. When the valve is switched for carbon monoxide determination, the sample flow is bypassed and the carbon monoxide cell is placed in series with the entrance to the ball leak. Helium is used to purge the cell of residual sample gas and to carry the desorbing carbon monoxide past the ball leak.

The sample flow rate through the system will be established by the required frequency of analysis for the carbon monoxide and the lower detectable limits. Assuming a four-hour analysis time interval and a lower detectable limit of 1 PPM, the sample flow rate may be determined in the following manner. An electrometer signal of 1×10^{-12} amps should provide an acceptable measurement over the noise and background levels (10^{-13} amps of m/e 28) in the M.S. This corresponds to an ion source pressure of 10^{-6} torr at a sensitivity of 1×10^{-6} amps/torr (typical



A-288C

FIGURE 7
Accumulator Cell

for the Two Gas Sensor) or a carbon monoxide concentration of 5000 PPM in the gas stream during desorption. Assuming a helium flow rate during desorption of 0.5 cc/min and a time interval of 5 minutes for actual desorption of carbon monoxide, the total amount of CO required is 12.5 μ l (at STP). To obtain this amount of CO from a sample containing one PPM requires a volume of 125 liters, which over a four hour sampling period implies a flow rate of about 50 cc/min. If the helium flow rate is increased or the sampling time period decreased, the atmospheric gas sample flow rate must be increased accordingly. For example, if analysis is required at one-hour intervals, the sample flow rate must be increased to 200 cc/min. These estimates are conservative to the extent that they are based on the average carbon monoxide concentration during desorption. The peak carbon monoxide signal will be considerably higher. These conditions should prove satisfactory for operation aboard a spacecraft. If the necessity arises for increasing the frequency of carbon monoxide analysis, the flow rate can be increased accordingly.

Based on experience with CO determination in the Laboratory Contaminant Sensor development program, a 6-inch tube with 0.1 inch O.D. packed with 0.25 gm. of palladium charcoal should prove adequate as a sorbent cell. The tube can be made of Nichrome V and heated directly. The ends of the tube can be thermally and electrically isolated from the valve and the M.S. leak with ceramic insulators. A similar section can be used for the organic scrubber. At intervals established by experimental study, the scrubber could be heated after the carbon monoxide determination is completed to regenerate the sorbent.

The total operation sequence would proceed as follows: over a four-hour period, the normal atmospheric components would be monitored continuously, the gas stream being pumped through a narrow channel past the ball leak, through the organic prescrubber, and through the CO sorbent cell. At the end of that time interval, an automatic device would open the helium tank and switch the sample valve to the carbon monoxide determination mode. Helium would flow through the cell at 0.5 cc/min or a linear flow rate of 10 cm/min for a time period of five minutes to purge residual air from the system. The accumulator cell would then be heated at a rate of 20°C/min to a temperature of 200°C. The decrease in the oxygen signal at m/e 32 could be used to initiate the heating cycle for the palladium-charcoal cell. As the CO desorbs, it is monitored in the M.S. At the conclusion of the desorption period, the charcoal cell could be heated for regeneration if necessary. The cells would be allowed to cool under helium flow for a predetermined time period and the helium flow shut off and the sampling valve returned to the sampling position.

An estimate of weight of the system and the power required for operation may be made on the basis of commercially available hardware. This estimate is conservative and the weight and power can be reduced by designing special equipment for the flight hardware.

The additional power required for the carbon monoxide determination is that for (1) heating the accumulator cell, (2) actuating the valve switching mechanism, (3) operating the timing circuit and possibly, (4) heating the prescrubber for regeneration. The power requirements depend on the frequency with which the

analysis is performed. It is assumed that in normal operation, the carbon monoxide analysis will be performed at four-hour intervals. However, during start-up, and if the carbon monoxide concentration appears to be increasing to a dangerously high level, a shorter analysis time may be required. The total energy consumed for cell heating is, of course, much higher if frequent carbon monoxide determination are required.

The accumulator cell consists of a thick walled (.001) nichrome V tube, 1/8 inch in diameter and 6 inches long insulated with 1 inch of glass wool. The power required to heat the cell is estimated to be a few watts and the heating time period is estimated at 10 minutes. The weight of the cell is estimated at 5 ounces. A motor driven valve positioner will be utilized and will require an estimated 1 watt of power. The helium consumed is approximately 25 standard cc per determination. Helium will be supplied from a pressurized tank with the flow rate controlled through a capillary restriction and the tank pressure controlled with a reducing gauge. Assuming that during the first eight hours of the mission carbon monoxide is monitored at 30-minute intervals and thereafter, at 4-hour intervals, a total volume of 10 standard liters are needed. A 150 ml cylinder pressurized to 1800 psig should prove adequate. The weight of the cylinder is 1.5 pounds; the weight of the pressure regulator is estimated at 0.5 pounds.

The power supply for heating the charcoal cell is the same as that required for the CO accumulator cell. Since the frequency of regeneration is less, the power requirement for recharging the cell is less by approximately the same factor. Thus, if the charcoal scrubber is regenerated after every ten carbon monoxide determinations, at the four-hour sampling interval the power required to regenerate the scrubber is less than 0.1 watt.

The power and weight factors for the accumulator cell hardware are tentative estimates, at present. A program to develop optimum hardware for this purpose is planned, and the results of this program should furnish more realistic values for the power consumption and the weight of this hardware.

SUMMARY OF SOLUTIONS TO CO PROBLEM

Direct solutions to the CO measurement problems:-

- (1) Increasing resolution
- (2) Low energy mass spectrometry
- (3) Hydrocarbon scrubber

All have serious drawbacks. Increasing the resolution is of little value unless the resolution is increased to about one part in 3,000. The attainment of such high value of resolution is far from being obtainable, at this time, in a flight mass spectrometer. The restraints imposed by weight, power, and size requirements eliminate this method of approach.

The low energy mass spectrometry method is, in general, not effective in reducing fragmentation around mass 28. For a number of compounds studied,

fragmentation around mass 28 increases with low energy electrons. This fact, coupled with the result that the sensitivity for CO greatly decreases at the low electron energies required, eliminates the low energy mass spectrometry method from practical consideration.

Of the direct methods, the hydrocarbon scrubber offers the greatest possibility for effective operation. But in an N_2 - O_2 atmosphere, or in an hc - O_2 atmosphere in which CO_2 or N_2 levels are high, the scrubber becomes practically useless. This is due to the fact that the scrubber can only eliminate organics and does not scrub N_2 or CO_2 . Also, the sensitivity of the instrument is not enhanced by the scrubber and 10 PPM of CO is still the lower detectable limit. For concentrations lower than 10 PPM of CO, another method must be used.

The direct methods are lacking in one or more of the major capabilities required. These failures cause a more indirect method to be considered: the accumulator cell. The accumulator cell eliminates the effects of N_2 and CO_2 contributions to m/e 28 in two ways. First, the system is flushed with He purging the system of the gasses present. Second, the CO is stored in the cell and then released giving a signal considerably higher than 10 PPM in the 5000 PPM range. By use of these two steps, background effects are effectively eliminated. Even the effect of CO produced by the filament is dwarfed by the large CO signal from the accumulator cell. If the concentration of CO present is very small, a longer accumulation time is required. The disadvantages of the accumulator cell method is that being an indirect method, additional power, weight, and complexity is required. Another disadvantage is that the CO measurement requires an interruption in the monitoring of atmospheric gases. In spite of the disadvantages, the accumulator cell approach offers the most effective method of dealing with the CO measurement problem.

ANALYZER LAYOUT

The Analyzer Layout is shown in the Mechanical Design and Packaging Section below. The design of the analyzer housing has been changed from previous Two Gas Sensor designs. The analyzer is enlarged to permit the location of the additional collectors. The focal points for m/e 2 and m/e 4 are located in the magnetic field. The collectors for these two masses are located in the magnetic field and connected to the same collector support. The collector for m/e 47-120 is not connected to the collector flange but is suspended from the analyzer housing. Also, a m/e 15 collector has been added. The m/e 15 and m/e 18 collectors share the same collector support.

SUPPORT ELECTRONICS SUBSYSTEM

Based on the analysis performed during the course of this study plus the results of various tests performed on the Two Gas Analyzer, it has been determined that the support electronics should consist of the following functional units. (See Figure 8.)

- | | |
|---------------------|----------------------------------------------------------------------|
| (1) Input Regulator | Regulates the incoming power line voltage and reduces conducted EMI. |
|---------------------|----------------------------------------------------------------------|

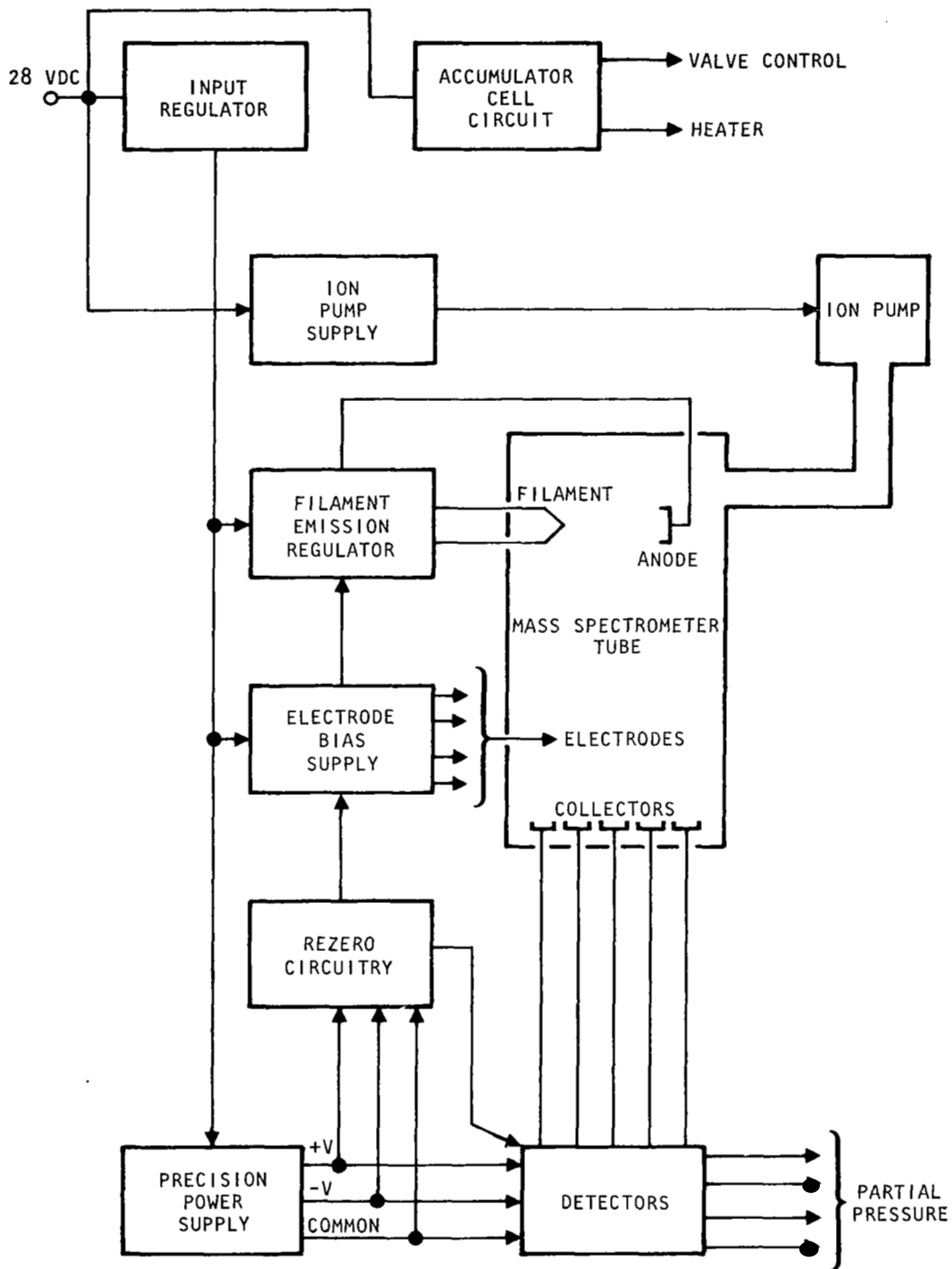


FIGURE 8
Support Electronics Block Diagram

A-115C-A

(2) Filament Emission Regulator	Provides controlled power to the filament so that constant anode current is maintained.
(3) Electrode Bias Supply	Provides the potentials required by the analyzer electrodes.
(4) Detectors	Provide output voltages proportional to the number of ions reaching the ion collectors.
(5) Rezero Circuitry	Performs the switching functions necessary for the rezero cycle.
(6) Ion Pump Supply	Provides the power necessary to operate the ion pump.
(7) Accumulator Cell Electronics	Controls the power used by the accumulator cell and valving.

Units (2) through (5) above are essentially improved versions of the circuits used on the Two Gas Sensor System. The other units are based on circuitry previously developed by Perkin-Elmer Aerospace Systems for similar applications. Following is a detailed circuit description.

Input regulator.- The input regulator consists of five sections as shown in Figure 9 and is a switching regulator preceded by an electromagnetic interference filter and utilizes ripple detection regulation. The ripple developed between the filter inductors is amplified and used to switch a bistable trigger circuit. The output of the trigger circuit is a pulse train which is applied through a driver to the series switch. The ripple does not appear at the output, due to the filter action of the output capacitor. This method provides adequate regulation with an efficiency of approximately 80%.

The electromagnetic interference filter serves two purposes: attenuates conducted interference in both directions and reduces the effect of line transients on the operation of the instrument.

Filament emission regulator.- The filament emission regulator maintains a constant emission current by controlling the AC power supplied to the filament. A block diagram of this system is shown in Figure 10. Basic operation of the system is as follows: The inverter produces squarewaves which are supplied to the 20Vdc regulator, the output amplifier, and as synchronization pulses to the voltage controlled oscillator (VCO). The error amplifier monitors a voltage proportional to the emission current level, compares it to a reference voltage, and amplifies the difference between the two voltages. The amplified difference voltage is supplied to the input of the VCO. The VCO is reset each time the squarewave sync signal changes polarity. After being reset, the VCO delays a finite time interval and then produces a pulse. The length of the time delay is determined by the magnitude of the error amplifier output voltage. Each VCO output pulse turns the output switching amplifier on. It then remains on until the squarewave voltage from the inverter changes polarity. The overall effect is that

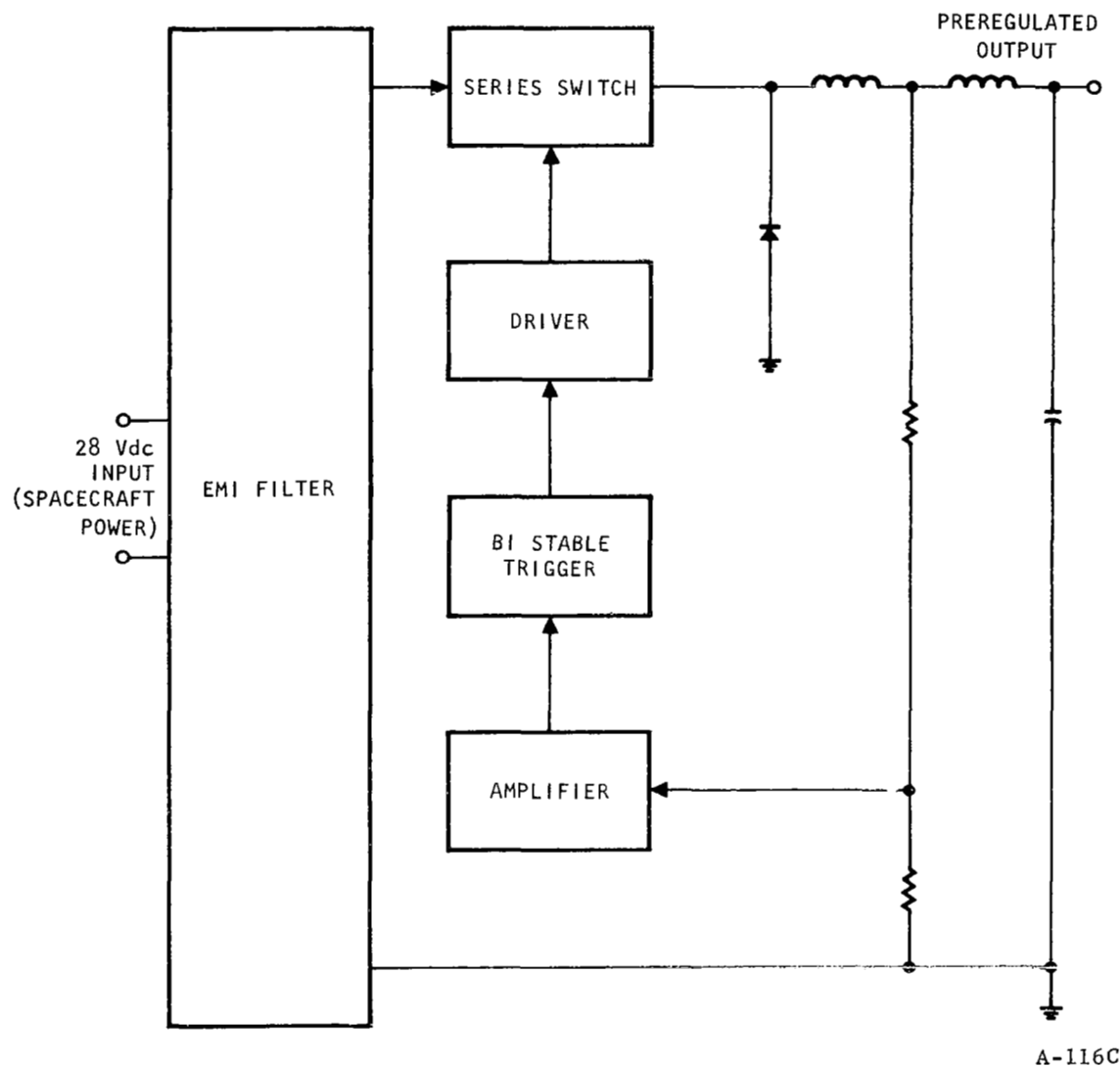


FIGURE 9
Input Regulator Block Diagram

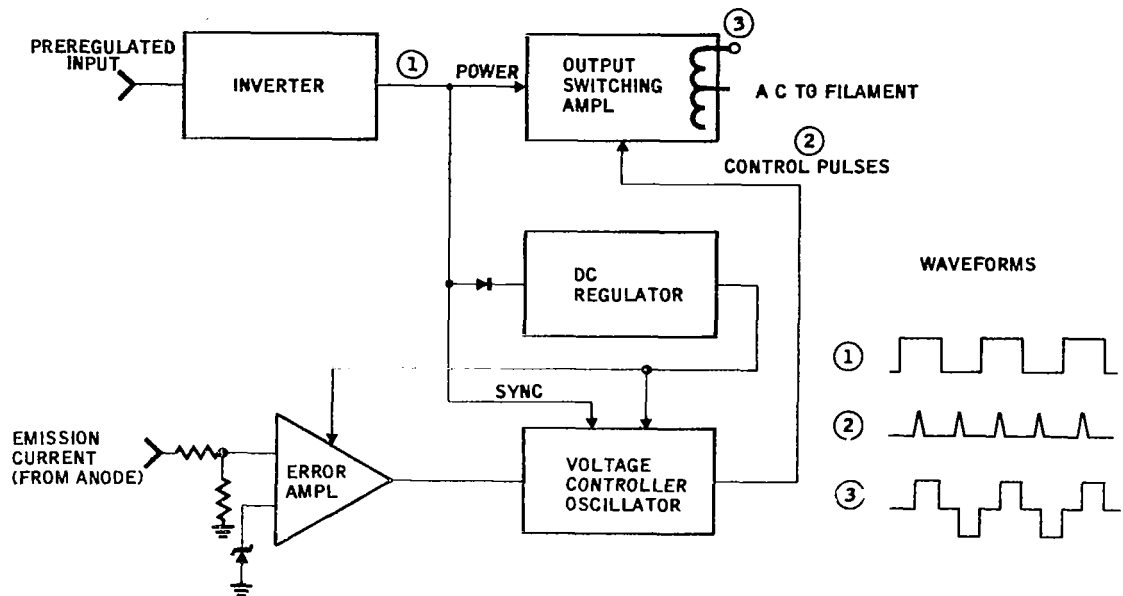


FIGURE 10
Filament Supply and Emission Regulator

A-117A

the output switching amplifier passes only a portion of the squarewave. The percentage of the squarewave passed is determined by the amount of power required by the filament to produce the desired magnitude of emission current.

By making modifications in the VCO and the error amplifier, three areas of operation will be improved. First, a broader range of filament power will be available so that filament aging does not effect the sensor operation; second, AC stability at low anode currents will be improved (the present circuit was designed and analyzed to operate at five times the anode current expected for this instrument); third, temperature stability will be improved to help meet the sensitivity requirements of the system. The methods for making these improvements have been identified and may be readily implemented.

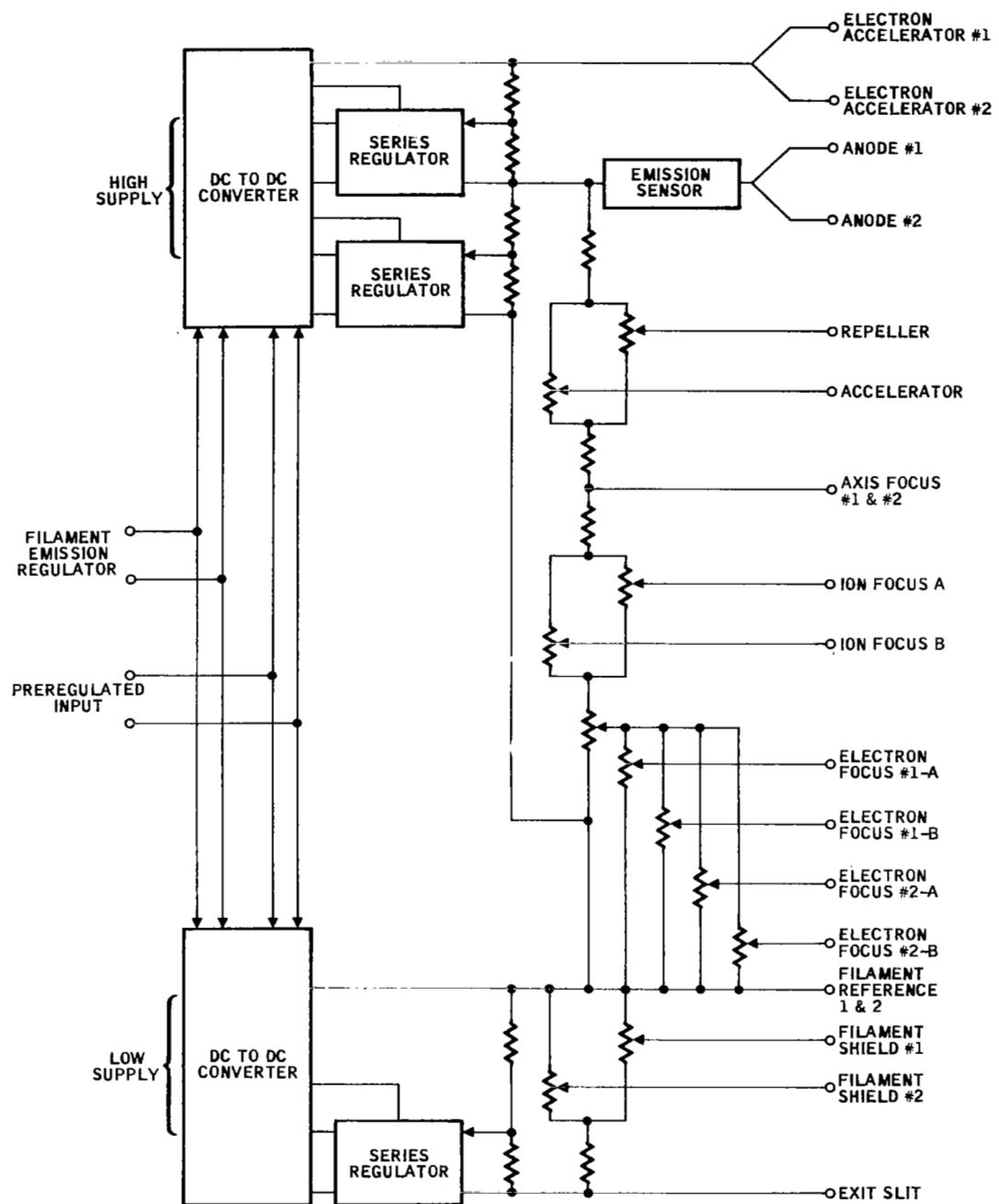
Electrode Bias Supply.- The electrode bias supply shown in Figure 11, consists of two DC/DC converters, three series regulators, and a resistive voltage divider string. The electrode bias supply function is to provide the potentials required by the analyzer electrodes.

The converters are driven by a signal from the filament supply so that the operating frequency of both modules are synchronized. Each transformer has multiple windings and several windings have multiple taps; in this way, a wide range of output voltages is obtained and the operation of the module is highly flexible.

The series regulators are adjustable over the range required for proper analyzer performance. The output of a semiregulated winding is placed in series with the regulator and a sample of the total voltage is sensed by the regulator feedback loop. This produces a regulated voltage that is much greater than the regulator alone is capable of providing. The three series regulators are identical and the following description applies to all three. The series regulator may be considered as an operational amplifier with a differential input. A temperature-compensated reference diode establishes a fixed voltage at the noninverting input and the feedback voltage divider presents a portion of the output at the inverting input. Any difference appearing between the two inputs results in an adjustment in the output that brings the voltage difference between the two bases back to zero. Therefore, the output is held constant at a value determined by the reference voltage and the feedback voltage divider.

The resistive divider string consists of fixed resistors connected in a series-parallel combination that provides the proper potentials to the electrodes of the analyzer. The string is made up of wire wound resistors with excellent temperature characteristics so that the electrode potentials will not be affected by temperature to any significant extent.

This circuit has been changed from the original by the addition of a third series regulator. With the third regulator, the three current-carrying electrodes -- the filament reference, the anode, and the electron accelerator -- are each connected to a separate low impedance point. This enhances the stability of the source by maintaining all the electrodes at constant potential despite changes in current.



A-289A

FIGURE 11
Electrode Bias Supply Block Diagram

Precision power supply.- The precision power supply (Figure 12) consists of a driven DC/DC converter and two series regulators to deliver +10Vdc and -10Vdc at 0.1% regulation to the detectors and associated circuitry. In the Two Gas Sensor system, it was called the detector power supply.

The positive and negative regulators are essentially the same, so only the positive unit will be described here.

There are four sections in the regulator; a pass element, a temperature compensated voltage reference, a difference amplifier, and a feedback network. The feedback network supplies a fraction of the output voltage to one input of the difference amplifier and the other input is connected to the voltage reference. The output of the difference amplifier drives the pass element so that the voltage between the amplifier inputs remains at zero. The level of the output voltage is controlled by the percentage of the output voltage that is fed back to the difference amplifier.

The only modification to this unit is to increase the power capability by adjusting component values and increasing the current capability of the series pass transistor. The circuit is more than adequate in every other way.

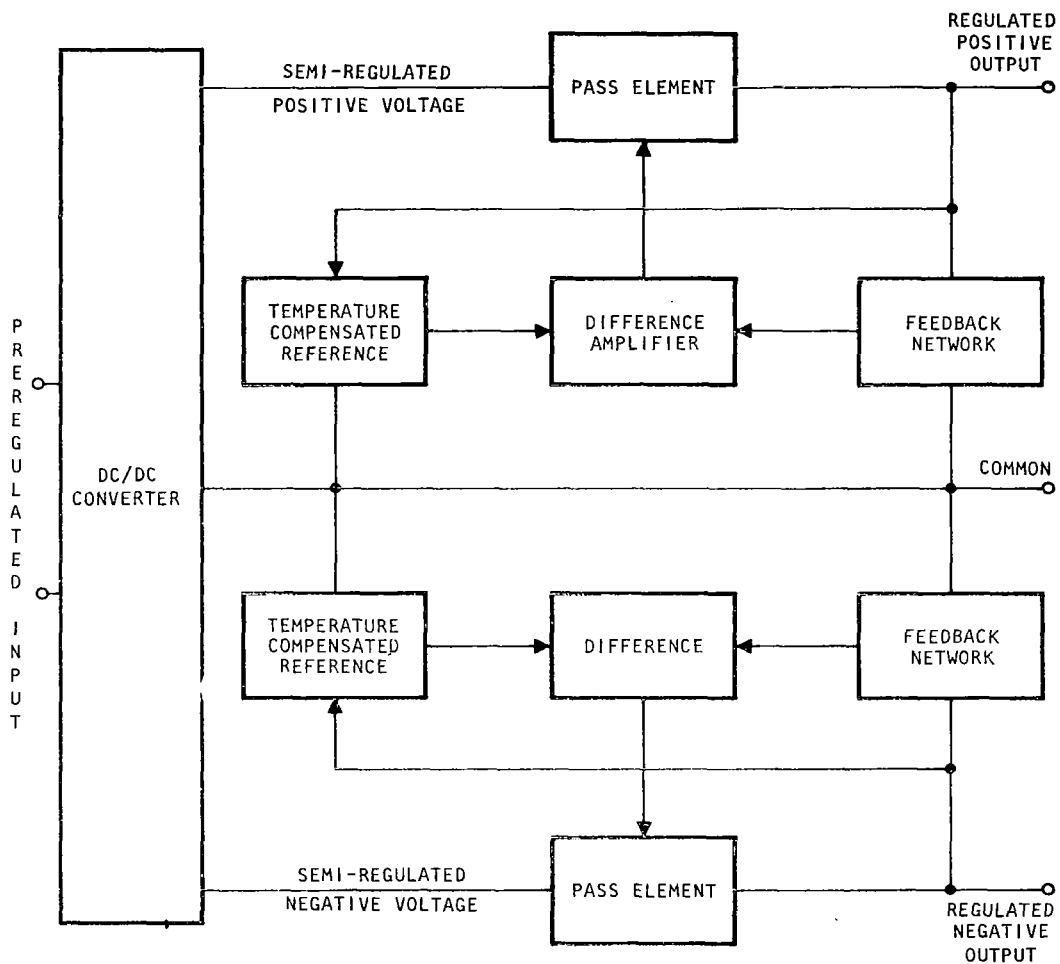
Detectors.- The detectors are solid-state electrometer amplifiers capable of amplifying the minute ion current developed in the analyzer to the required positive output voltage levels.

As shown in Figure 13, Detector Block Diagram, the circuitry is divided into three parts.

The preamplifier utilizes a metal oxide semiconductor field effect transistor (MOSFET) as its input device, to provide the necessary input impedance with adequate circuit performance.

The active filter is a low-pass two-pole type which is used to set the bandwidth to the required value while minimizing output noise. The minimum open loop gain of the combined preamplifier and filter is greater than 1000 so that the closed loop-gain error is less than 0.1%.

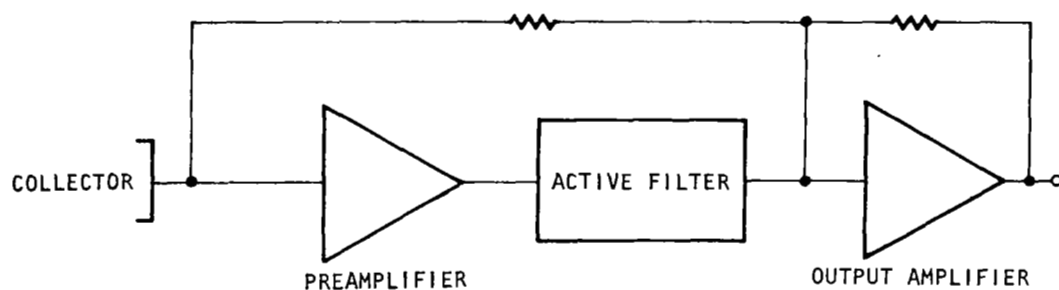
The actual units will use the same block diagram, but the circuitry will change considerably to meet the 1×10^{-15} ampere minimum detectable signal requirement of this sensor. A new MOSFET input device that takes advantage of recent advances in low-noise MOSFET technology should enhance the signal-to-noise ratio of the detectors significantly, while the addition of a temperature-compensation network and a rezero network will reduce the effects of the temperature drift and component aging. The rezero scheme is shown in Figure 14. The ion beam is deflected away from the collectors to place the input at zero. The capacitor C_z is charged to the output voltage which in the electrometer configuration equals the input offset voltage. The capacitor is then momentarily switched to the input, thus counteracting the error voltage and bringing the output to zero. In this way, the effects of various sources of output error are negated.



Precision Power Supply

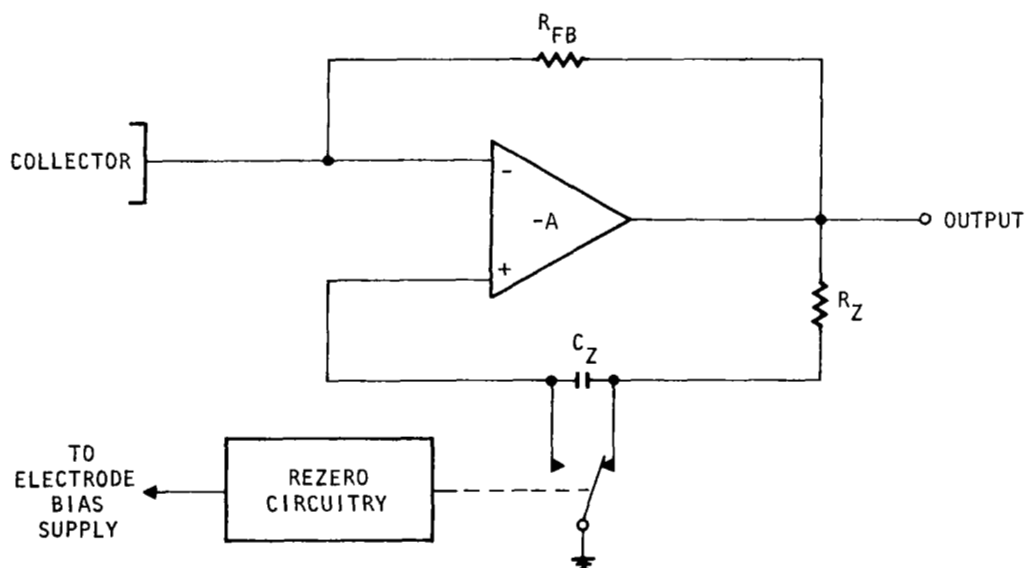
A-120C

FIGURE 12
Precision Power Supply



A-121C

FIGURE 13
Detector Block Diagram



A-290C

FIGURE 14
Detector Rezero Method

Rezero circuitry.- The rezero circuitry block diagram is shown in Figure 15. The rezero circuitry consists of a rezero oscillator and two switching circuits. The oscillator maintains the proper timing relationships during the rezero cycle while one switch causes the ion beam to be deflected and the other controls the rezero function within the detector. The rezero circuitry is powered by the precision power supply.

Ion pump supply.- The ion pump supply, as shown in Figure 16, provides the potential necessary to operate the ion pump cells and consists of a driven multivibrator, a step-up transformer, and a voltage-doubling rectifier circuit. The multivibrator is driven by a signal developed in the Filament Power Regulator so that the switching transients occur simultaneously and can be more easily filtered. The transformer is a high efficiency tape-wound type with a very large step-up turns ratio.

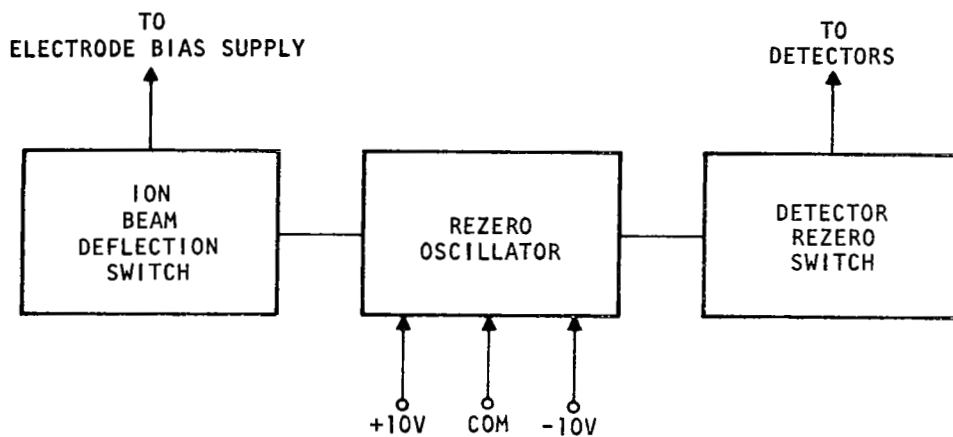
A starting-mode has been added to allow the supply to furnish the high current required for starting while still maintaining reasonable efficiency when running at very low currents.

Accumulator cell electronics.- The accumulator cell electronics consist of the four units shown in Figure 17. The DC/DC converter provides the low voltage required by the constant current source as well as the voltages used by the sequencer. The constant-current source charges the battery at the proper rate and in the proper manner. The valve control circuit applies power to the valving only long enough to cause proper activation, thus conserving power. The sequencer controls the sequence of events required in the operation of the cell.

POWER SUMMARY

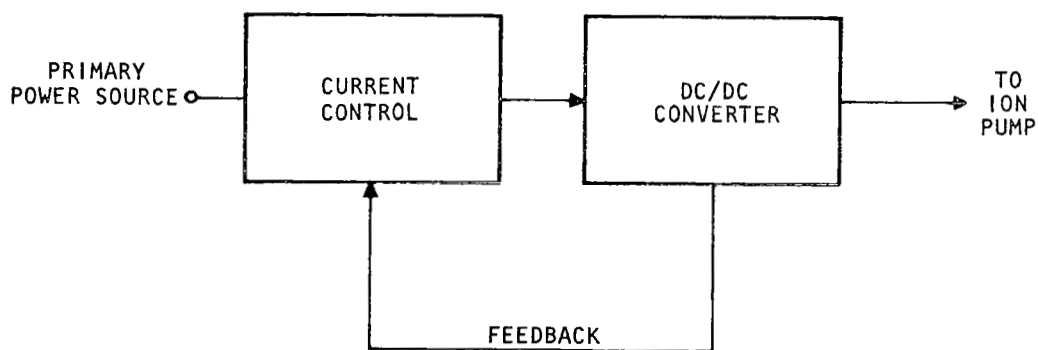
The power figures given below are calculated at nominal source voltage and normal system operation. The figures do not include the power consumed and valving by the accumulator cell, these functions are summarized in the Accumulator Cell and Valves discussion below.

(1) Input Regulator	1.80 W
(2) Filament Emission Regulator (Including Filament Dissipation)	2.60 W
(3) Electrode Bias Supply	0.75 W
(4) Precision Power Supply	0.75 W
(5) Detectors (at 0.15 W each)	1.20 W
(6) Ion Pump Supply	2.00 W



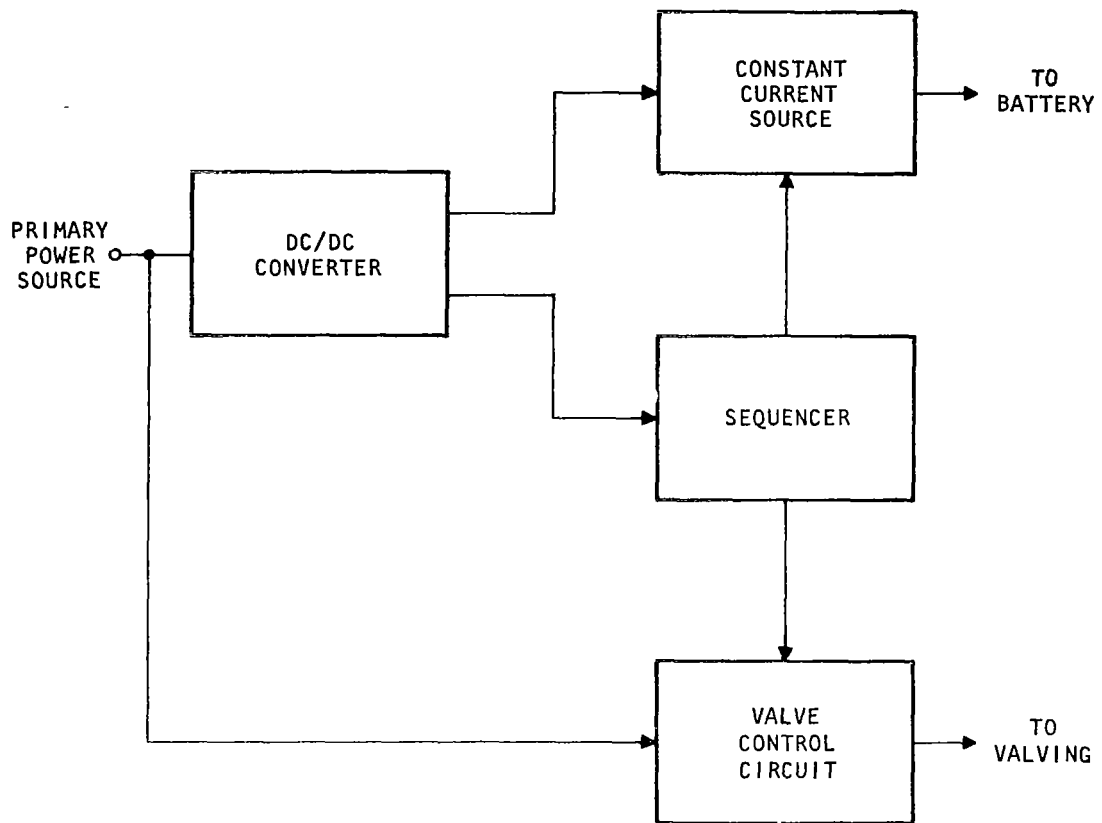
A-291C

FIGURE 15
Rezero Circuitry Block Diagram



A-292C

FIGURE 16
Ion Pump Supply Block Diagram



A-293C

FIGURE 17
Accumulator Cell Electronics Block Diagram

(7) Rezero Circuit	0.5 W
(8) Accumulator Cell Circuit	0.20 W
Total Power	<u>9.80 W</u>

PUMPING

The Atmospheric Sampling System requires a 10^{-7} torr vacuum source of approximately 3 liter/second, for maintenance of operation. During the development of the Two Gas Sensor, venting to outer space through the spacecraft cabin is as investigated. By connecting the Atmospheric Sampling System to outer space through an 18 inch long x 1.125 diameter tube, a pumping speed of 4 liters per second can be maintained. The 18 inch length was assumed to be sufficient to pass through the bulkhead of the spacecraft. The end of the line was to be capped with a break-off hat which would maintain the mass spectrometer in an evacuated condition during pre-launch, launch, and ascent. The break-off hat is ruptured and ejected by the action of a redundant pyrotechnic squib and spring assembly. During ground check-out an auxiliary pumping station would be employed to supply the necessary evacuation.

The vent to outer space would reduce the system weight and power requirements by eliminating the need for a self-contained vacuum apparatus. The tradeoff being that a separate vacuum line through the wall of the capsule would be required. For this application Perkin-Elmer Aerospace Systems is proposing a self-contained vacuum system. Should the pump-out tube approach be acceptable in terms of the spacecraft interface, it could of course be adopted, but no further consideration of this method will be given at this time.

Perkin-Elmer proposes the "sputter" or "getter" ion pump for this application, as this is the only type of pump compatible with space environments capable of pumping inert gases such as helium at a rate sufficient for this application. Briefly, the operation of an ion pump can be described as follows: the ion pump consists of open-ended cylindrical anodes suspended between two cathode plates inside of a vacuum envelope. (Figure 18.) A magnetic field is applied parallel to the axes of the anode cells and a high-positive voltage is applied to the anode cells. This voltage causes a Penning discharge to be established in the cell region. Electrons formed in the discharge are trapped by the magnetic field. Ions formed are accelerated toward the titanium cathodes. The ions strike the cathode surfaces with sufficient momentum to cause sputtering of the titanium. This sputtered material coats the anode and the opposing cathode with clean titanium, gettering active gases such as nitrogen, oxygen, carbon dioxide and water vapor, thereby pumping them.

Inert gas is pumped by burial of the inert gas energetic ions and neutrals with newly sputtered titanium. This process is not as efficient as gettering, producing a lower pumping speed for inert gases than for active gases. Several types of ion pumps are available in which inert gas pumping has been enhanced by various techniques. These include slotting the cathode surface, employing two

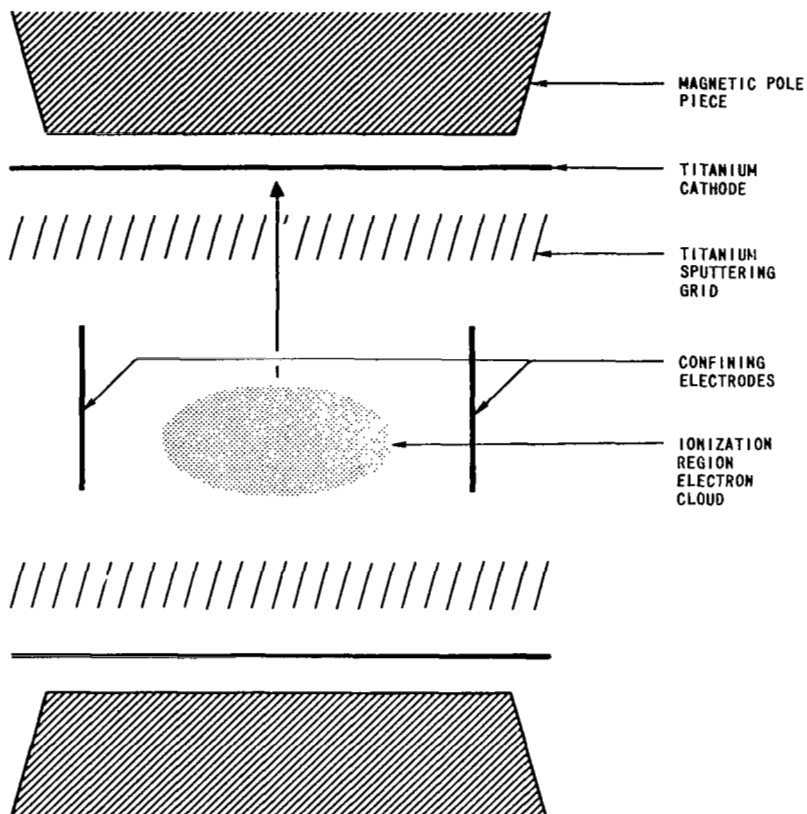
1. AN ELECTRON CLOUD IS SET UP BY A BREAKDOWN OF THE GAS DUE TO THE VOLTAGE BETWEEN THE CONFINING ELECTRODES

2. THE MAGNETIC FIELD, SPUTTERING GRIDS AND CONFINING ELECTRODES CONSTRAIN THE ELECTRON CLOUD.

3. IONS ARE FORMED BY COLLISION WITH THE GAS MOLECULES AND ARE ACCELERATED TOWARD THE SPUTTERING GRIDS.

4. IONS STRIKE THE TITANIUM SPUTTERING GRIDS AND GLANCE OFF TOWARD THE CATHODE EACH GLANCING BLOW DISLODGES SEVERAL TITANIUM MOLECULES WHICH COAT THE CATHODE SURFACE.

5. PUMPING ACTION IS OBTAINED BY BURIAL OF IONS IN CATHODE SURFACE AND GETTERING ACTION OF THE ACTIVE GASES BY THE CLEAN TITANIUM SURFACES.



A-112C

FIGURE 18
Ion Pump

different cathode materials with different sputtering rates, and employing another electrode called a grid or sputter cathode. All of these techniques are aimed at obtaining differential sputtering from one area of the pump to another in order to supply fresh material for burial of inert species. The best inert pumping ion pumps will pump helium at approximately 30% of the speed of air, which is sufficient for this application.

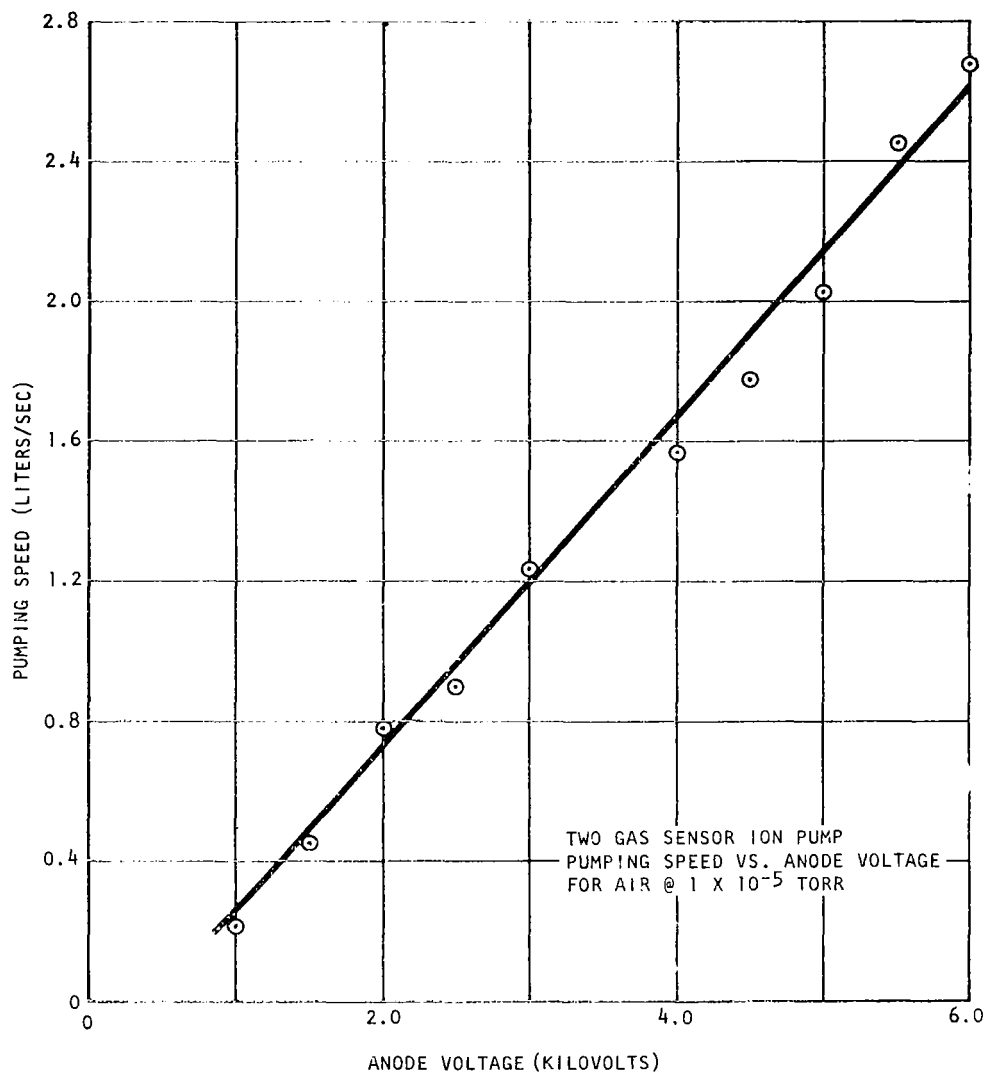
The pumping speed requirements are reviewed in detail in the Analyzer Subsystem Considerations discussion below. Generally, however, an active gas pumping speed of two or three liters per second is required, providing a corresponding speed for helium of a little less than one liter per second. The Two Gas Sensor program included development of a pump essentially having these properties. Two pumping speed curves versus anode voltage for air and oxygen for this ion pump are shown in Figures 19 and 20. With continued development, this ion pump will be capable of achieving the required performance. Helium pumping has not yet been attempted with this ion pump, this not being a requirement under the present effort. Perkin-Elmer Aerospace Systems has investigated a 1 liter/second Differential Sputter Ion Pump manufactured by the Ultek Division of Perkin-Elmer. It demonstrated pumping speeds for helium in the range of 25 to 35% of the speed for air, which is consistent with the manufacturers specifications.

For the CAS System, Perkin-Elmer proposes to modify the ion pump developed during the Two Gas Sensor program by incorporating the differential sputtering configuration employed by Ultek to obtain the necessary helium pumping speed. This conversion can be readily accomplished, requiring only the use of a different cathode material for one cathode. Additional improvements are expected to be incorporated in this ion pump prior to completion of the present program.

Additional areas of interest relative to the operation of the ion pump will be briefly discussed in the following paragraphs. Ion pumps have been in use since 1957 and have attained wide popularity in a short period of time primarily due to the simplicity of their construction which leads to inherent reliability; their cleanliness which avoids difficulties due to oil contamination; their long operating life with trouble-free performance (in excess of 10^4 hours at 1×10^{-6} torr of air and longer at lower pressures); and the low ultimate pressures they can achieve.

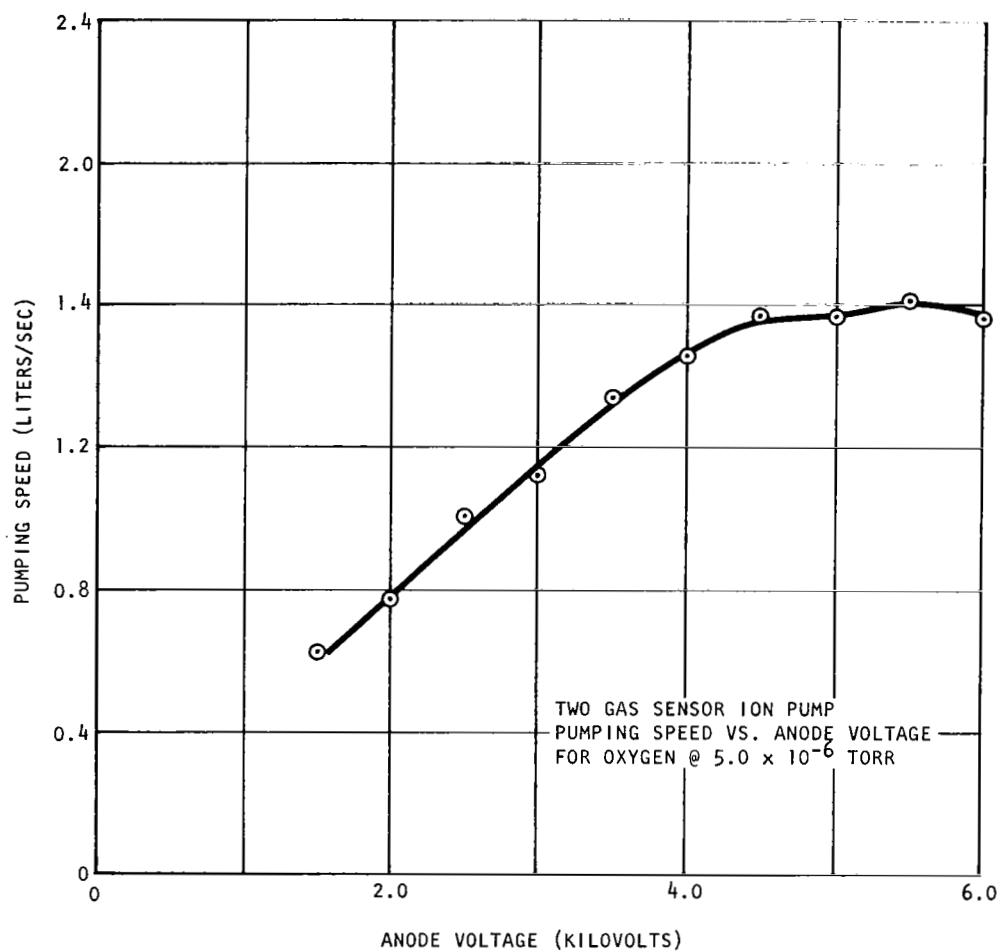
The ion pump is operated from a high voltage DC power supply which for the proposed pump would have a voltage of about 6 Kv. The power required for the pump is proportional to the operating pressure and to the I/p ratio. For commercial ion pumps the I/p ratio is approximately 10 amps/torr for each liter/second of pumping speed for air. Therefore, for a three liter/second ion pump, pumping air at 1×10^{-6} torr, the load power in the pump would be 180 milliwatts which is certainly compatible with the power requirements for the overall system. With an efficiency of 20%, the ion pump power supply would require less than 1 watt.

As described earlier, the pumping requirement for helium presents a special consideration. The pumping speed for helium will vary somewhat more than for the other gases due to the different mechanism by which it is pumped. These effects will be diminished by the differential pressure ratio which exists between the



A-11.3C

FIGURE 19



A-114C

FIGURE 20

ion source and the analyzer as described in the Ion Source discussion below. In the case of helium, the reduction will not be as substantial for two reasons. First, the pumping speed of the pump for helium is lower than for the active gases; and second, the conductance of the ion source for helium is higher due to lower molecular weight (and consequently higher thermal velocity at a given temperature). The combination of these effects reduces the differential pressure ratio for helium to approximately 8. As a result, variations in helium pumping speed or the helium background level in the analyzer region will be diminished by a factor of 8 in the ion source. This will aid in reducing ion source partial pressure variations due to changes in the ion pump; the reduction will be as great as in the case of the active gases and will result in greater reduction of accuracy of the helium measurement through pump-speed variations. During the majority of the operating period, when the controlled atmosphere is being monitored, the pump characteristics should be sufficiently stable that this will not be a significant concern. Furthermore, since the sample flow within the entire mass spectrometer system is molecular and therefore, on a non-interfering basis, variations in the helium partial pressure within the ion source will not affect the partial pressures of the other constituents.

Adjusting the flow of helium into the mass spectrometer is necessary so that the helium partial pressure in the ion pump will be maintained in the range where stability pumping occurs. This level is in the 10^{-6} torr range. The Ultek Division of Perkin-Elmer has been operating one of their differential sputtering ion pumps continuously since 1966 with a helium pressure of 1×10^{-6} torr with no degradation of pumping speed. Therefore, assume that operation at this level can be safely maintained. To allow the sensor to sample the cabin atmosphere under all test conditions was found unfeasible with this restriction placed upon the instrument. In particular, those periods during which the cabin will be pressurized to 16 or 20 psia would work a particular hardship upon the ion pump. Since these periods are specified as non-operational for the sensor, exposure of the inlet to environments is felt unnecessary. In this way potential instability in the ion pump due to excessive helium partial pressure will be eliminated. Closure will be accomplished by employing a pulse operated solenoid valve just ahead of the leak. The valve will be actuated by a control circuit sensing the helium channel output of the sensor. When the output goes above a preset level the valve is actuated to the closed position. The valve is re-opened by an external command, supplied when the excessive helium pressure has been reduced. Since the pump can experience higher helium partial pressures for shorter periods of time, commanding the valve open is possible, and if the helium partial pressure is still too high the valve will simply reclose. The closure level for the helium partial pressure has been tentatively set at 2.0 psia, 33% above the nominal on-orbit pressure of 1.5 psia.

When put in operation, the pump is expected to operate continuously through the pre-launch, launch, ascent, and on-orbit periods. In this way, the necessary vacuum will be continuously maintained along with the cleanliness of the internal surfaces. This condition would be interrupted in the case of a power failure. The possibility of a power failure for a period of up to 18 seconds is described in the power system specification. The maximum expected flow rate (for example during sampling air at 14.7 psia) is approximately 2×10^{-3} torr cc/sec. The

where M is the molecular weight of the component under consideration. Note that the conductances which are obtained are easily obtainable by the rough ball leak.

Values for the inlet partial pressures for all constituents were established. In the case of CO₂, CH₄, H₂, and H₂O, estimated values were used. In the case of He and O₂, values given in the oxygen partial pressure analyzer specification were used. For N₂ the value for air at 14.7 psia was selected as the maximum partial pressure. From these partial pressures values for the analyzer partial pressures and sample partial pressure flows were established.

The conductance of the ion source for N₂ was assumed to be 40 cc/sec as in the case of the Two Gas Sensor ion source. Source conductances for the other gases were then computed. With this information, the ion source partial pressures can be calculated from the following flow relation:

$$\frac{P_s}{P_a} = 1 + \frac{S}{C_s}$$

where P_s is the ion source partial pressure. The values which are obtained for both the ion source and analyzer partial pressures are lower than the design values which were utilized for the Two Gas Sensor. This has three significant results. First, the ion source will suffer no noticeable effects due to ion space charge, therefore, good linearity will be achieved. Second, the analyzer partial pressure for oxygen is at such a low level that the necessary filament life is assured. Therefore, the possibility exists that the redundant filament and electron gun assembly can be eliminated thereby giving a lower ion source conductance, and increased differential pumping. This possibility will be given careful consideration. Third, the ion source output currents are reduced somewhat from the design levels for the Two Gas Sensor thereby requiring amplification of the electrometer output signals.

The values for P_s/P_a are also tabulated along with a set of reduction coefficients, K. These coefficients are nothing more than the inverse of the differential pressure ratio and represent the reduction of pressure effects in the analyzer when they are observed in the ion source. In equation form:

$$\frac{dP_s}{P_s} = -K \frac{ds}{S}$$

and

$$\frac{dP_s}{P_s} = K \frac{dQ}{Q}$$

where

$$dP_s/P_s = \text{Fractional change in source pressure}$$

$$ds/S = \text{Fractional change in pumping speed}$$

dQ/Q = Fractional outgassing flow in the pump
and analyzer region relative to the sample
inlet flow.

From the tabulated values note that if ds/S and dQ/Q are of moderate proportions, the effects in the ion source will be negligible. In the case of helium, K is somewhat smaller and the accuracy of the helium measurement could be reduced.

An ion source sensitivity for the Atmospheric Sensor of 1.5×10^{-6} amps/torr for nitrogen was assumed based upon the performance of the Two Gas Sensor. Sensitivities for the other constituents were computed based upon relative sensitivity data given by the American Petroleum Institute and considered to be representative of the proposed ion source. Some flexibility should be noted in these source sensitivity figures since the ionizing electron beam current level is adjustable. Higher levels can be used, if necessary, in view of the lower ion source pressure and the lower oxygen partial pressure in the vicinity of the filament. From the values for ion source partial pressure and ion source sensitivity, ion source output currents were computed using the relation:

$$I^+ = S P_s$$

where

$$I^+ = \text{Ion source output current (amps)}$$

$$S = \text{Ion source sensitivity (amps/torr)}$$

Values for the electrometer amplifier feedback resistor were then selected to give output voltages at a reasonable level. A maximum resistor value of 5×10^{12} ohms was used to keep the electrometer impedances at a safe level and avoid leakage effects.

Two analyzer subsystem tables were made to provide an idea of the problems to be overcome. In Table 3 the standard inlet conductance of 2.75×10^{-6} cc/sec for nitrogen was used. This conductance leads to an analyzer or pump pressure of 1.93×10^{-6} torr for helium. This pressure is too high for the 3 liter pump to handle. The pump is capable of handling a helium partial pressure of less than 1×10^{-6} torr. Lowering the helium source pressure to 1×10^{-6} requires a 6 liter/sec pump, or a reduction in the inlet leak conductance. In Table 5, the leak conductance is cut in half. Notice that the ion currents are also cut in half.

Signals from the CO and CH₄ detectors drop to 0.45×10^{-2} volts and 0.124 volts respectively. The voltages are not impossible to work with because an accumulator cell is proposed for the CO measurement and the CH₄ reading is still several times above the noise level of about 10 millivolts. If the method of reducing the inlet leak conductance is not acceptable, work must be initiated in producing a larger ion pump.

TABLE 5.- ANALYZER SUBSYSTEM

COMP	Sample PRESS. (Torr)	Inlet Leak Conductance (cc/sec)	Source Conductance (cc/sec)	Pumping Speed (cc/sec)	Sample Flow (Torr- cc/sec)	Analyzer PRESS. (Torr)	Ion Source PRESS. (Torr)	DIFF PRESS. Ratios	RED. COFF	Ion Source Sensitivity (Amps/Torr)	Ion CUR. (Amps)	Electrometer Resistor (Ohms)	Electrometer Output Voltage (max.)	Post Amp Gain	Signal Noise = 1×10^{-15} Amps	Lower Detectable Limit for Signal/Noise=1
	P _o max. Num.	C _o	C _s	S	Q max.	P _a max.	P _s max.	P _s /P _a	K	S	I+ max.	R	V max.	C		
H ₂	16 UND*	0.52 $\times 10^{-4}$	1.50 $\times 10^2$	5.70 $\times 10^3$	0.83 $\times 10^{-3}$	1.45 $\times 10^{-8}$	5.7 $\times 10^{-7}$	39	2.57 $\times 10^{-2}$	1.2 $\times 10^{-6}$	6.8 $\times 10^{-13}$	5×10^{12}	3.4	3.70	0.68 $\times 10^3$	60.0
H _e	200 180	3.64 $\times 10^{-5}$	1.06 $\times 10^2$	7.50 $\times 10^2$	0.73 $\times 10^{-3}$	0.96 $\times 10^{-6}$	7.2 $\times 10^{-6}$	8.04	1.24 $\times 10^{-1}$	2.89 $\times 10^{-7}$	2.21 $\times 10^{-12}$	2×10^{12}	4.41	1.11	2.21 $\times 10^3$	226.0
H ₂ O	20 UND	1.72 $\times 10^{-6}$	4.99 $\times 10^1$	3.09 $\times 10^3$	3.43 $\times 10^{-5}$	1.15 $\times 10^{-7}$	7.1 $\times 10^{-7}$	61	1.64 $\times 10^{-2}$	1.05 $\times 10^{-6}$	1.20 $\times 10^{-12}$	2×10^{12}	2.4	2.08	1.2 $\times 10^4$	64.6
N ₂	200 180	1.37 $\times 10^{-6}$	4.00 $\times 10^1$	3.0 $\times 10^3$	2.75 $\times 10^{-4}$	0.92 $\times 10^{-7}$	6.9 $\times 10^{-6}$	76	1.32 $\times 10^{-2}$	1.5 $\times 10^{-6}$	1.04 $\times 10^{-11}$	5×10^{11}	5.2	1	1.05 $\times 10^4$	47.6
O ₂	200 180	1.28 $\times 10^{-6}$	3.74 $\times 10^1$	2.10 $\times 10^3$	2.52 $\times 10^{-4}$	1.23 $\times 10^{-7}$	6.87 $\times 10^{-6}$	56.2	1.76 $\times 10^{-2}$	1.13 $\times 10^{-6}$	0.78 $\times 10^{-11}$	5×10^{11}	3.9	1.28	0.78 $\times 10^4$	64.8
CO ₂	20 UND	1.11 $\times 10^{-6}$	3.20 $\times 10^1$	3.0 $\times 10^3$	2.21 $\times 10^{-5}$	7.3 $\times 10^{-9}$	7.0 $\times 10^{-7}$	95	1.05 $\times 10^{-2}$	1.65 $\times 10^{-6}$	1.16 $\times 10^{-12}$	5×10^{12}	5.80	1	1.16 $\times 10^3$	54.2
CH ₄	.36 ---	1.82 $\times 10^{-5}$	5.28 $\times 10^1$	3.0 $\times 10^3$	0.65 $\times 10^{-5}$	3.4 $\times 10^{-10}$	1.89 $\times 10^{-8}$	58	1.70 $\times 10^{-2}$	1.32 $\times 10^{-6}$	2.48 $\times 10^{-14}$	5×10^{12}	1.24 $\times 10^{-1}$	41	2.48 $\times 10$	80.0

*UND = UNDETERMINED

SAMPLE INLET

The mass spectrometer system requires a high operational internal vacuum, at least 2×10^{-4} torr, and must provide means for admitting the gas to be sampled to that vacuum from atmospheres 10 orders of magnitude higher in pressure. This is the function of the sample inlet system. The required pressure reduction must be accomplished without distorting the sample and must cause the internal pressure to vary linearly with the external pressure.

In conventional mass spectrometry this is accomplished by one of two standard methods. The first is the expansion volume technique in which a portion of sample is expanded to a lower pressure which is then suitable for sampling by a molecular leak. The conductance of a molecular leak is independent of total sample pressure, flow through the leak at a rate determined by their differential partial pressures. Molecular flow is obtained when the mean free path of the gas on the high side of the leak is greater than the leak diameter by approximately a factor of three. The expansion volume technique is not continuous in nature and therefore, other methods must be used.

The viscous flow pressure divider is commonly employed and is the technique used for sampling on the Two Gas Sensor. With this method the sample passes through a long tubular channel in which there is viscous flow. The diameter of the channel is much larger than the mean free path of the gas and results in a flow mechanism in which the flow rate is not directly proportional to the pressure difference, and each partial pressure has an effect upon the bulk flow. At an appropriate point on the line, where the pressure is sufficiently reduced, the sample is exposed to a molecular leak. This approach has the feature that the capillary line length allows the sampling point to be well removed from the mass spectrometer, while providing its own sample transport technique. This method also requires a pumping media at the end of the viscous line. While the flow through the line is small in terms of the quantity of gas consumed (less than 0.5 pounds in 120 days), flow is significant in terms of pump capacity. A mechanical rough pump or cryogenic sorption pump is generally employed. For an application such as MOL, the possibility exists that the necessary pumping mechanism can be obtained by venting the end of the capillary line to outer space. This would require access to a vacuum line with a pressure of about 10 microns and a large conductance. Also worth noting is that the sample transport times obtainable with a viscous flow sample inlet system are compatible with the time response requirements for this instrument.

Logic dictates seeking a technique by which the sample can be continuously and directly admitted to the mass spectrometer without resorting to auxiliary pumping mechanisms. A direct sampling system must be accomplished by the use of a direct molecular leak since the linear relationship between sample and ion source pressures must be maintained. The basic requirement is for a leak with cross-sectional dimensions less than the mean free path of the gas in the sample environment. For oxygen at 3.5 psia, this corresponds roughly to 2.8×10^{-4} mm. Since linear flow is maintained well into the transition region, dimensional requirements for the leak are somewhat larger than given above.

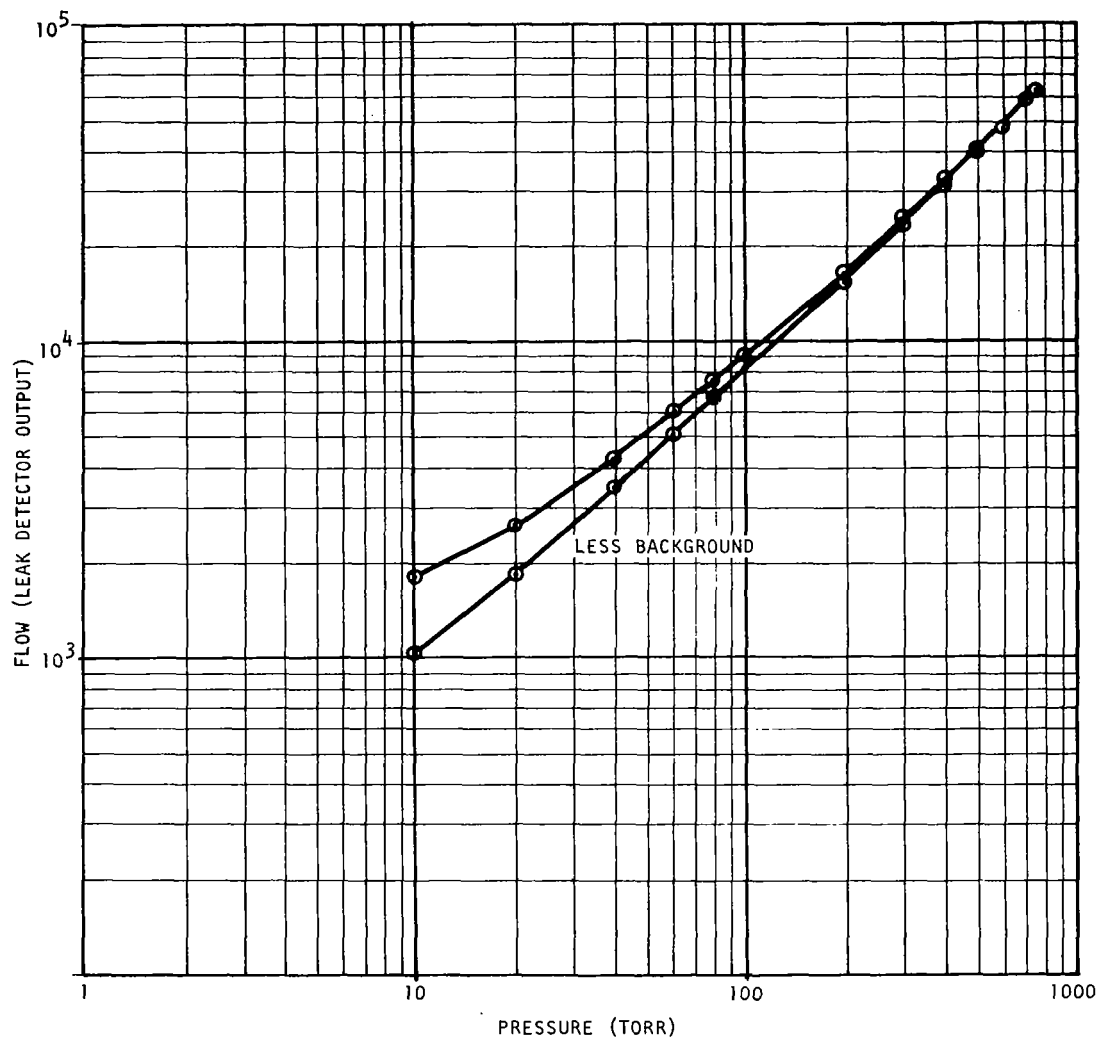
Perkin-Elmer Aerospace Systems has studied several techniques for manufacturing molecular leaks which will perform at normal ambient pressures. A type known as a rough ball leak is currently under investigation. Basically, this leak is obtained by pressing a rough stainless steel ball against a circular knife edge seat. By adjusting the pressure on the ball leak, the conductance can be varied over a wide range. A performance curve for an early version of this leak is shown in Figure 21. The leak is presently undergoing evaluation, after some design refinements, intended to improve adjustability and temperature characteristics. The rough ball leak will give controlled conductance in the 10^{-7} cc/sec region; more than a decade less than the value required for this application. This margin should aid in assuming stable operation at the expected conductance levels. A cross-section drawing of the ball leak assembly is shown in Figure 22.

One of the important aspects of sample introduction is maintaining a constant inlet leak conductance against possible contamination effects. This can only be accomplished with the aid of appropriate filtering. Due to the small dimensions of the leak, a filter having correspondingly small dimensions is necessary to prevent admission of particles capable of plugging or otherwise changing the conductance of the leak. The existing ball leak now under test employs a sintered stainless steel filter with a 0.5 micron-mean pore diameter. Sintered silver filters are available with mean pore diameters down to 0.2 micron. Furthermore, due to the large length to diameter ratios (250 for the sintered silver type), they can reliably stop particles of smaller size than the mean diameter. The metal filters are preferable since they can be permanently mounted to the leak assembly and can survive decontamination bakeout temperatures. Finer cellulose ester filters are available and could be used if necessary.

The rough ball leak will be undergoing continued investigation and development during the months ahead and should achieve reliable flight status over this period of time. Therefore, this device is proposed to be employed as the direct sample inlet technique for the CAS System.

ACCUMULATOR CELL AND VALVES

The components required for carbon monoxide determination are an accumulator cell, a prescrubber cell, three two-way switching valves, a valve actuator, and the necessary power supplies for the cell heaters and valve actuator. The accumulator and prescrubber cell will be made from thin Nichrome V tubing (1/8" O.D. mil wall). Tentatively assume that a tube six inches in length will be adequate to retain carbon monoxide under the anticipated operating conditions. The exterior surface of the tube will be insulated to minimize power requirements during heating. The ends of the tube will be isolated from the switching valve and ball leak with ceramic washers. Sorbents will be retained in the tube with small plugs of glass wool. A tube section is shown in Figure 23.



A-110A

FIGURE 21
Performance Curve (Leak)

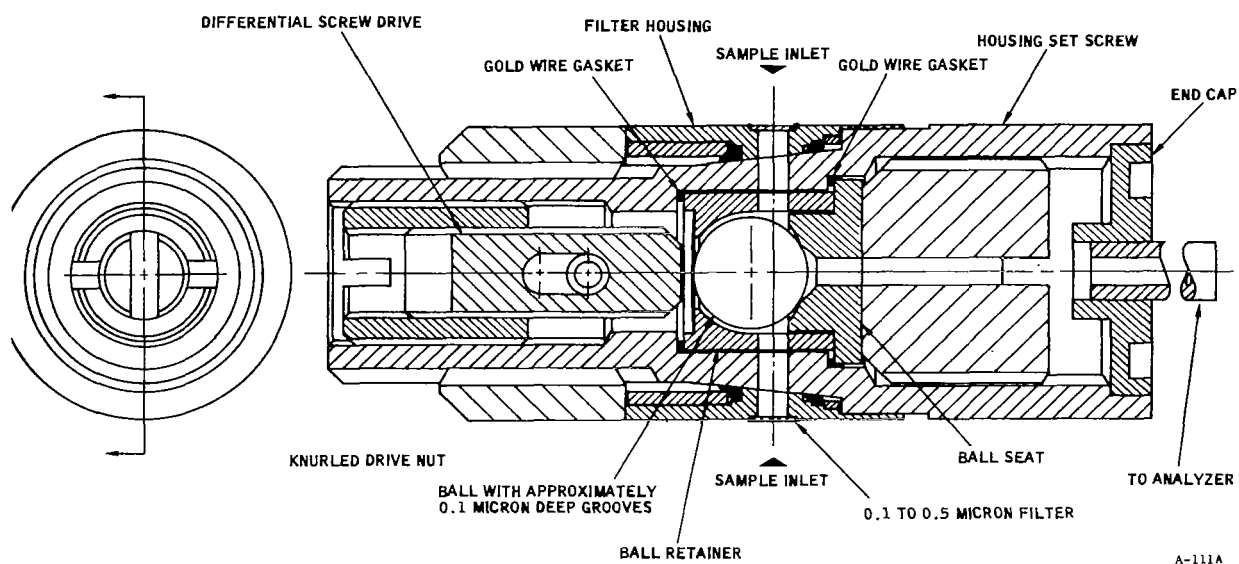


FIGURE 22
Ball Leak Assembly

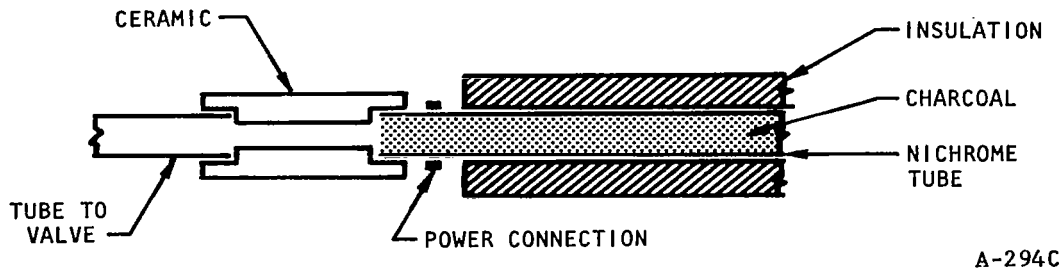


FIGURE 23
Tube Section

Three four-way switching valves provide the necessary plumbing to permit sampling and desorption of carbon monoxide. These valves are ganged on a single shaft so that all three are actuated simultaneously. The flow pattern schematic is shown in Figure 24.

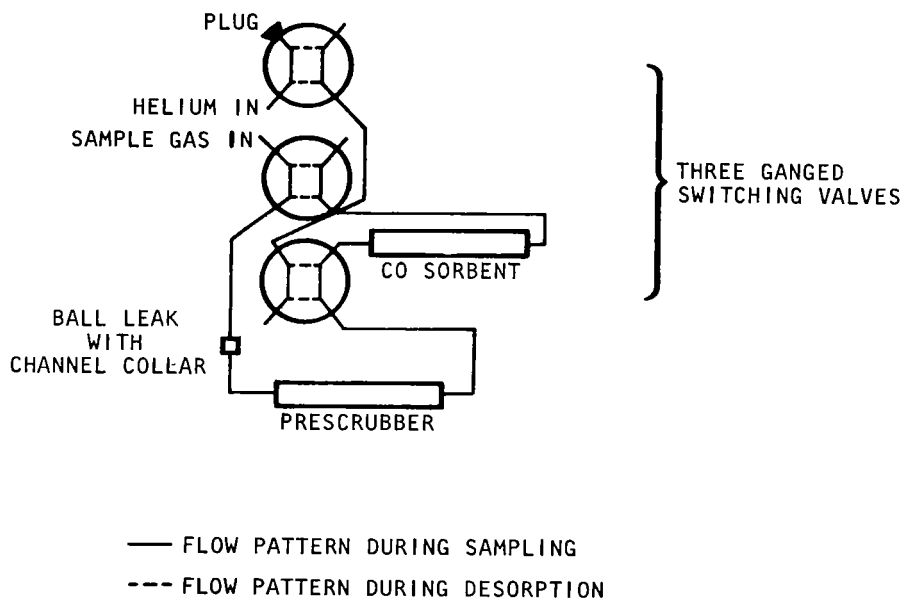


FIGURE 24
Flow Pattern Schematic

Suitable commercially-available valves of this type are made of stainless steel with teflon compound sealing surfaces. These are typically operated under considerable tension to maintain leak-free performance under a large pressure differential. Since only low pressure gradients are encountered in this application, less tension to retain the valve seals may be possible. Also, the use of lighter-weight materials for the valve may be considered.

Valve positions will be changed with a solenoid device designed for this purpose. A latching mechanism will be employed to minimize power consumption.

Heater power will be supplied by nickel cadmium cells which will be trickle charged from the main 28Vdc power supply through a DC/DC converter.

A mechanical timing device will be employed to control the sequence of operations which includes switching the valve to helium purge position, turning the heater on, and switching the valve back to the sampling position.

The ball leak will be provided with a disc-type collar through which the gas sample flows. A small pump will be used to pump the atmospheric gas sample through the valves and the sorbent cells.

The helium supply will be contained in a stainless steel pressure vessel. A pressure reducing diaphragm regulator will be used to maintain constant delivery pressure. The flow rate will be controlled by a capillary restriction in the line.

ION SOURCE

The ion source of a mass spectrometer performs the following functions:

- (1) Receives sample gas from the sample inlet system
- (2) Provides a means for ionizing the sample.
- (3) Accelerates and focuses the resulting ions into a beam which is then projected toward the magnetic sector where a portion of the beam passes through the object slit and enters the resolving region.

In performing these functions the ion source must meet several important criteria:

- (1) The output ion current from the source must vary linearly with the pressure in the ion source.
- (2) The intensity of ion current coming from the ion source must be sufficient to achieve the desired detection levels for the various constituents.
- (3) The divergence, energy, and energy spread of the ion beam must be compatible with the requirements of the magnetic sector to achieve the necessary resolving power.

- (4) The ion source must maintain the above characteristics consistently and reliable for the required period of operation.

The proposed ion source is essentially the same one as is used in the present Two Gas Sensor System. The source is a dual filament, electron bombardment, nonmagnetic type. This type of source was selected for several reasons.

The electron bombardment type of ion source employing a thermionic emitter electron source is the most conventional, well understood, and most sensitive type of ion source and was selected early in the Two Gas Sensor development program as most likely to result in successful flight instrumentation. The available reliability data on thermionic emitters, operating under the projected flight environments, caused Aerospace Systems to choose the dual filaments approach for redundancy. Since that time more data on filaments have been gathered, and there may be justification for ultimately reverting to a single filament source, if this would be advantageous.

Test filaments have been operated for 4,680 hours without failure. A new tungsten-rhenium alloy (97% W - 3% Re) has demonstrated superior properties with respect to increasing filament resistance with age and has been incorporated into the current design. Modifications in the sample inlet and pumping system will lead to reduced pressures in the analyzer, greatly increasing filament life. In tests on 3 mil diameter (which is the size currently used) tungsten-rhenium alloy filament performed at lower pressures, the filament operated for 4,000 hours with very slight changes in the characteristics. There is therefore every reason to believe that additional tests will demonstrate the reliability of the filament sufficiently to allow elimination of redundancy. At that time the modification could be readily made. The chief advantage of eliminating one of the filaments is the elimination of the electron beam entrance aperture, thereby lowering the ion source conductance. The advantages of a lower ion source conductance are discussed later in this section.

Establishment of the dual filament approach led to a particular configuration for the ion source. The most feasible arrangement determined for the filaments was to place them in separate electron guns and mount them at right angles to each other with the electron beams entering a common ionizing region, leading to a requirement that the ion source be nonmagnetic. In the nonmagnetic ion source the electron beam is focused entirely by electrostatic fields, providing a distinct advantage by eliminating mass discrimination which would result from a magnetic field existing in the ion source. This factor becomes important in this type of instrument where simultaneous monitoring of heavy and light constituents is contemplated. The nonmagnetic feature is important because hydrogen is to be measured.

The operating characteristics of the ion source have been demonstrated in repeated testing. The sensitivity of the source is between 1 and 1.5×10^{-6} amps/torr. This is a factor of 2 to 3 greater than the original design value and allows considerable flexibility in adapting the system to various applications. The linearity of the ion source output with pressure has also been established. A typical linearity run is shown in Figure 25. In order to maintain linearity, maintaining the source pressure below approximately 2×10^{-4} torr is essential, thereby avoiding effects due to ion space charge.

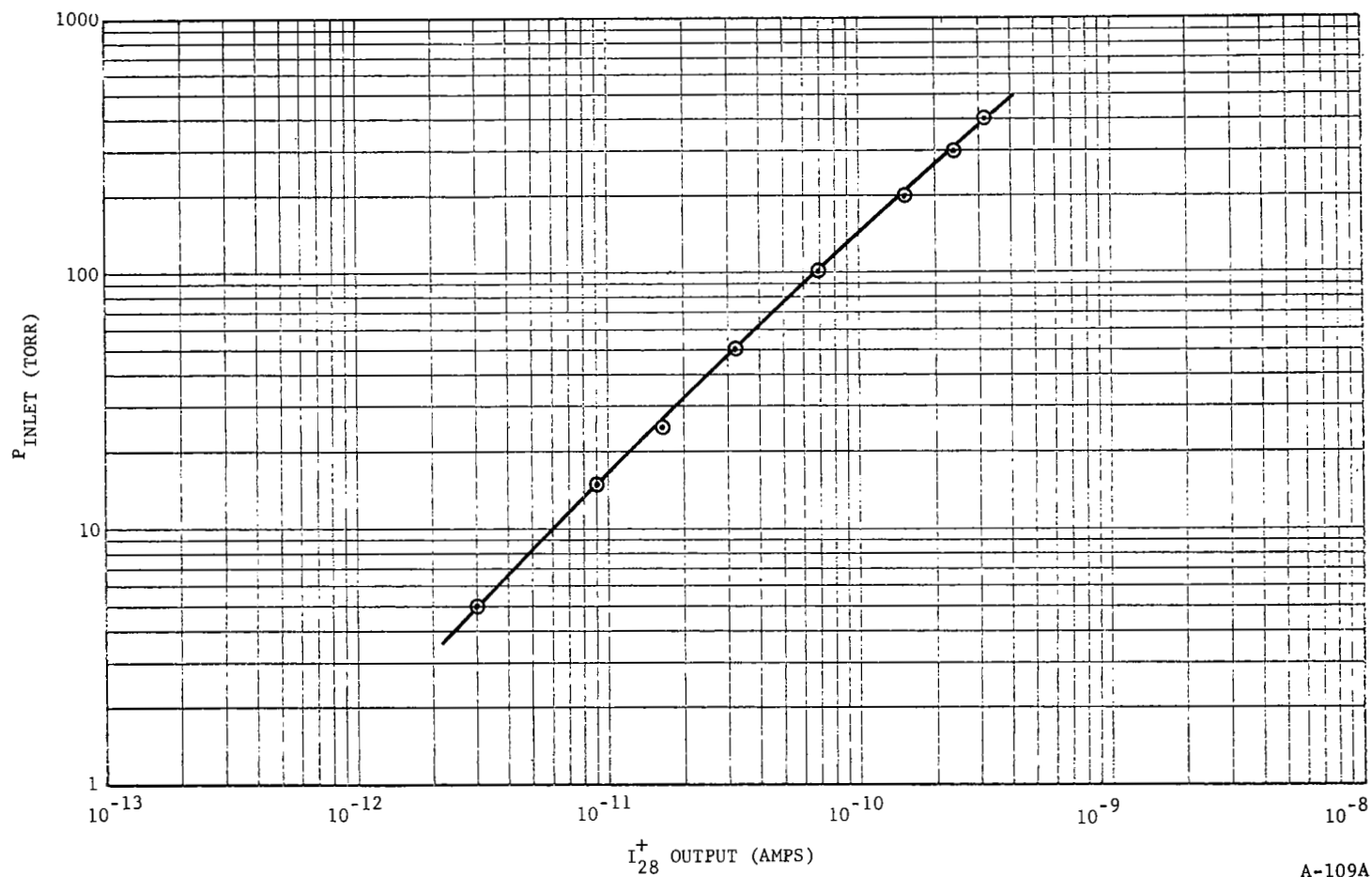


FIGURE 25
Typical Linearity Run

A-109A

For the proposed application the source pressure will be maintained well below 2×10^{-4} torr by the inclusion of an ion pump. The compatibility of the source with the magnetic sector in terms of beam divergence and ion energy spread is verified by the resolution, obtained as demonstrated in the preceding section,

The reliability and stability of the ion source have been demonstrated over many hours of testing. This testing has included the functional testing of nine ion sources at Perkin-Elmer Aerospace Systems, calibration testing of a mass spectrometer for the OGO-F satellite at the Space Physics Laboratory of the University of Michigan, and the 60-day space cabin simulator test at McDonnell Douglas Aircraft Company.

In examining an ion source, it is possible to identify several potential failure modes. During the design of this ion source each of these was carefully examined and steps were taken to prevent their occurrence. Surface charge up has been eliminated as a source of instability by combination of efforts which chiefly occurs at surfaces under electron bombardment, for example, through reducing the number of surfaces receiving electron bombardment to a minimum proper focusing of the electron beam. The anode surface receiving the controlling ionizing current was located outside of the ionizing region where positional stability of the electron beam is required. Contamination would also be suspect. Careful preparation and cleaning of all ion source surfaces assures that they will be free of contaminating materials. The 60-day test at McDonnell Douglas demonstrated that contamination from the sample gas itself is not a source of concern. The anode surface on the electron gun which was operated for over 30 days showed no visible contamination.

Another important factor in the design is the positional stability of the electron beam. Studies of this area have been conducted in which the position of the filament was viewed during operation. That the filament moves initially after turn on was noted but no further motion occurs. An electron gun has been operated continuously and with cycled operation for a period in excess of one year and demonstrated consistent operation. Regulation of only that part of the emission current reaching the anode allows slight fluctuations in the source characteristics without affecting stability. The net results of these factors is an ion source with extremely stable characteristics.

Another area which has been given careful attention is the possibility of shorts occurring between the ion source electrodes. Maximum clearances were designed between all electrodes. Rigid cleaning procedures and the use of nonmagnetic electrodes eliminate the possibility of contamination causing shorts. All parts are deburred and electropolished and carefully inspected. Through these precautions no shorts have occurred during testing of the nine ion sources.

These factors are mentioned primarily as a demonstration of the thorough design, test and process control implemented to develop the mass spectrometer from a laboratory instrument into a reliable system for manned space flight applications.

An important feature of the ion source design is limited conductance to the rest of the analyzer. This causes a pressure difference to exist between the ion source and the rest of the analyzer. This differential pressure ratio is important in achieving analytical accuracy for the instrument since the ratio reduces effects of sample interaction at the filament and variations in the pumping speed of the pump system. The ion source has a conductance for air of approximately 40 cc/sec which will give a differential pressure ratio of 50 with a 2 liter/sec pumping system. With this pressure ratio any variations as mentioned above will be reduced by 50:1 so that they will not be significant in determining the accuracy of the instrument.

MECHANICAL DESIGN AND PACKAGING

The following paragraphs describe the proposed approach to the packaging of the analytical system. The envelope of the system is shown in Figure 26. A preliminary weight analysis indicates a total weight not to exceed 15 pounds plus less than 4 pounds for the accumulator subsystem. A weight program will be initiated at the beginning of the program and maintained for the duration of the contract in order to attain minimum system weight.

A structural and dynamic analysis will be performed to assure positive margins of safety and also to indicate areas for weight reduction where margins of safety are more than required.

System package.- An exploded view of the package is presented in Figure 27. The enclosure is an aluminum casting with mounting blocks, flanges, and standoffs to mount the analyzer, magnet structure, ion pump, and electronics modules. Attachment of the electronics modules to the casting minimizes the internal thermal resistance of the mounting surface.

A cover plate is mounted to the enclosure casting and moisture sealed by a gasket. Reinforcing braces and stiffeners are added to the enclosure. Mounting feet or pads are provided on the outside walls of the enclosure. The location of the sample inlet ports and controls are optional.

The heaviest components, such as the magnet and the ion pump, are rigidly mounted to the enclosure in the center of gravity plane and close to the mounting feet to minimize vibration and shock sensitivity.

Inlet leak assembly and mounting.- A typical Perkin-Elmer inlet leak is shown in Figure 28. The inlet leak consists of a ball retainer assembly, differential drive screw arrangement, filter assembly, housing, and connecting tube. The ball, in the ball retainer assembly, is held against the knife edge of the seat by the spring tension of a diaphragm, which is welded to the retainer. This assembly is secured in the housing by a special set screw and sealed by a gold gasket. The differential screw arrangement is designed for minimum longitudinal travel to turn ratio, providing adjustment for a specific molecular flow. The filter assembly provides a filtering capability of 0.1 to 0.5 micron particle size.

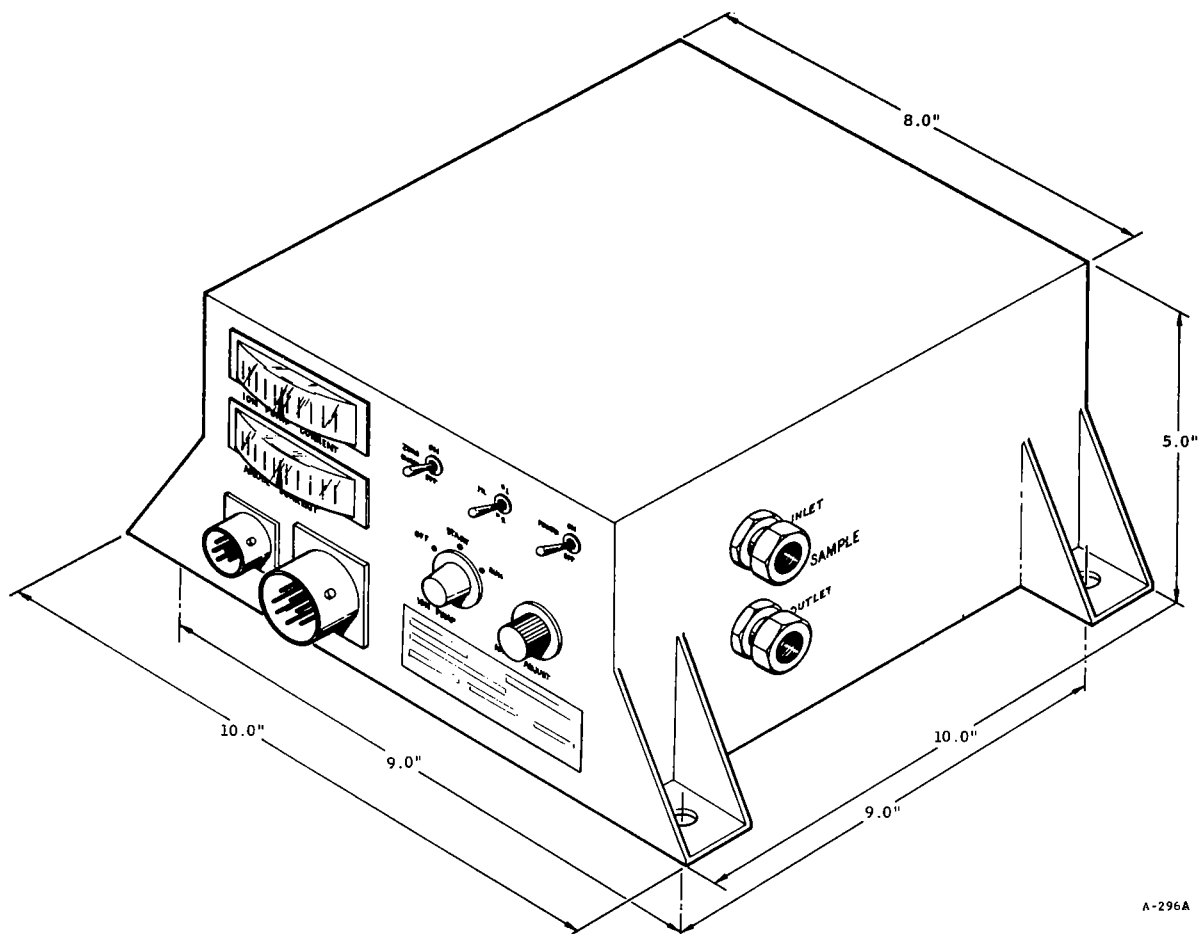
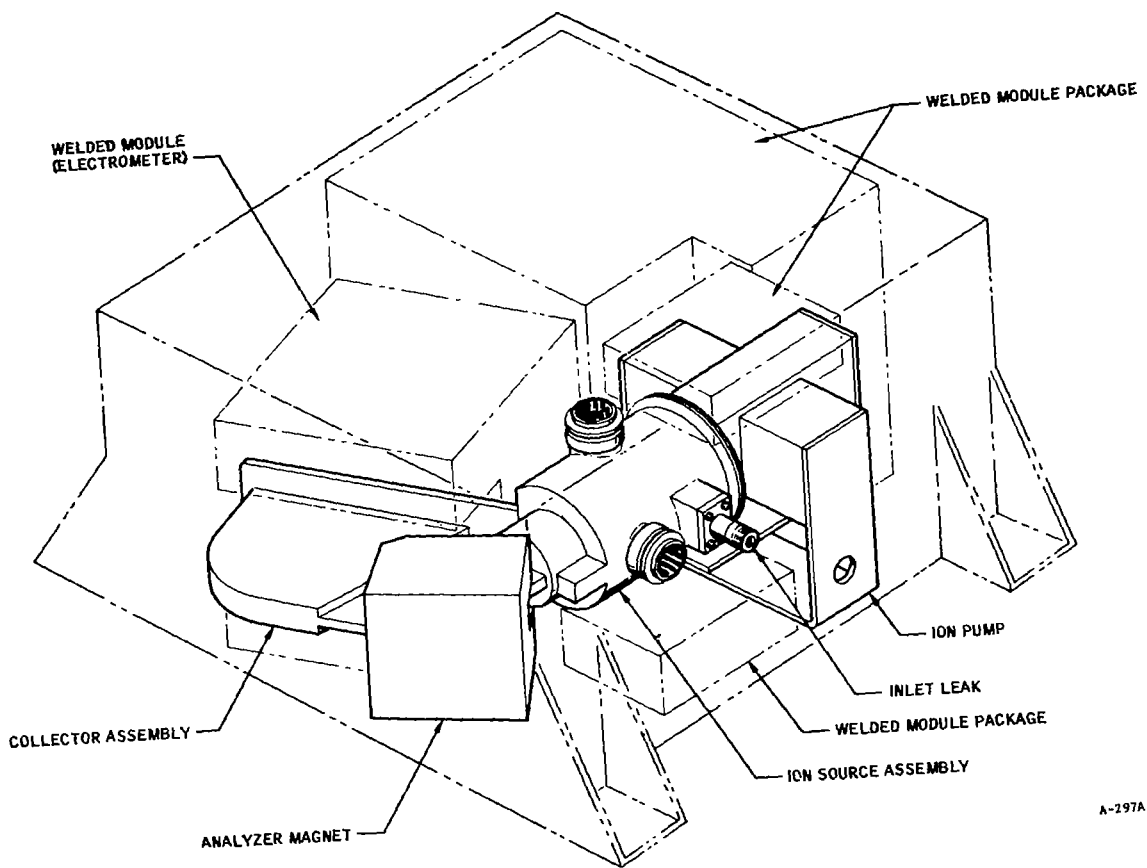


FIGURE 26
Analytical System Envelope Packaging



A-297A

FIGURE 27
Contaminant Atmospheric Sensor Analyzer Assembly
(Sheet 1 of 2)

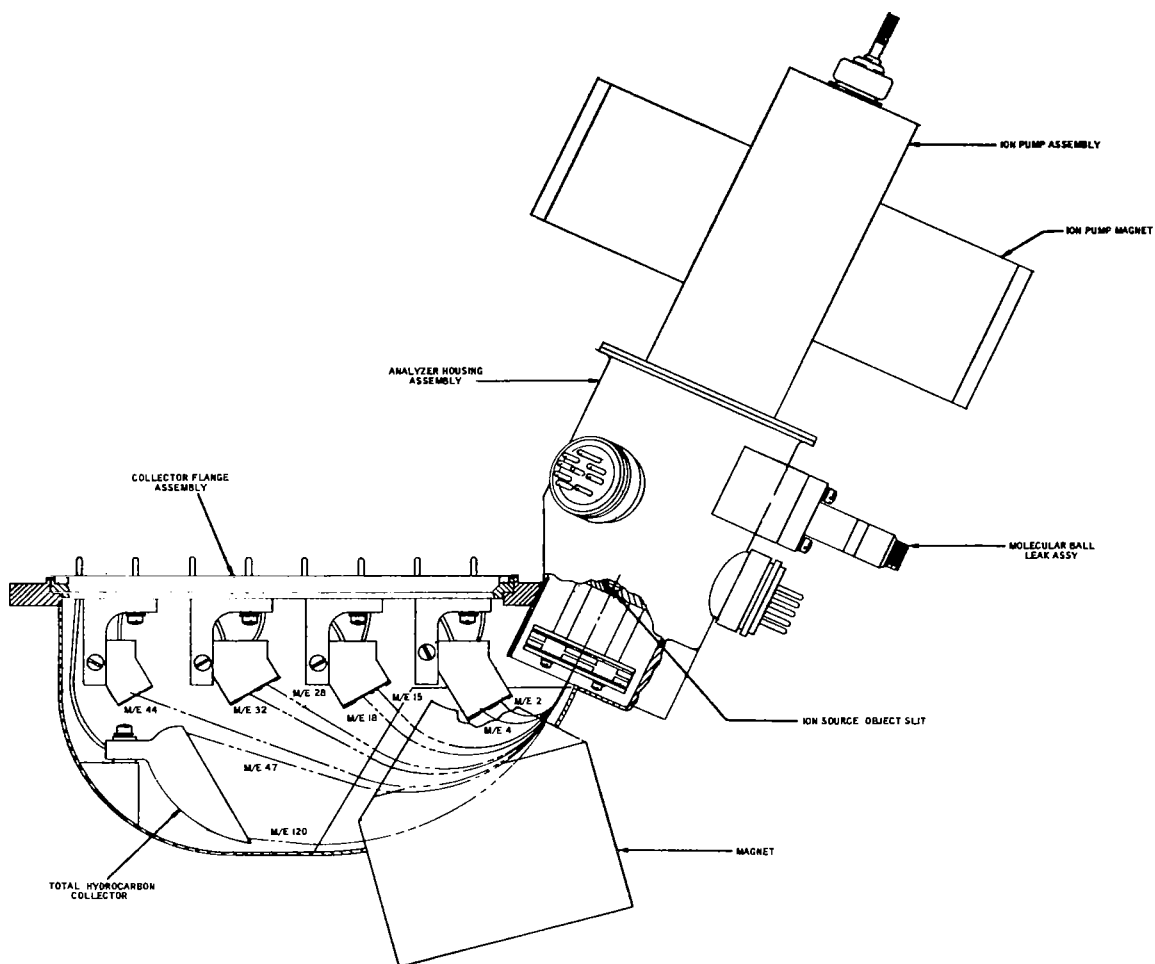


FIGURE 27
 Contaminant Atmospheric Sensor Analyzer Assembly
 (Sheet 2 of 2)

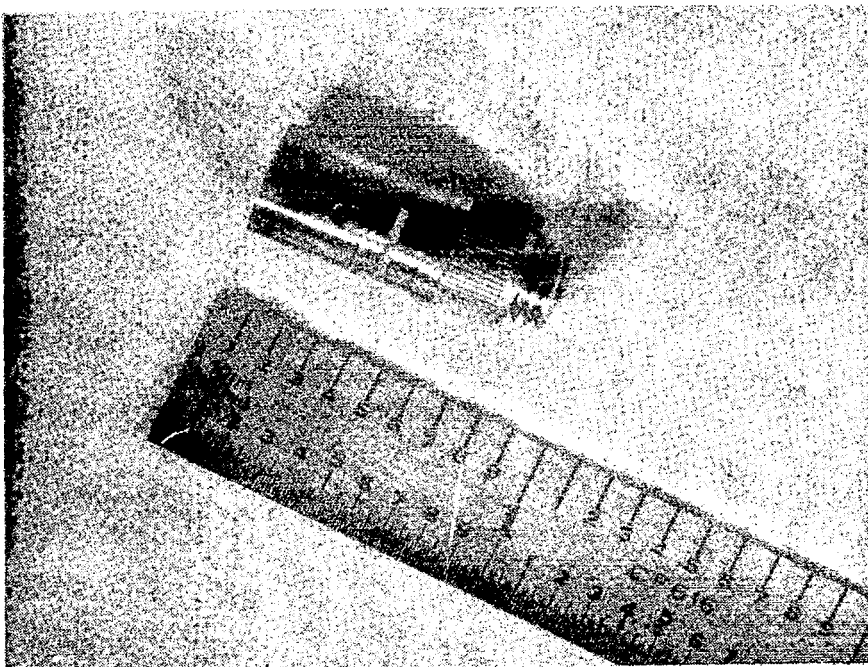


FIGURE 28
Typical Inlet Leak

Sample inlet lines are welded into the leak housing and connected to the system enclosure inlet ports. The ports can be connected to an accumulator subsystem. The leak is mounted to an analyzer mounting boss and sealed by a gold gasket.

Ion source assembly.- The ion source is shown in Figure 29 . An exploded view of the ion source is presented in Figure 30 . The ion source proposed has been used successfully in an instrument for NASA/Langley Research Center under contract NAS 1-6387. The design permits the ion source to be completely assembled and then aligned under a traveling microscope before installation in the analyzer housing. All of the ion source parts are gold plated to minimize secondary emission and surface interaction problems. The construction embodies locating counterbores throughout to obtain location of the electron guns, and the ion focusing system. The filaments are tungsten-rhenium alloy wire mounted on filament posts and spring tensioned with a thin strip of similar ribbon material. Tensioning is required to hold the filaments in position because of thermal expansion during operation. The z-axis focus assembly is a split assembly which will allow the ion beam to be deflected in the event of misalignment.

Analyzer envelope and interfaces.- An exploded view of an analyzer, developed for NASA/Langley Research Center, is shown in Figure 31.

The analyzer housing provides a vacuum-tight chamber, housing the ion source and collector assemblies and provides an interface with the inlet system. The housing consists of a cylindrical ion source housing and a flat-sided curved section housing the collector assembly. They are joined by inert arc welding. The housing material is 304 stainless steel which has good vacuum properties, is nonmagnetic, and is weldable. Elimination of heavy flanges in the envelope is accomplished by welding the entire final assembly after test, which improves the reliability by omitting gasket seals and decreases the weight. The ion pump is welded to the end-of-the-source housing. The entire housing, when sealed, is bakeable to over 300°C in order to outgas the internal surfaces.

Voltages are introduced to the ion source by the use of three nine pin feedthroughs. Single pin headers are provided to bring the collected ion currents out to the electrometers.

Analyzer magnet and support structure.- The analyzer magnet is a five piece assembly consisting of two Armco iron pole pieces, two Alnico V magnet arms, and an Armco iron yoke. The magnet assembly is supported by a bracket, which is attached to the enclosure at the approximate center of gravity plane.

Collector assembly.- A typical collector flange assembly is shown in Figure 32. The collector assembly consists of ion collectors and shields for each mass mounted onto moveable frames. Each of the frames can be moved about the theoretical position along the collector flange for proper alignment. In addition, the collectors and their shields can be moved up or down on the frames parallel to the ion paths. The necessary isolation between the collectors and their shields is obtained with ruby washer insulators. Wires are attached from the collectors to the feedthrough pins in the collector flange. After the collectors have been properly positioned, shields are spot welded between the

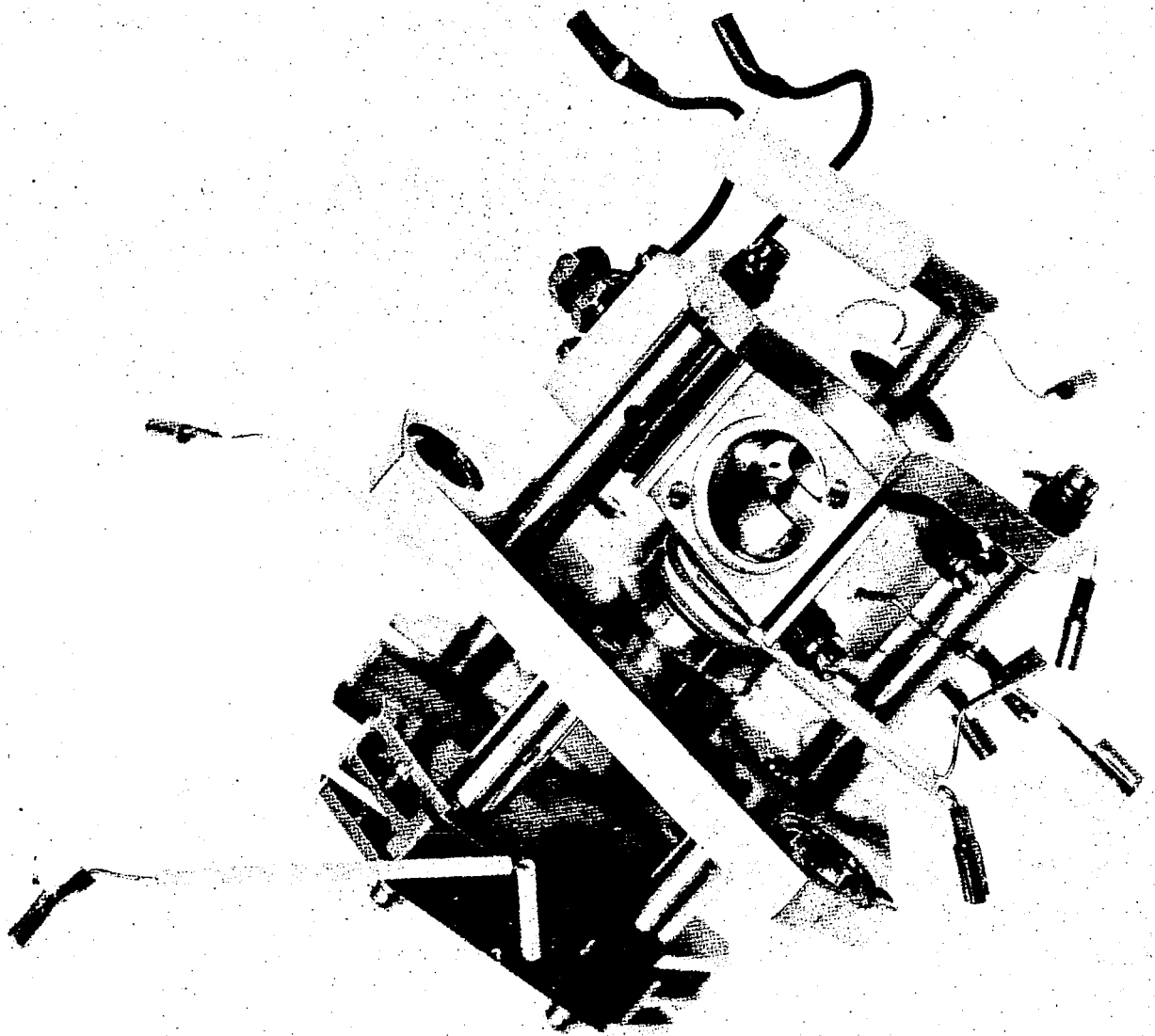


FIGURE 29
Ion Source

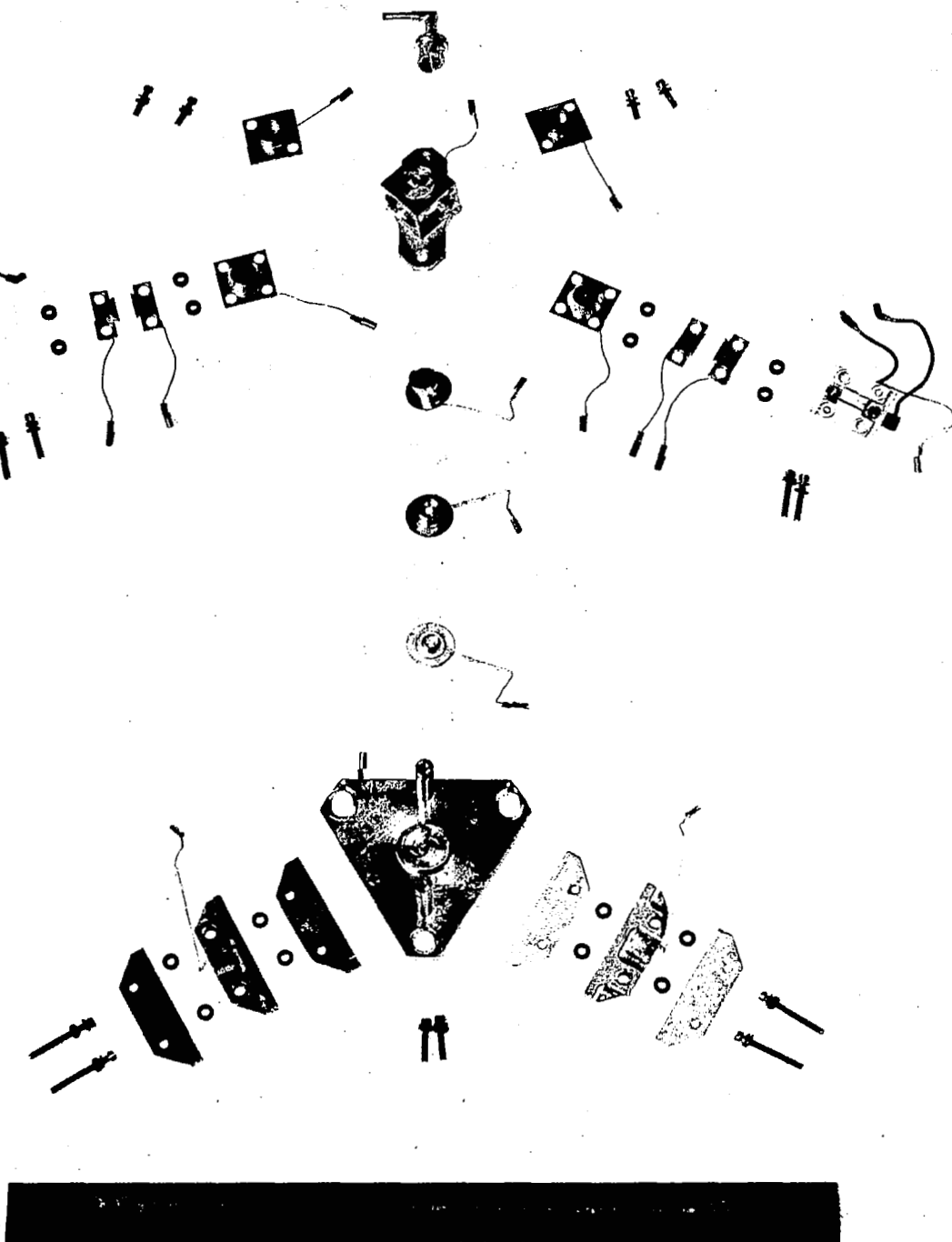


FIGURE 30
Exploded View of Ion Source

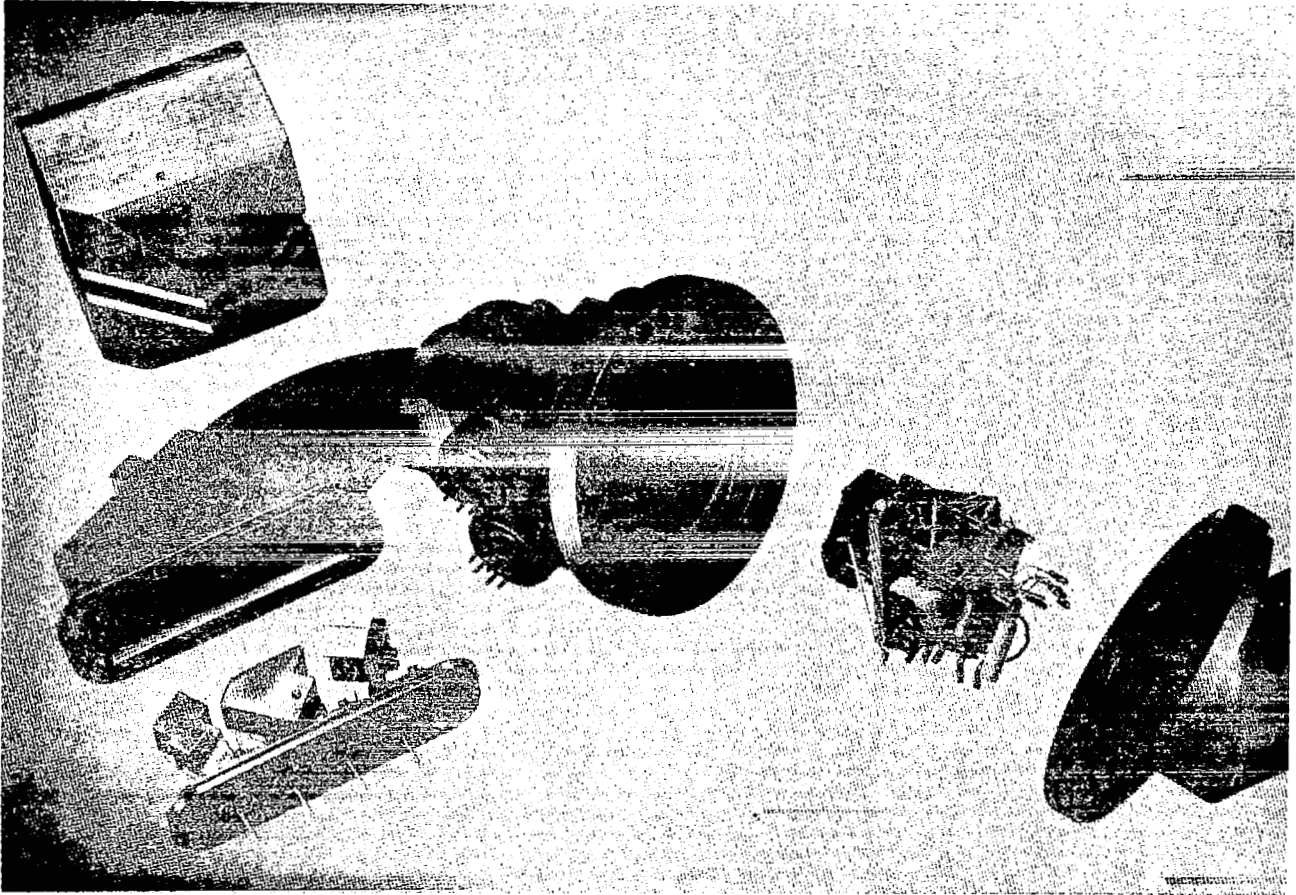


FIGURE 31
Exploded View of Analyzer

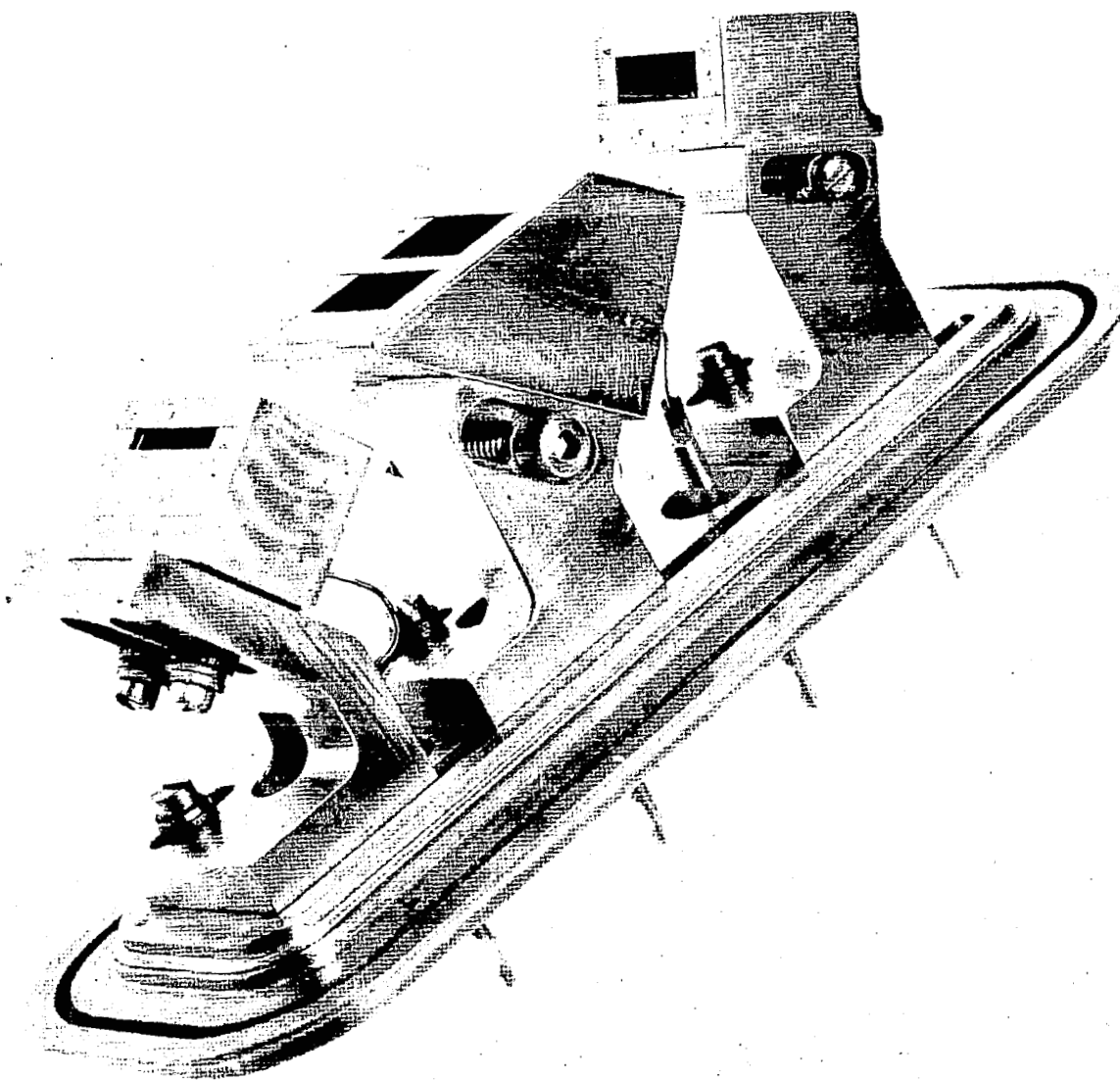


FIGURE 32
Collector Flange Assembly

collectors, to shield the feedthrough pins and connections, to prevent registration of stray ions. The collector flange assembly is then welded to the flange of the analyzer housing.

Ion pump assembly and mounting.- A prototype Perkin-Elmer ion pump is shown in Figure 33 . The ion pump assembly consists of four major subassemblies: the cathode/anode assembly, the housing assembly, the magnets, and the magnet mounting. The cathode/anode assembly features an integrally machined anode, which is mounted on contained ceramic washers to the cathod structure. The housing assembly is an all-welded construction, with welded-in pole pieces to minimize the airgap between the magnets. The magnet assembly consists of two magnets and a yoke. The magnets are soldered to the yoke. After the magnet assembly is positioned the yoke is secured to a bracket on the pump housing. The yoke is also mounted to bosses of the system enclosure. The flange of the pump housing is welded to the analyzer housing.

Electronics modules assembly and mounting.- The electronic packages consist of cordwood welded modules and associated discrete components mounted on printed circuit boards. A typical welded module is shown in Figure 34 . The printed circuit boards are shaped and the modules located so that minimum additional volume is required.

Only those modules and components requiring additional thermal paths are hard potted. Where thermal conditions permit, the electronics packages are protected from shock and vibration with foamed epoxies. Silicone rubbers and foam epoxy provides an effective corona suppression. The packages are hard wired together with the instrument during assembly.

CONCLUSIONS

An analytical study of the necessary modifications which would allow the Two Gas Sensor to monitor the atmospheric constituents selected contaminants and summation of contaminants has been performed for both helium-oxygen and nitrogen-oxygen atmospheres. Several approaches utilizing the Two Gas Sensor as the basic component were analyzed. The accumulator cell approach offered the most feasible solution to the problems encountered. The results of the study lead to the definition of a contaminant and atmospheric sensor, utilizing the accumulator cell, meeting the performance goals specified in the contract while still having acceptable weight, power, and size specifications.

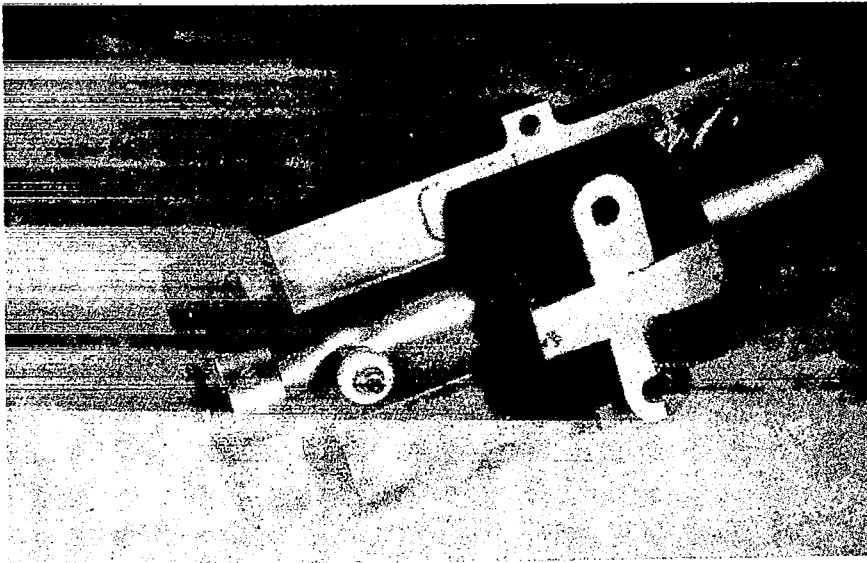


FIGURE 33
Typical Ion Pump

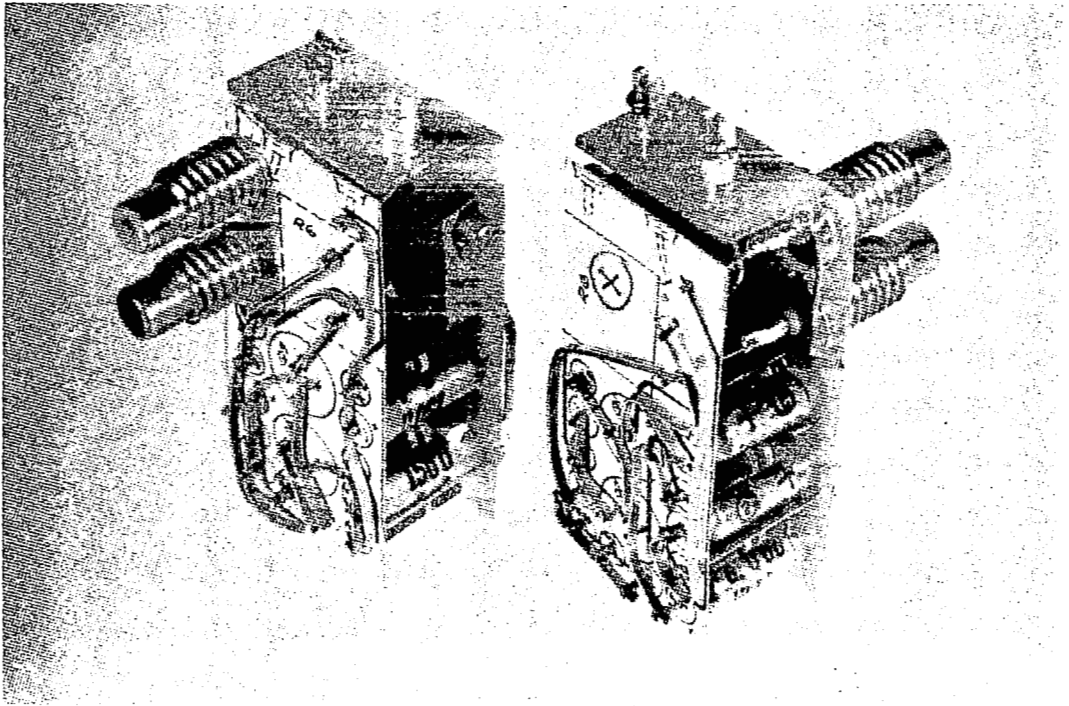


FIGURE 34
Typical Welded Module

APPENDIX A

RESOLUTION AND SENSITIVITY NEEDED FOR THE MEASUREMENT OF TOTAL HYDROCARBONS AND CO

Measurement of total hydrocarbons requires determination of resolution and sensitivity requirements. The instrument is to measure THC in an oxygen-helium atmosphere in which little is known about the composition and concentrations of contaminants present. Studies for MOL applications have given the concentration of organics to be 50 to 500 mg/m³. These values are used in this analysis primarily because of the lack of more desirable data. The 50 contaminants to be considered were chosen from lists of contaminants found in helium-oxygen atmosphere, as given in the Laboratory Contaminant Sensor contract, NAS 1-7266. The partial spectra of the 50 elected contaminants is displayed in Table A1. The largest peak in the spectra is called the 100% peak, other peaks are given as a percentage of the 100% peak. Table A2 shows the spectra weighted as to their relative nitrogen sensitivity. Since the sensitivities given vary with several parameters the decision was made to weigh the spectra with respect to sensitivity in this manner:

if S equals:	multiply by:
0 - 0.25	the given sensitivity
0.25 - 0.75	0.5
0.75 - 1.25	1.0
1.25 - 1.75	1.5
1.75 - 2.25	2.0
2.25 - 2.75	2.5
2.75 - 3.25	3.0

The next decision was to compute the PPM for each of the 50 contaminants at m/e 15, 27, 28, 29, and 47-120, as if they occupied the atmosphere by themselves. This computation combined with an estimate of the percentages of the contaminants expected provides an idea of the sensitivities needed.

Changing $\frac{\text{mg}}{\text{m}^3}$ to PPM

$$\frac{\text{mg}}{\text{m}^3} = \frac{1}{\text{M.W.}} \frac{10^{-3} \text{ gms} \quad 6.023 \times 10^{23} \text{ molecules}}{\text{molecules}} = \frac{\text{molecules}}{(\text{meter})^3}$$

$$= \frac{6.023 \times 10^{20}}{\text{M.W.}} \frac{1}{\text{m}^3} = \frac{6.023 \times 10^{20}}{\text{M.W.}} \frac{1}{\text{m}^3}$$

number of molecules in 1 m^3 at 380 torr (1/2 atmosphere)

$$= \frac{6.023 \times 10^{23}}{22.4} (10^3) (1/2)$$

$$\therefore \text{PPM} = \frac{6.023 \times 10^{20}}{\text{M.W.}} = \frac{(22.4)}{\text{M.W.}} (2) (10^{-6})$$

$$\frac{6.023 \times 10^{26}}{22.4} (1/2)$$

$$\therefore \frac{44.8}{\text{M.W.}} \text{ PPM for each } \frac{\text{mg}}{\text{m}^3} \text{ of gas (M.W. in grams)}$$

Table A3 is composed by use of this relation. Now the expected concentrations of all the constituents can be expressed in PPM as follows:

Helium	0 to 500,000 PPM
Oxygen	0 to 500,000 PPM
Carbon Dioxide	0 to 50,000 PPM
Water Vapor	0 to 50,000 PPM
Carbon Monoxide	0 to 48 PPM
Methane	0 to 1,950 PPM
Total Hydrocarbons	0 to 1,000 PPM ($\sim 1000 \frac{\text{mg}}{\text{m}^3}$ assuming an average M.W. of 50)

PPM values presented were computed at 50 to 500 mg/m^3 . The values were chosen as a low and moderately high estimate of the contaminants levels to be expected.

The Two Gas Sensor can be made to operate with an ion source sensitivity of 2×10^{-6} amps/torr. This sensitivity along with the normal operating pressure of 2×10^{-4} torr gives an output current of 4×10^{-10} amps for N_2 . In a 380 torr

atmosphere a signal of 13 PPM is detectable. This would provide an ion current of 5×10^{-15} amps, well above the present detector noise level of 1.5×10^{-15} with a one second 0 to 90 percent rise time. This value of 13 PPM sets a lower limit of constituents to be examined with the present Two Gas Sensor of:

Oxygen	13 (9.3 mg/m^3) to 500,000 PPM
Helium	13 (1.14 mg/m^3) to 500,000 PPM
Carbon Dioxide	13 (12.8 mg/m^3) to 50,000 PPM
Water Vapor	13 (5.25 mg/m^3) to 50,000 PPM
Carbon Monoxide	13 (8.15 mg/m^3) to 48 PPM
Methane	13 (4.29 mg/m^3) to 1,950 PPM
Total Hydrocarbons	13 (12.1 mg/m^3) to 1,000 PPM

The lower limit on the concentrations of 13 PPM assumes that all the components have the same sensitivity as nitrogen. Correcting for this assumption we obtain:

	Sensitivity	Lower Detectable Limit
Oxygen	0.73	17.8 PPM
Helium	0.185	70.0 PPM
Water Vapor	0.68	19.1 PPM
Carbon Dioxide	1.1	11.8 PPM
Carbon Monoxide	1.0	13.0 PPM
Methane	0.825	15.75 PPM
Total Hydrocarbons	1.5*	8.45 PPM

Therefore, note that the present Two Gas Sensor is capable of detecting hydrocarbons of a concentration of greater than 10 PPM. By examining the spectra a concentration considerably greater than 10 PPM can be expected. Sufficient sensitivity is expected for a hydrocarbon measurement. The present Two Gas Sensor has a resolution of 18. This is quite sufficient to separate 44 from 47. Therefore, the resolution is adequate even though the analyzer may need to be enlarged to allow masses 44 and 47 to be placed at their optimum focal points.

*Average sensitivity of 50 selected contaminants

TABLE A1.- SELECTED CONTAMINANTS PARTIAL SPECTRA

Compound	S	m/e Major	12	14	15	27	28	29	49-120
Allyl Alcohol		57	0.16	0.78	1.46	18.97	12.32	39.11	----
Acetone	1.42	43	1.11	8.55	43.69	8.01	1.74	4.29	----
Acetaldehyde	0.904	29	3.97	17.46	42.07	4.93	4.00	100.0	----
Ammonia	0.457	17	----	22.0	7.5	----	----	----	----
Benzene	1.95	78	0.60	----	1.52	3.48	----	----	----
Butene ⁻¹	1.28	41	0.8	2.90	7.32	33.19	28.01	17.64	----
Carbon Dioxide	1.1		9.7	----	----	----	11.0	----	----
1,4-Dioxane	1.56	28	0.79	6.24	16.42	18.21	100.0	42.73	----
Ethylacetate	2.32	43	0.81	7.36	21.52	13.5	4.60	25.01	----
Ethylene Dichloride	0.175	62	0.95	4.1	1.0	31.0	91.2	4.8	----
Formaldehyde	0.314	29	5.2	6.33	----	----	30.31	100.0	----
Methane	0.79	16	3.8	20.09	88.76	----	----	----	----
Methanol	1.02	31	0.58	6.97	36.44	----	5.93	59.86	----
Methylene Chloride	1.28	50	3.3	8.4	72.3	----	----	----	----
Nitrous Oxide	0.79	44	----	17.03	----	----	15.81	----	----
Nitroic Oxide	1.14	30	----	11.44	2.71	----	3.76	0.04	----
Toluene	1.67	91	0.09	0.13	(0.27)	0.65	----	----	----
					1.26				
Vinyl Chloride	1.055	27	3.49	3.04	1.09	100.0	2.70	----	----
M-Xylene	1.44	91	----	----	2.89	9.64	0.67	----	----
Sulfurdioxide	0.67	64	----	----	----	----	----	----	----
Ethyl Alcohol	0.74	31	----	----	----	22.2	5.5	22.48	----
Iso-Propyl Alcohol	0.16	45	----	----	----	16.3	1.2	10.0	----
Methyl Ethyl Ketone	0.1575	--	----	----	----	15.4	2.79	23.6	----
Cyclohexane	0.72	56	----	0.30	3.56	24.22	12.65	11.96	----
Iso Pentane	1.0	43	0.10	0.74	5.65	35.61	4.05	44.33	----
Methyl n-Butyrate	<u>25.6</u> 50	43	n.d.	n.d.	n.d.	43.72	9.03	17.10	----
Ethylether	1.05	31	0.23	3.14	9.88	24.07	6.21	54.0	----
Ethylene	0.9	28	1.64	5.01	0.52	64.72	100.0	2.31	----

TABLE A1.- SELECTED CONTAMINANTS PARTIAL SPECTRA - Concluded

Compound	S	m/e Major	12	14	15	27	28	29	49-120
Acetic Acid	---	43	----	----	----	0.40	5.55	15.6	----
Acetonitrile	1.0	41	7.12	13.47	2.36	2.39	3.79	----	----
Butanal	0.35	27	----	----	----	100.0	26.55	95.59	83.0
n-Butane	1.35	43	----	1.78	9.28	43.49	32.96	43.37	17.0
Carbontetrachloride .	1.1	117	9.96	----	----	----	----	----	330.0
2,3 Dimethylpentane .	1.7	57	----	0.74	8.22	25.0	4.21	30.7	194.0
Ethylbenzene	2.5	91	----	----	----	7.47	0.86	0.51	245.0
Formic Acid	68.0	100	3.32	----	----	----	17.21	100.0	108.0
2 Propanol	1.8	45	0.48	4.52	14.49	17.53	1.65	12.49	60.0
Methyl Acetate . . .	2.1	43	----	----	----	0.84	1.94	10.50	22.00
Methyl Mercaptan . .	1.0	47	1.49	5.38	12.07	----	1.08	----	200.0

TABLE A2. - SPECTRA WEIGHTED TO RELATIVE NITROGEN SENSITIVITY

Compound	SEN	m/e MAJOR	12	14	15	27	28	29	47-120
Allyl Alcohol		57	0.16	0.78	1.46	18.97	12.32	39.11	38.2
Acetone	1.42	43	1.67	12.75	66.1	12.01	2.61	6.41	44.0
Acetaldehyde	0.902	29	3.97	17.46	42.07	4.93	4.00	100.0	--
Amonia	0.457	17	--	1.1	3.75	--	--	--	--
Benzene	1.95	78	1.2	--	3.04	6.96	--	--	392.0
Butene ⁻¹	1.28	41	1.2	4.35	10.9	--	--	--	286.0
Carbon Dioxide	1.1	44	9.7	--	--	--	11.0	--	--
1-4 Dioxane	1.56	23	119.0	9.36	24.63	27.31	150.0	63.36	156.0
Ethyl Acetate	2.32	43	2.03	18.30	54.55	33.9	11.5	62.5	62.5
Ethylene Dichloride	0.17	62	0.168	0.72	0.175	5.45	15.9	0.84	34.0
Formaldehyde	0.31	29	2.6	3.17	--	--	15.15	50.0	--
Methane	0.79	16	3.8	20.09	88.76	--	--	--	--
Methanol	1.02	31	0.58	6.97	36.44	--	5.93	59.86	--
Methyl Chloride	1.28	50	5.0	12.6	108.4	--	--	--	239.0
Nitrous Oxide	0.79	44	--	17.03	--	--	15.81	--	--
Nitric Oxide	1.14	30	--	11.44	2.71	--	3.76	0.04	--
Toluene	1.67	91	0.013	0.17	1.89	0.98	--	--	400.0
Vinyl Chloride	1.05	27	3.49	3.04	1.09	1.00	2.70	--	127.0
m-Xylene	1.44	91	--	--	4.33	14.46	1.00	--	295.0
Sulfur dioxide	0.67	64	--	--	--	--	--	--	155.0
Ethylalcohol	0.75	31	--	--	--	22.2	5.5	22.48	--
Cyclohexane	0.72	56	--	0.15	1.78	12.11	6.33	5.98	138.0
Iso Pentane	1	43	0.10	0.74	5.65	35.61	4.05	44.33	200.0
Methyl Ethyl Keytone	0.16		--	--	--	2.0	1.55	3.8	N.A.
Methyl n Butyrate	0.75	43	n.d.	n.d.	n.d.	43.72	9.03	17.10	187.0
Ethyl ether	1.05	31	0.23	3.14	9.88	24.07	6.21	54.0	--
Ethylene	0.9	28	1.64	5.01	0.52	64.72	100.0	2.31	--
Acetic Acid	1.2	43	--	--	--	0.40	5.55	15.6	--
Acetonitrile	1.0	41	7.12	13.47	2.36	2.39	3.79	--	--
Betenal	0.35	27	--	--	--	50.0	13.28	47.8	85.0
Carbon Tetrachloride	1.0	117	9.96	--	--	--	--	--	330.0

TABLE A2. - SPECTRA WEIGHTED TO RELATIVE NITROGEN SENSITIVITY - Concluded

Compound	SEN	m/e MAJOR	12	14	15	27	28	29	47-120
2,3 Dimethyl 100 Pentane	1.7	57	--	1.11	12.33	37.5	6.31	46.1	291.0
Ethyl-Benzene	2.5	91	--	--	--	18.75	2.05	1.27	612.0
Formic Acid	1.8	100	6.64	--	--	--	17.21	200.0	216.0
2-Propanol	1.8	45	0.48	9.06	29.00	35.06	3.30	24.98	12.0
Methyl Acetate	2.1	43	--	--	--	1.68	3.88	21.00	44.00
Methyl Mercaptan	1.0	47	1.49	5.38	12.07	--	1.08	--	200.0
n-Hexane	1.15	57	--	1.15	9.30	55.59	15.30	60.29	183.0
Methyl Z Pentanone	1.6	43	--	--	--	--	2.92	22.2	120.0
2-Butanol	N.A.	45	--	--	--	17.0	3.20	15.0	26.0
Furfuryl Alcohol	--	--	--	--	--	2.4	0.41	2.96	20.5
Furan	N.A.	39	2.1	4.0	--	0.8	1.5	15.8	130.0
Isopropyl Alcohol	N.A.	45	0.5	1.5	14.5	17.5	1.7	12.5	37.0
1-Pentene	1.2	42	--	1.1	5.6	32.2	4.9	27.0	40.0
Benzaldehyde	2.1	27	--	--	--	200.0	53.0	191.0	140.0
Ethyl Formate	N.A.	31	--	--	--	43.0	72.0	65.0	10.0
m-Propanol	1.8	31	--	40.0	3.6	37.2	12.6	34.4	36.0
Propylene	1.2	41	1.2	3.1	50.0	38.5	1.6	0.6	--
Nephthalene	2.9	128	--	--	--	5.34	--	--	615.0
Hexane	1.15	57	--	1.16	9.30	55.59	15.30	60.29	183.0
Methyl-2-Pentom	1.6	43	--	--	--	--	1.95	14.87	80.0
Butanol	--	45	--	--	--	17.0	3.20	15.0	26.0
Furfuryl Alcohol	0.05	98	--	--	--	48.0	8.2	59.5	410.0
Furon	N.A.	39	2.1	4.0	--	0.8	1.5	15.8	130.0
Isopropyl Alcohol	--	45	0.5	1.5	14.5	17.5	1.7	12.5	37.0
Pentene	1.2	42	--	1.1	5.6	32.2	4.9	27.0	40.0
Benzaldehyde	2.1	27	--	--	--	100.0	26.5	95.6	70.0
Ethyl Formate	--	31	--	--	--	43.0	72.0	65.0	10.0
n-Proponal	1.8	31	--	2.0	1.8	18.6	6.3	17.2	18.0
Propylene	--	41	1.2	3.1	50.0	38.5	1.6	0.6	--
Naphthalene	2.9	128	--	--	--	1.78	--	205.0	--

TABLE A3.- PPM VALUES FOR MASS NUMBERS OF INTEREST

	PPM15	PPM27	PPM28	PPM29	PPM47-120
Butanol					
50 $\frac{\text{mg}}{\text{m}^3}$	0.0	15.5	4.13	14.8	26.3
500 $\frac{\text{mg}}{\text{m}^3}$	0.0	155.0	41.3	148.0	263.0
Carbon Tetrachloride					
50 $\frac{\text{mg}}{\text{m}^3}$	0.0	0.0	0.0	0.0	45.0
500 $\frac{\text{mg}}{\text{m}^3}$	0.0	0.0	0.0	0.0	450.0
2,3 Dimethyl Pentane					
50 $\frac{\text{mg}}{\text{m}^3}$	2.77	8.35	1.410	10.3	65.0
500 $\frac{\text{mg}}{\text{m}^3}$	27.77	83.5	14.10	103.0	650.0
Ethylene					
50 $\frac{\text{mg}}{\text{m}^3}$	0.416	51.6	80.0	185.0	0.0
500 $\frac{\text{mg}}{\text{m}^3}$	4.16	516.0	800.0	1850.0	0.0
Acetic Acid					
50 $\frac{\text{mg}}{\text{m}^3}$	0.0	0.15	2.04	5.75	75.0
500 $\frac{\text{mg}}{\text{m}^3}$	0.0	1.5	20.4	57.5	750.0

TABLE A3.- PPM VALUES FOR MASS NUMBERS OF INTEREST - Continued

	PPM15	PPM27	PPM28	PPM29	PPM47-120
Acetonitrile					
50 $\frac{\text{mg}}{\text{m}^3}$	1.27	1.28	2.05	0.0	0.0
500 $\frac{\text{mg}}{\text{m}^3}$	12.7	12.8	20.5	0.0	0.0
m-Xylene					
50 $\frac{\text{mg}}{\text{m}^3}$	1.90	6.3	0.43	0.0	127.0
500 $\frac{\text{mg}}{\text{m}^3}$	19.0	63.0	4.3	0.0	1270.0
Sulfur Dioxide					
50 $\frac{\text{mg}}{\text{m}^3}$	0.0	0.0	0.0	0.0	54.2
500 $\frac{\text{mg}}{\text{m}^3}$	0.0	0.0	0.0	0.0	542.0
Ethyl Alcohol					
50 $\frac{\text{mg}}{\text{m}^3}$	0.0	10.7	2.8	10.7	0.0
500 $\frac{\text{mg}}{\text{m}^3}$	0.0	107.0	28.0	107.0	0.0
Ethyl-Benzene					
50 $\frac{\text{mg}}{\text{m}^3}$	0.0	9.2	1.00	0.601	299.0
500 $\frac{\text{mg}}{\text{m}^3}$	0.0	92.0	10.0	6.01	2990.0

TABLE A3.- PPM VALUES FOR MASS NUMBERS OF INTEREST - Continued

	PPM15	PPM27	PPM28	PPM29	PPM47-120
Formic Acid					
50 $\frac{\text{mg}}{\text{m}^3}$	0.0	0.0	7.9	92.0	98.5
500 $\frac{\text{mg}}{\text{m}^3}$	0.0	0.0	79.0	920.0	985.0
2-Propanol					
50 $\frac{\text{mg}}{\text{m}^3}$	10.7	13.0	11.4	9.25	4.34
500 $\frac{\text{mg}}{\text{m}^3}$	107.0	130.0	114.0	92.50	43.4
Acetone					
50 $\frac{\text{mg}}{\text{m}^3}$	25.5	46.20	10.1	2.47	17.0
500 $\frac{\text{mg}}{\text{m}^3}$	255.0	462.0	101.0	24.7	170.0
Acetaldehyde					
50 $\frac{\text{mg}}{\text{m}^3}$	10.0	2.46	2.00	50.0	0.0
500 $\frac{\text{mg}}{\text{m}^3}$	100.0	24.6	20.0	500.0	0.0
Ammonia					
50 $\frac{\text{mg}}{\text{m}^3}$	5.62	0.0	0.0	0.0	0.0
500 $\frac{\text{mg}}{\text{m}^3}$	56.2	0.0	0.0	0.0	0.0

TABLE A3.- PPM VALUES FOR MASS NUMBERS OF INTEREST - Continued

	PPM15	PPM27	PPM28	PPM29	PPM47-120
Benzene					
50 $\frac{\text{mg}}{\text{m}^3}$	8.6	19.8	0.0	0.0	112.0
500 $\frac{\text{mg}}{\text{m}^3}$	86.0	198.0	0.0	0.0	1120.0
Butene					
50 $\frac{\text{mg}}{\text{m}^3}$	4.0	0.0	0.0	0.0	115.0
500 $\frac{\text{mg}}{\text{m}^3}$	40.0	0.0	0.0	0.0	1150.0
Carbon Dioxide					
50 $\frac{\text{mg}}{\text{m}^3}$	0.0	0.0	5.5	0.0	0.0
500 $\frac{\text{mg}}{\text{m}^3}$	0.0	0.0	55.0	0.0	0.0
Methanol					
50 $\frac{\text{mg}}{\text{m}^3}$	25.5	0.0	4.15	41.6	0.0
500 $\frac{\text{mg}}{\text{m}^3}$	255.0	0.0	41.5	416.0	0.0
Methyl Chloride					
50 $\frac{\text{mg}}{\text{m}^3}$	50.0	0.0	0.0	0.0	107.0
500 $\frac{\text{mg}}{\text{m}^3}$	500.0	0.0	0.0	0.0	1070.0

TABLE A3.- PPM VALUES FOR MASS NUMBERS OF INTEREST - Continued

	PPM15	PPM27	PPM28	PPM29	PPM47-120
Nitrous Oxide					
50 $\frac{\text{mg}}{\text{m}^3}$	0.0	0.0	7.9	0.0	0.0
500 $\frac{\text{mg}}{\text{m}^3}$	0.0	0.0	79.0	0.0	0.0
Nitric Oxide					
50 $\frac{\text{mg}}{\text{m}^3}$	1.82	0.0	2.56	0.027	0.0
500 $\frac{\text{mg}}{\text{m}^3}$	18.2	0.0	25.6	0.27	0.0
Tolulene					
50 $\frac{\text{mg}}{\text{m}^3}$	0.46	0.22	0.0	0.0	97.6
500 $\frac{\text{mg}}{\text{m}^3}$	4.6	2.2	0.0	0.0	976.0
Vinylchloride					
50 $\frac{\text{mg}}{\text{m}^3}$	0.40	39.0	1.11	0.0	50.0
500 $\frac{\text{mg}}{\text{m}^3}$	4.0	390.0	11.1	0.0	500.0
1-4 Dioxane					
50 $\frac{\text{mg}}{\text{m}^3}$	6.25	6.8	3.75	15.8	38.0
500 $\frac{\text{mg}}{\text{m}^3}$	62.5	68.0	37.5	158.0	380.0

TABLE A3.- PPM VALUES FOR MASS NUMBERS OF INTEREST - Continued

	PPM15	PPM27	PPM28	PPM29	PPM47-120
Ethyl Acetate					
50 $\frac{\text{mg}}{\text{m}^3}$	15.4	9.4	3.0	17.7	17.3
500 $\frac{\text{mg}}{\text{m}^3}$	154.0	94.0	30.0	177.0	173.0
Ethylene Dichloride					
50 $\frac{\text{mg}}{\text{m}^3}$	0.039	1.21	3.55	0.2	7.6
500 $\frac{\text{mg}}{\text{m}^3}$	0.39	12.1	35.5	2.0	76.0
Formaldehyde					
50 $\frac{\text{mg}}{\text{m}^3}$	0.0	0.0	11.2	37.0	0.0
500 $\frac{\text{mg}}{\text{m}^3}$	0.0	0.0	112.0	370.0	0.0
Methane					
50 $\frac{\text{mg}}{\text{m}^3}$	123.0	0.0	0.0	0.0	0.0
500 $\frac{\text{mg}}{\text{m}^3}$	1230.0	0.0	0.0	0.0	0.0
Methyl Acetate					
50 $\frac{\text{mg}}{\text{m}^3}$	0.0	0.504	1.16	6.30	13.0
500 $\frac{\text{mg}}{\text{m}^3}$	0.0	5.04	11.6	63.0	130.0

TABLE A3.- PPM VALUES FOR MASS NUMBERS OF INTEREST - Continued

	PPM15	PPM27	PPM28	PPM29	PPM47-120
Methyl Mercaptan					
50 $\frac{\text{mg}}{\text{m}^3}$	5.4	0.0	0.46	0.0	90.0
500 $\frac{\text{mg}}{\text{m}^3}$	54.0	0.0	4.6	0.0	90.0
n-Hexane					
50 $\frac{\text{mg}}{\text{m}^3}$	0.241	14.5	4.0	15.7	47.6
500 $\frac{\text{mg}}{\text{m}^3}$	2.41	145.0	40.0	157.0	476.0
Cyclohexane					
50 $\frac{\text{mg}}{\text{m}^3}$.467	3.24	1.67	1.59	37.0
500 $\frac{\text{mg}}{\text{m}^3}$	4.67	32.4	16.7	15.9	370.0
Iso Pentane					
50 $\frac{\text{mg}}{\text{m}^3}$	1.75	11.1	1.24	13.7	62.0
500 $\frac{\text{mg}}{\text{m}^3}$	17.5	111.1	12.4	137.0	620.0
Methyl Ethyl Keytone					
50 $\frac{\text{mg}}{\text{m}^3}$	0.0	0.62	.48	1.18	N.A.
500 $\frac{\text{mg}}{\text{m}^3}$	0.0	6.2	4.8	11.8	N.A.

TABLE A3.- PPM VALUES FOR MASS NUMBERS OF INTEREST - Continued

	PPM15	PPM27	PPM28	PPM29	PPM47-120
Methyl n Butyrate					
50 $\frac{\text{mg}}{\text{m}^3}$	n.d.	9.65	1.96	3.76	41.2
500 $\frac{\text{mg}}{\text{m}^3}$	n.d.	96.5	19.6	37.6	412.0
Ethyl Ether					
50 $\frac{\text{mg}}{\text{m}^3}$	2.92	7.45	1.87	16.2	N.A.
500 $\frac{\text{mg}}{\text{m}^3}$	29.2	74.5	18.7	162.0	N.A.
Benzaldehyde					
50 $\frac{\text{mg}}{\text{m}^3}$	0.0	44.0	11.6	42.0	28.6
500 $\frac{\text{mg}}{\text{m}^3}$	0.0	440.0	116.0	420.0	286.0
Ethyl Formate					
50 $\frac{\text{mg}}{\text{m}^3}$	0.0	12.9	21.6	19.5	3.0
500 $\frac{\text{mg}}{\text{m}^3}$	0.0	129.0	216.0	195.0	30.0
n-Propanol					
50 $\frac{\text{mg}}{\text{m}^3}$	1.33	1.35	4.66	14.4	13.3
500 $\frac{\text{mg}}{\text{m}^3}$	13.3	13.5	46.60	144.0	133.0

TABLE A3.- PPM VALUES FOR MASS NUMBERS OF INTEREST - Continued

	PPM15	PPM27	PPM28	PPM29	PPM47-120
Furan					
50 $\frac{\text{mg}}{\text{m}^3}$	0.0	0.264	0.524	5.24	43.0
500 $\frac{\text{mg}}{\text{m}^3}$	0.0	2.64	5.24	52.4	430.0
Isopropyl Alcohol					
50 $\frac{\text{mg}}{\text{m}^3}$	5.40	6.52	0.633	4.65	13.8
500 $\frac{\text{mg}}{\text{m}^3}$	54.0	65.2	6.33	46.5	138.0
1-Pentene					
50 $\frac{\text{mg}}{\text{m}^3}$	1.88	10.5	1.52	7.3	12.8
500 $\frac{\text{mg}}{\text{m}^3}$	18.8	105.0	15.2	73.0	128.0
Methyl 2 Pentanone					
50 $\frac{\text{mg}}{\text{m}^3}$	0.0	0.0	0.640	5.0	26.6
500 $\frac{\text{mg}}{\text{m}^3}$	0.0	0.0	6.40	50.0	266.0
2-Butanol					
50 $\frac{\text{mg}}{\text{m}^3}$	0.0	5.10	0.96	1.50	7.2
500 $\frac{\text{mg}}{\text{m}^3}$	0.0	51.0	9.6	15.0	72.0

TABLE A3.- PPM VALUES FOR MASS NUMBERS OF INTEREST - Concluded

	PPM15	PPM27	PPM28	PPM29	PPM47-120
Furfuryl Alcohol					
50 $\frac{\text{mg}}{\text{m}^3}$	0.0	0.553	0.0957	0.677	4.70
500 $\frac{\text{mg}}{\text{m}^3}$	0.0	5.53	0.957	6.77	47.0
Propylene					
50 $\frac{\text{mg}}{\text{m}^3}$	25.5	19.3	0.80	0.32	0.0
500 $\frac{\text{mg}}{\text{m}^3}$	255.0	193.0	8.0	3.2	0.0
Napthalene					
50 $\frac{\text{mg}}{\text{m}^3}$	0.0	0.945	0.0	0.0	108.0
500 $\frac{\text{mg}}{\text{m}^3}$	0.0	9.45	0.0	0.0	1080.0
Allyl Alcohol					
50 $\frac{\text{mg}}{\text{m}^3}$	0.55	7.1	4.72	14.9	14.7
500 $\frac{\text{mg}}{\text{m}^3}$	5.5	71.0	47.2	149.0	147.0
1-Propanethial					
50 $\frac{\text{mg}}{\text{m}^3}$	N.A.	13.0	1.70	1.40	49.0
500 $\frac{\text{mg}}{\text{m}^3}$	N.A.	130.0	17.0	14.0	490.0

APPENDIX B

CROSSTALK AND ORGANIC FRAGMENT INTERFERENCE AT MASS 28

Only at mass 28 is crosstalk from adjacent masses a problem. In Appendix A the discussion concerning the sensitivity and resolution of hydrocarbons found m/e 27 and m/3 29 averaged over the 50 contaminants, are nearly the same size as m/e 28 (actually m/e 27 and 29 were found to be larger than m/e 28 due to hydrocarbons). The present two gas sensor has a resolution of 18. This resolution is not sufficient to separate m/e 27 and 29 from m/e 28. The mass 28 collector is primarily for the detection of CO. Since the instrument is not able to separate the three masses, the ion current at mass 28, assuming that spectra data obtained in Appendix A is indicative of the true situation, will be roughly a sum of m/e 27, m/e 28, and m/e 29. Assuming that m/e 27, 28 and 29 are each about 20 PPM leads to the realization that m/e 28 current, due to hydrocarbons, is greater than the maximum expected CO current, about 40 PPM. The increase in resolution to 28 would decrease the hydrocarbon contribution to m/e by a conservative factor of 3. There is no simple method known to subtract out the hydrocarbons contribution to mass 28, therefore, decreasing hydrocarbon contribution as much as possible is desirable.

A physical method, which can be used to prevent the clouding of the CO measurement of m/e 28, requires the use of an organic scrubber in the mass spectrometer inlet system that will remove the organics. Scrubbers are composed of a mixture of sorbents such as charcoal and molecular sieve. While the use of the scrubber would eliminate total hydrocarbon measurement, methane would not be scrubbed effectively and could still be monitored by the mass spectrometer. The use of the scrubber offers an alternative method to increasing the resolution of the instrument. Without the scrubber there is no simple way to know how much of the m/e 28 current is due to CO and how much is due to fragments of hydrocarbons. At this time the most logical approach suggested would be to operate the mass spectrometer without the scrubber for normal operation, then if the 28 level is higher than would be expected from CO, or if a significant change in the 28 level appeared, the scrubber could then be brought into service in order to obtain an improved measurement. This type of operation calls for the scrubber to be rarely used.

If all 50 contaminants are considered to occupy the atmosphere in equal proportion as to weight, the following concentrations are computed:

for 50 $\frac{\text{mg}}{\text{m}^3}$

PPM 15	PPM 27	PPM 28	PPM 29	PPM 47-120
6.78	8.20	4.62	13.35	39.40

for 500 $\frac{\text{mg}}{\text{m}^3}$

PPM 15	PPM 27	PPM 28	PPM 29	PPM 47-120
67.8	82.0	46.20	133.50	394.0

The ratio of 27 +29 to 47-120 taken at 70 e.v. is 0.563 for the 50 contaminants. While the ratio of 28 to 47-120 is 0.117. Judging by these figures note that having a resolution of 28 decreases interference at mass 28 by a factor of 5. The expected amount of CO to be present in the atmosphere is about 40 PPM. Using 40 PPM CO as a representative number note that in an atmosphere with 50 mg/m^3 contaminants the percentage of mass 28 interference is about 10% of the total m/e 28 current, a negligible amount. If we have a high concentration of organics, 500 mg/m^3 , the 28 interference due to organics is about 50% of the 28 ion current. This is not a good measurement but in some cases 100% accuracy can be obtained because the 47-120 ion current provides a rough idea of how much of the 28 peak is due to organics. Analyzing the data of the 50 contaminants weighted equally as to weight yields these directions.

- (1) Resolution of 28 is needed to limit organic interference at m/e 28 only to ions of m/e 28.
- (2) For low concentrations of contaminants scrubber is not needed. When less than 50 mg/m^3 of contaminants are present the scrubber need not be used.

APPENDIX C

EVALUATION OF THE EFFECT OF LOWERING THE ELECTRON ENERGY ON FRAGMENTATION AND SENSITIVITY

As noted, decreasing the electron energy, in a number of cases, decreases fragmentation but, unfortunately, causes an accompanying reduction in sensitivity,^{1,2,3}. A method for decreasing fragmentation would decrease interference at mass 28 due to organics, enabling the attainment of data more indicative of the CO present. Masses 47-120 are to be monitored as an indication of the total hydrocarbons present. A large reduction in sensitivity would eliminate the possibility of obtaining a good THC measurement. Therefore, to weigh the positive advantage of reduced fragmentation against the disadvantage of reduced sensitivity is essential. In order to determine the value of a low energy electron method, a survey of existing literature and an analysis of contaminant spectra taken from the Laboratory contaminant contract were performed.

Data obtained from 9 contaminants run at 4 different electron voltages is shown in Table C1. The largest peak in the spectra is given the value 1, other peaks are given values relative to the major peak. The summation of masses 27, 28 and 29 is given along with masses 47-120. Masses 27, 28 and 29 are indicative of the current received at mass 28 because the Two Gas Sensor has a resolution of 18 and is not able to separate 27 and 29 from 28.

Examining the data provided in Table C1, shows no strong justification for the premise that intensity of fragment peaks at 27, 28 and 29 is reduced relative to the 47-120 intensity. An ascending value of the ratio of 27 and 28 and 29 to 47-120 as the electron energy is increased shows that fragmentation in the region of interest is decreased with a decrease in electron energy. An indication of how the intensity of the major peak varies with electron energy is given by the relative sensitivity values. Also, this sensitivity value gives a rough indication of how the 47-120 intensity varies with electron voltage. The correlation would be better if the major peak always fell in the 47-120 mass range, but this is not always the case. Only three of the nine compounds presented show an increase in ratio with increasing electron energy. These three compounds are Acetone, Butene-1, and Toluene. Even for these three cases the changes in ratio are not large. The ratio changes by a factor of 6.15 for Acetone, by 1.82 for Butene-1, and by a factor of 7 for Toluene when the ratios at 8 and 70 e.v. are compared. Also, remember that even in these three compounds, the decrease in fragmentation is accompanied by a decrease in sensitivity. Sensitivity decreases by a factor of 6.55 for Acetone, 8.7 for Butene-1, and 9.6 for Toluene when the same values at 70 volts and 8 volts are compared.

The data in the literature which can be directly applied to this study is, indeed, rare. Several papers concerning low voltage mass spectrometry have been written but in these papers sensitivity was no problem, due to large amounts of sample, and detection methods and resolution was sufficient to allow the attainment of clear and relatively complete data of all the spectra.

TABLE C1.- CONTAMINANTS RUN DATA*

Electron energy	m/e 27+28+29	m/e 47-120	Ratio 27+28+29 to 47-120	Relative sensitivity of major peak
Acetone				
8	0.0366	0.4481	0.0817	0.153
12	0.0786	0.5170	0.1515	0.341
16	0.1026	0.4445	0.2305	0.560
70	0.1756	0.3506	0.5010	1.00
Benzene				
8	0.0243	1.2014	0.0202	0.123
12	0.0355	1.1462	0.0310	0.496
16	0.0425	1.3266	0.0320	0.753
70	0.0320	1.9680	0.0163	1.00
Allyl Alcohol				
8	1.285	1.479	0.869	0.167
12	0.948	1.370	0.792	0.40
16	1.014	1.331	0.763	0.75
70	1.334	1.356	0.965	1.00
Butene-1				
8	0.713	1.126	0.633	0.115
12	0.544	0.843	0.646	0.440
16	0.594	0.730	0.814	0.685
70	0.808	0.700	1.155	1.000
Toluene				
8	0.003	1.083	0.003	0.104
12	0.006	1.352	0.004	0.418
16	0.033	1.783	0.018	0.620
70	0.049	2.319	0.021	1.000

TABLE C1.- CONTAMINANTS RUN DATA* -Concluded

Electron energy	m/e 27+28+29	m/e 47-120	Ratio 27+28+29 to 47-120	Relative sensitivity of major peak
Freon-11				
8	1.00	φ	und.	0.005
12	0.018	1.721	0.0105	0.175
16	0.014	1.791	0.008	0.523
70	0.007	2.382	0.003	1.000
1-4 Dioxane				
8	1.173	0.550	2.130	0.227
12	1.210	0.710	1.705	0.370
16	1.229	0.695	1.770	0.575
70	1.406	0.563	2.490	1.000
Ethyl Acetate				
8	0.719	0.406	1.772	0.032
12	0.326	0.410	0.795	0.232
16	0.346	0.328	1.055	0.420
70	0.341	0.260	1.310	1.000
Ethylene Dichloride				
8	1.043	0.320	3.070	0.233
12	1.093	1.331	0.822	0.412
16	1.149	1.259	0.912	0.564
70	1.183	1.821	0.652	1.000

* Values of electron energy given as 8, 12 and 16 volts, are about 4 volts low.

These luxuries are not afforded to flight mass spectrometers. The paper by Stevenson and Wagner ¹ presents curves showing how the intensity of the parent ion and several of its fragment varies with electron energy within about 8 volts of the ionization potential. The curves are presented in this section and are shown in Figures C1 thru C5.

The compounds presented in the Stevenson and Wagner paper are relatively simple organics. Fragments are formed by removing one or more hydrogens. The data does indicate that in order to considerably decrease fragmentation for simple organics, that operating within 4 volts of the ionization potential is necessary, but usually sensitivities are reduced by at least a factor of 10 when the electron energy is within 4 volts of the ionization potential. Lumpkin and Aczely's paper ², on the sensitivities of aromatic carbons, does give examples where lowered electron energy does give a decrease in selected fragmentation. As an example, their data for 1, 3, 5 - trimethylbenzene is presented in Table C2. The fragment peaks observed are caused by removing CH₂ from the ring, which accounts for the difference in mass by factors of 14 between the fragment peaks studies. For such special fragment peaks, the low electron energy method is a good one.

The most powerful argument against the use of lower energy electrons is the fact that the ionization potential of CO is several electron volts above that of most organics. The ionization potential of CO is given as 14.01 volts by KISER ⁴, while the ionization potential of most organics falls between 8 and 12 volts. Operating the mass spectrometer at an electron energy of 16 volts (4 volts above the 12 volt ionization potential) may reduce the fragmentation but the ion intensity is decreased by at least a factor of 10. Since the upper amount of CO expected is 48 PPM at an electron energy of 70 e.v., an electron energy of 16 e.v. would yield no more than 4.8 PPM CO. This amount of CO is not detectable on the present two gas sensor.

The results of the low energy mass spectrometry study are not favorable. The low energy method creates more problems than it solves and, therefore, is not practical.

According to King and Long ⁵, ionization efficiency curves fall into three distinct types. The first group of curves, labelled Type I, are for those ions whose fractional yield f_i varies inversely with the electron energy above the

-
1. D.P. Stevenson and C.D. Wagner, J. Amer. Chem. Soc., 72, 5612 (1950)
 2. H.E. Lumpkin and T. Aczely Anal. Chem., 36, 181, (1964)
 3. G.F. Crable, G.L. Kearns, and M.S. Norris, Anal. Chem., 32, 13 (1960)
 4. R.W. Kiser, Intro. to MassSpect. and its Applications, Prentice-Hall, Inc, Englewood Cliffs, N.J., 1965, pp 310.
 5. A.B. King and F.A. Long, J. Chem. Phys., 29, 374 (1958)

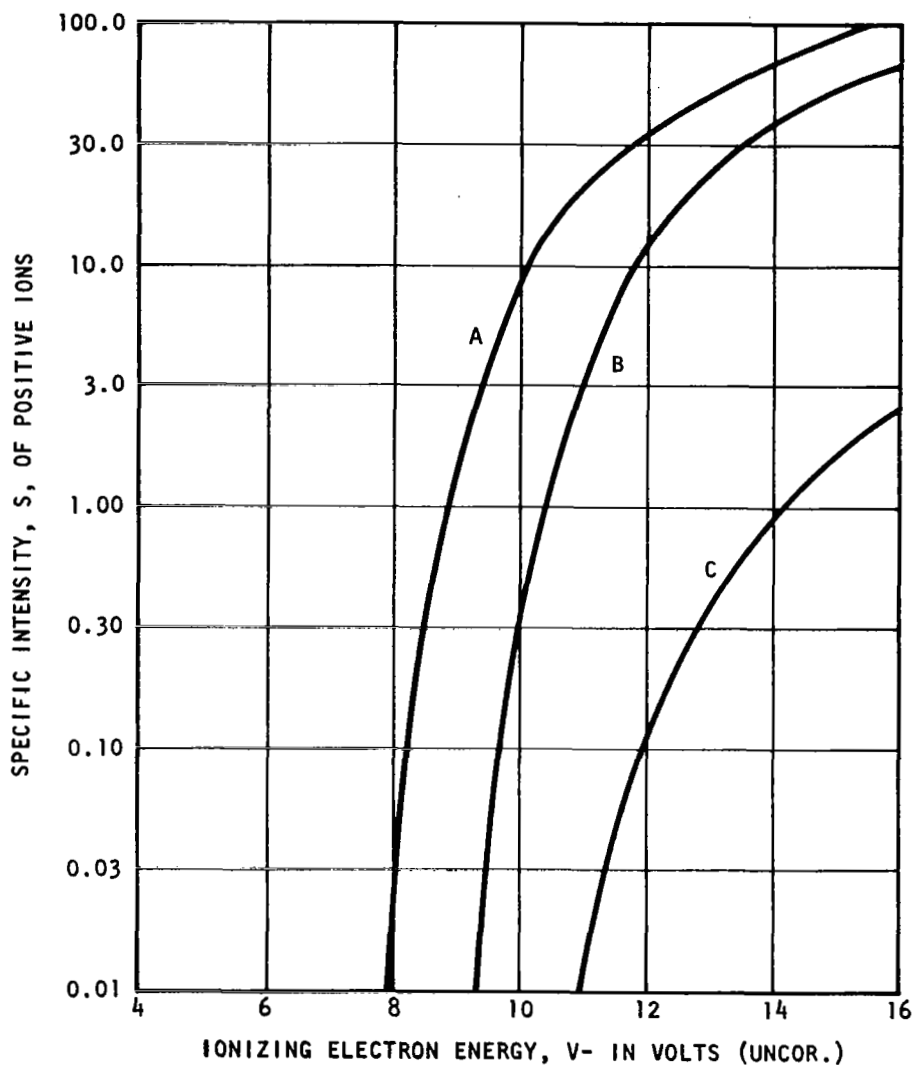
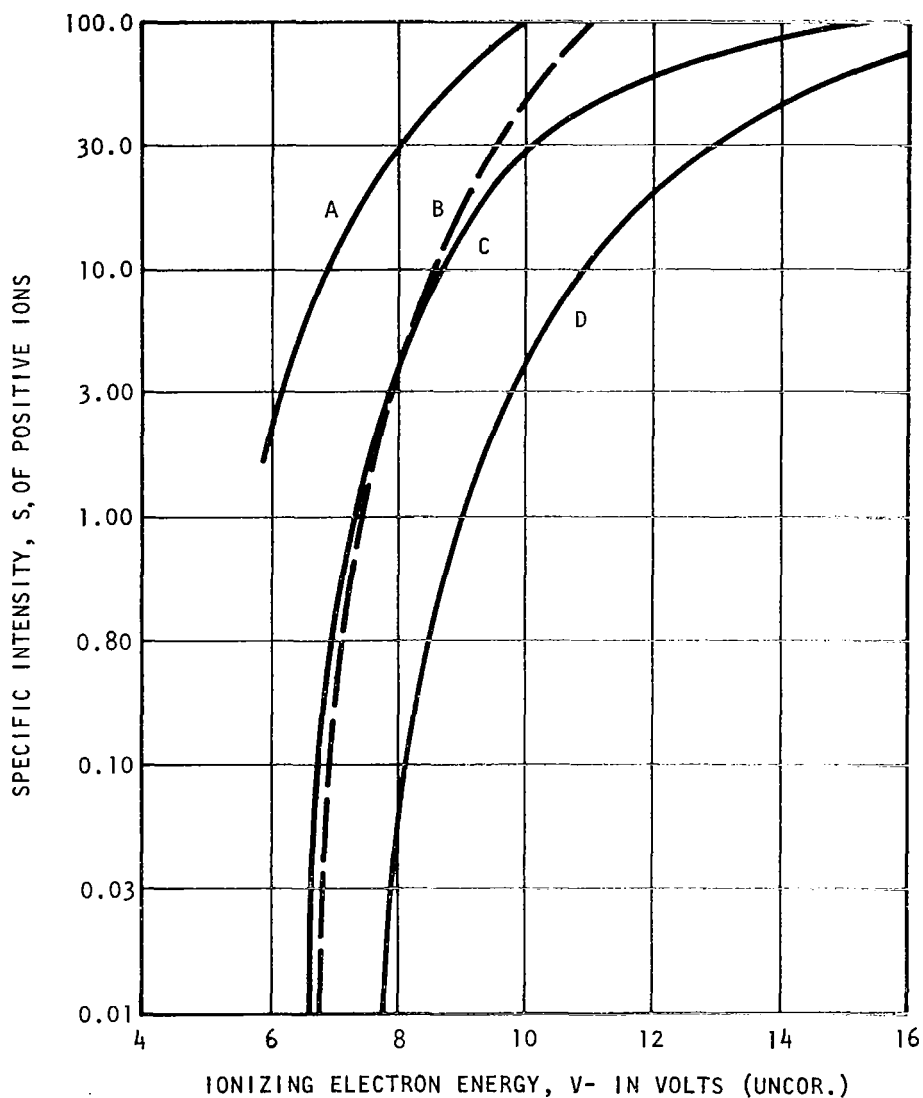


FIGURE C1

A-298C

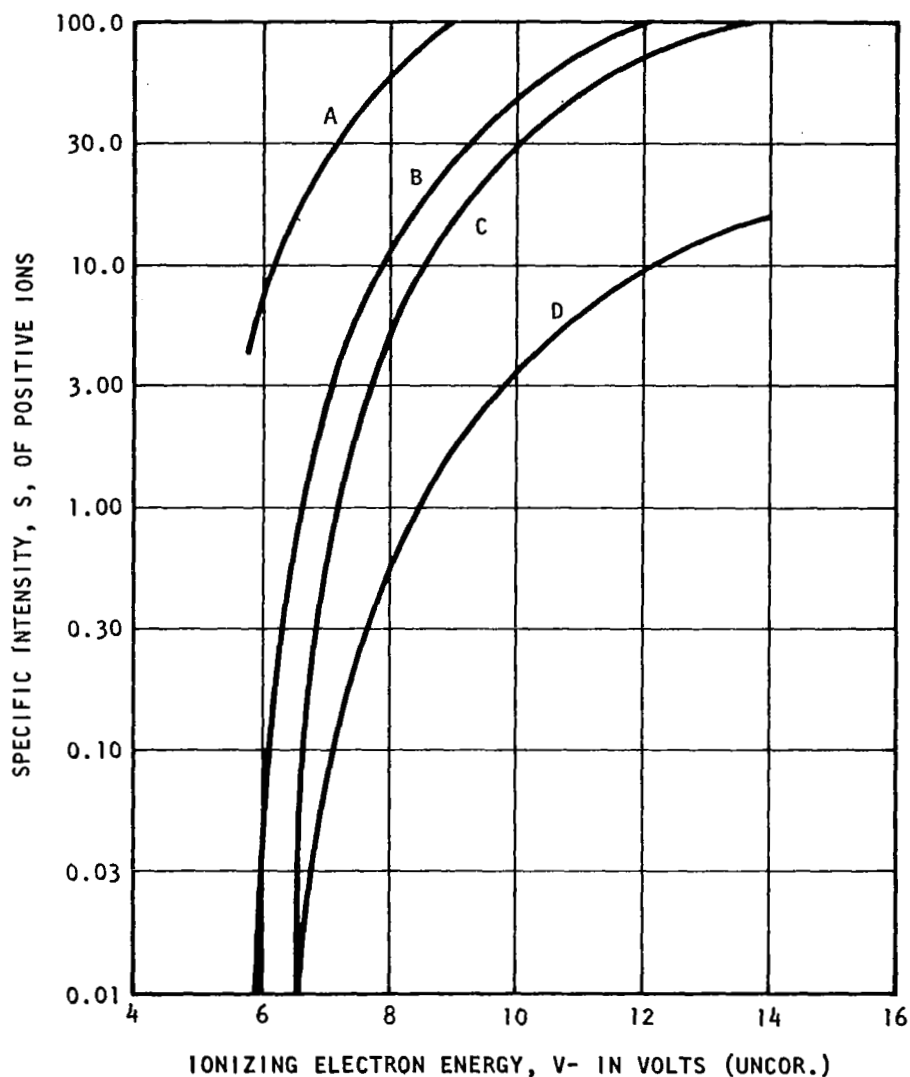
Ionization efficiency curves of the methane ions, CH_4^+ , CH_3^+ and CH_2^+ . The specific intensities at $V^- = 75$ volts are $\text{CH}_4^+ = 348$, $\text{CH}_3^+ = 261$ and $\text{CH}_2^+ = 25.8$. To correct voltage scale, V^- , to an absolute basis add 4.1 e.v. in this figure and Figs. C2 thru C5. (A) $\text{CH}_4 \rightarrow \text{CH}_4^+ + e^-$, (B) $\text{CH}_4 \rightarrow \text{CH}_3^+ + \text{H} + e^-$. (C) $\text{CH}_4 \rightarrow \text{CH}_2^+ + \text{H}_2 + e^-$.



A-299C

FIGURE C2

Ionization efficiency curves of the ethane ions, $C_2H_6^+$, $C_2H_5^+$ and $C_2H_4^+$, and the ethylene ion, $C_2H_4^+$. The specific intensities at $V^- = 75$ volts are: ethane, $C_2H_6^+ = 250$, $C_2H_5^+ = 167$, and $C_2H_4^+ = 784$; ethylene, $C_2H_4^+ = 572$. The specific intensity of $C_2H_5^+$ from ethane has been corrected for contribution from the ion $C^{12}C^{13}H_4^+$ due to the natural C^{13} content of the ethane. (A) $C_2H_4 \rightarrow C_2H_4^+ + e^-$, (B) $C_2H_6 \rightarrow C_2H_4^+ + H_2 + e^-$, (C) $C_2H_6 \rightarrow C_2H_6^+ + e^-$, (D) $C_2H_6 \rightarrow C_2H_5^+ + H + e^-$.



A-300C

FIGURE C3

Ionization efficiency curves of the propane ions, $C_3H_8^+$, $C_3H_7^+$ and $C_3H_6^+$ and the propylene ion $C_3H_6^+$. The specific intensities at $V^- = 75$ volts are: propane, $C_3H_8^+ = 310$, $C_3H_7^+ = 240$ and $C_3H_6^+ = 44.4$; propylene, $C_3H_6^+ = 362$. (A) $C_3H_6 \rightarrow C_3H_6^+ + e^-$, (B) $C_3H_8 \rightarrow C_3H_8^+ + e^-$, (C) $C_3H_8 \rightarrow C_3H_7^+ + H + e^-$, (D) $C_3H_8 \rightarrow C_3H_6^+ + H_2 + e^-$.

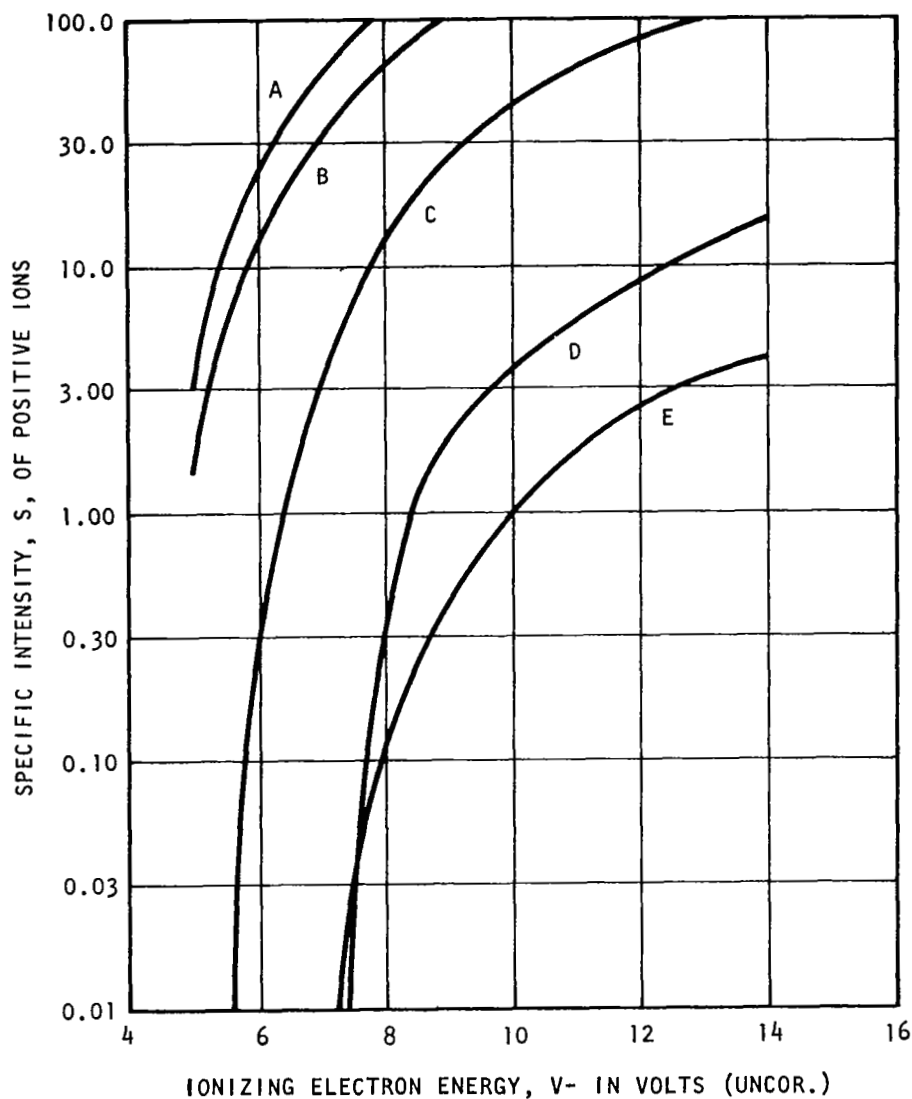
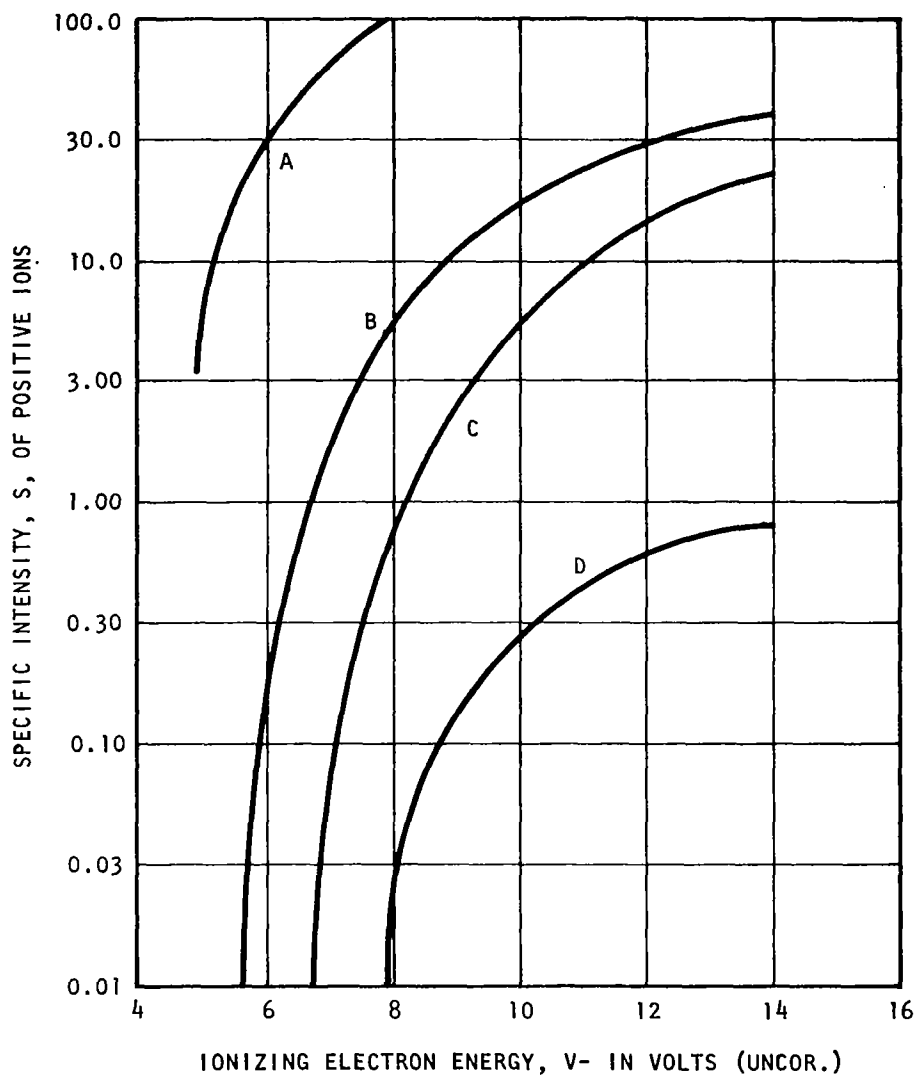


FIGURE C4

A-301C

Ionization efficiency curves of the n-butane ions, $C_4H_{10}^+$, $C_4H_9^+$ and $C_4H_8^+$ and the α - and cis- β butylene ions, $C_4H_8^+$. The specific intensities at $V^- = 75$ volts are: n-butane, $C_4H_{10}^+ = 220$, $C_4H_9^+ = 30.0$, $C_4H_8^+ = 8.24$; α -butylene, $C_4H_8^+ = 290$; cis- β -butylene, $C_4H_8^+ = 330$ (A) cis- β - $C_4H_8 \rightarrow C_4H_8^+ + e^-$, (B) α - $C_4H_8 \rightarrow C_4H_8^+ + e^-$, (C) n- $C_4H_{10} \rightarrow C_4H_{10}^+ + e^-$, (D) n- $C_4H_{10} \rightarrow C_4H_9^+ + H + e^-$, (E) n- $C_4H_{10} \rightarrow C_4H_8^+ + H_2 + e^-$.



A-302C

FIGURE C5

Ionization efficiency curves of the *i*-butane ions, $C_4H_{10}^+$, $C_4H_9^+$ and $C_4H_8^+$, and the isobutylene ion $C_4H_8^+$. The specific intensities at $V^- = 75$ volts are, isobutane $C_4H_{10}^+ = 71.6$, $C_4H_9^+ = 45.3$, $C_4H_8^+ = 5.32$; isobutylene, $C_4H_8^+ = 333$ (A) $i-C_4H_8 \rightarrow C_4H_8^+ + e^-$, (B) $i-C_4H_{10} \rightarrow C_4H_{10}^+ + e^-$, (C) $i-C_4H_{10} \rightarrow C_4H_9^+ + H + e^-$, (D) $i-C_4H_{10} \rightarrow C_4H_8^+ + H_2 + e^-$.

TABLE C2.- PARTIAL SPECTRA OF 1,3,5-TRIMETHYLVENZENE OBTAINED AT VARIOUS IONIZING VOLTAGES AND CURRENTS

Ionizing voltage, e.v.	Ionizing current, μ a	Parent peak sensitivity (relative to that at 10.1 e.v., 11 μ a.)	Σ 105 + 119 + 133 + 147 + 161	Fragment peak sensitivities, % of parent peak sensitivity							
				Polyisotopic values				Isotope corrected			
				106	120	134	148	106	120	134	148
10.1	11	1.00	1.06	---	---	---	---	---	---	---	---
	35	1.63	1.12	---	---	---	---	---	---	---	---
	45	1.11	---	---	---	---	---	---	---	---	---
11.5	11	2.15	12.10	---	---	1.35	0.61	---	---	0.46	0.11
	35	5.23	5.64	---	---	0.66	0.36	---	---	0.24	0.15
	45	5.09	3.64	---	---	0.64	0.33	---	---	0.18	0.19
14.5	11	3.66	81.90	---	---	6.30	4.59	---	---	1.47	0.21
	35	11.45	69.11	---	---	5.49	3.72	---	---	1.30	0.18
	45	13.18	64.61	---	---	5.30	3.41	---	---	1.26	0.22
17.5	11	4.37	156.03	0.70	0.42	10.08	8.87	0.09	0.10	2.10	---
	35	13.93	142.90	0.62	0.34	9.40	8.25	0.08	1.07	1.87	0.33
	45	16.79	136.21	0.56	0.24	9.19	7.76	0.07	0.07	1.95	0.23
70.0	11	6.48	407.09	5.10	1.73	20.87	23.74	0.59	0.25	4.46	0.98

ionization potential, ($V_e - I$). Ionization efficiency curves designated as Type II are for those ions whose relative yield rises to a maximum, about 10 volts above the ionization potential, and then drops off slightly at higher voltages. Ions whose relative yields rise slowly and do not level off until much higher voltages are designated as Type III. A typical example of ionization efficiency curves for ions of Type I, II and III is given by King and Long. This data is presented for methyl formate in Figure C6. Ions of Type I are clearly not favorably affected by a low-energy electron application because lowering the electron voltage increases rather than decreases fragmentation. Table C3 groups ions from methyl formate, methyl acetate, and ethyl formate into the three types. Notice that the parent peak usually fell into the Type I category. Therefore, some positive virtue in Type I ions was noted. A low-energy electron method would increase the 47-120 contribution because Type I behavior is usually experienced by the heavier ions. But, still the fact remains that fragmentation is not decreased by lowering the electron energy when Type I ions are considered. Type II ions rise so very quickly that they are of little or no help in decreasing fragmentation. Examining Figure C6, note that at 5 volts above the ionization potential the Type II ion presented (mass 29) has risen to 75% of its maximum value. Since the ionization potential of most organics is about 10 e.v. and the ionization potential of CO is about 14 volts, a value of 5 volts above the ionization potential of an organic is about 15 volts. By examining the CO ionization efficiency curve, Figure C7, and Figure C6, note that a 25% reduction in fragmentation is offset by about a 98% reduction in CO ion current. Type II ions are not helped by the low energy electron method. Type III ions do not rise as rapidly as Type II ions when the electron energy is increased. When operating 10 e.v. above the ionization potential, about 20 volts, Figure C6, gives a typical Type III current of about one-third its maximum value. But operation at 20 e.v. gives a CO value of about one-sixth of its maximum value. Since CO sensitivity is already a problem no net gain is accomplished for even Type III ions. Table C4 summarizes how fragmentation varies with electron energy for various groups of compounds.

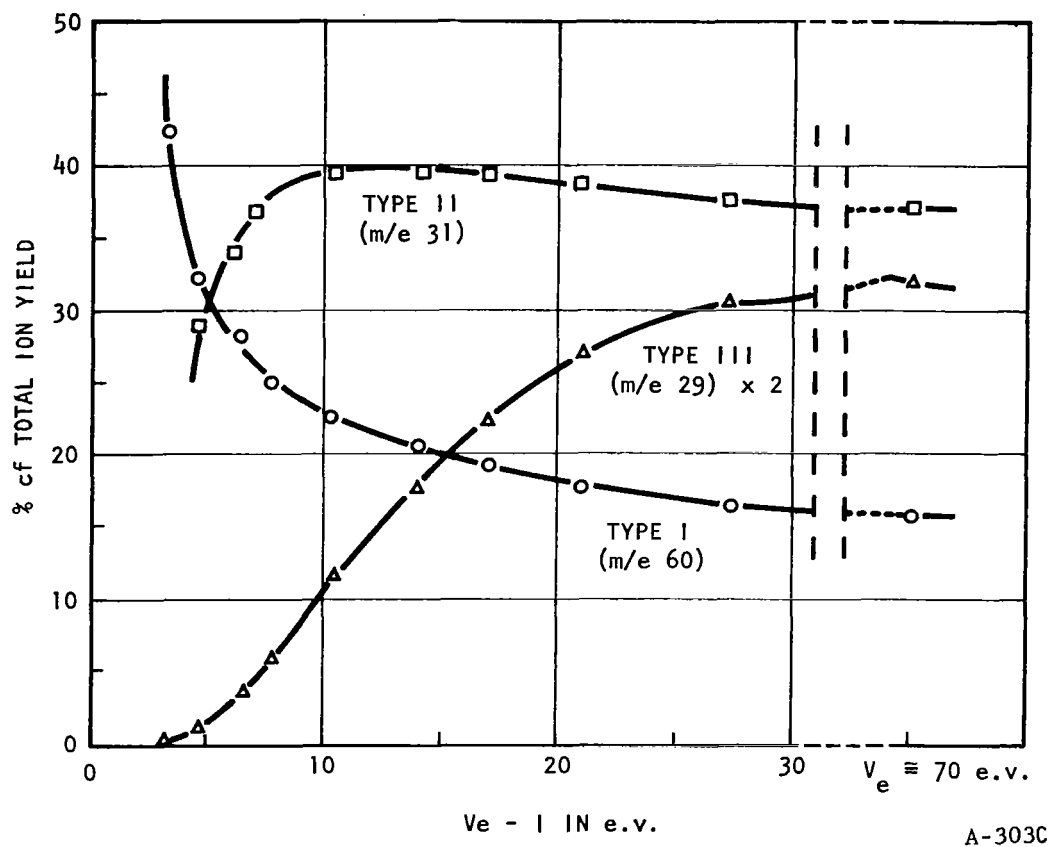


FIGURE C6
Low Voltage Yields of Three Ions From Methylformate

TABLE C3.- TYPES OF BEHAVIOR EXHIBITED BY PRINCIPLE
IONS AT LOW ELECTRON VOLTAGES

Mass peaks with type	Methyl Formate		Methyl Acetate		Ethyl Formate	
	m/e	60	m/e	74	m/e	74
I curve		32		--		73
		--		--		59
		--		--		56
		--		--		47
		--		--		46
		--		--		28
	m/e	59	m/e	73	m/e	45
II curve		31		59		31
		--		43		--
	m/e	45	m/e	42	m/e	44
III curve		44		41		43
		30		31		42
		29		30		30
		28		29		29
		15		28		27
		14		15		26
		--		14		19
		--		--		15

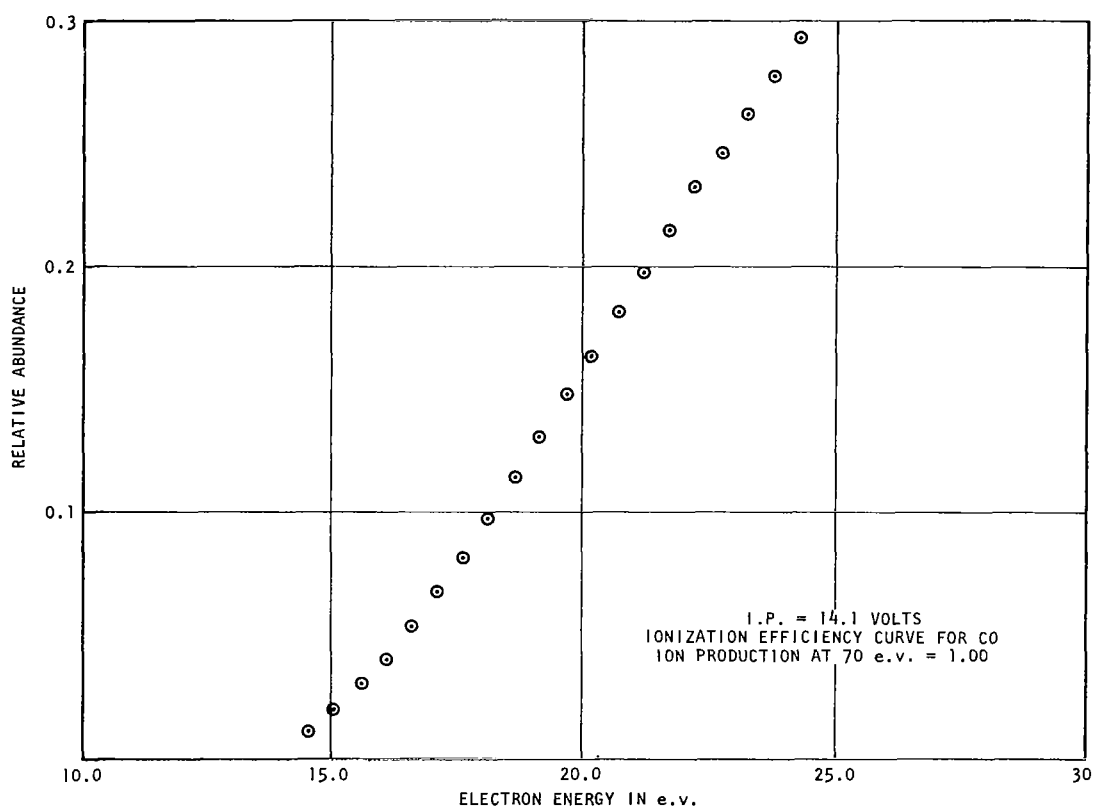


FIGURE C7

A-304C

TABLE C4.- FRAGMENTATION CHANGES WITH ELECTRON ENERGY

Compounds	Examples run	Fragmentation changes due to low energy electrons
1.	Hydrocarbons	
Aromatics	Benzene Toluene Xylene	Decreases overall fragmentation but not to a large degree at 27, 28 and 29
Aliphatics	Ethane	No 47-120 contribution, ratio of major peak to 27+28+29 decreases with increasing electron energy.
Olefins	Butene-1	Small decrease in fragmentation.
2.	Oxygen Compounds	
Alcohols	Allyl Alcohol Methyl Alcohol	Little change in fragmentation.
Ketones	Acetone	Some decrease in fragmentation but 27, 28 and 29 fairly small.
Ethers	Dioxane	No improvements, 28 major peak
Esthers	Ethyl Acetate	Very little improvement.
3.	Halogenated Compounds	
	Freon II	Fragmentation increases at lower voltages
	Ethylene Dicloride	

TABLE C4.- FRAGMENTATION CHANGES WITH ELECTRON ENERGY - Continued

HYDROCARBONSAliphatic

n-Butane
 Cyclohexane
 n-Decane
 2,2-Dimethylbutane
 Dimethylpentane
 Ethane
 n-Hexane
 Methylcyclohexane
 2-Methylpentane
 3-Methylpentane
 Propane
 1,1,3-Trimethylcyclohexane
 Trimethylhexane

Aromatic

Methylthylbenzene
 Phenylpentane
 o-Xylene
 p-Xylene

Oxygen CompoundsAcids

Acetic Acid
 Butyric Acid
 Isobutyric Acid
 p-Cresol
 Caprylic Acid
 Propionic Acid
 Valeric Acid

Olefins

cis-Butene-2
 Trans-Butene-2
 Isobutylene
 Dimethylbutene
 Ethylene
 1-Hexene
 Methylbutene
 2-Methylpropene
 Propylene
 Trimethylhexadiene

Acetylenic

Acetylene

Alcohols

Amyl alcohol
 t-Butanol
 1-Butanol
 2-Butanol
 n-Butyl alcohol
 Cyclohexanol
 2-n-Butoxyethanol (also an ether)
 Ethyl alcohol
 2-(2-Butoxybutoxy)ethanol
 Ethylene Glycol (dihydro alcohol
 or glycol)
 Isodecanol
 Isopropanol
 Isobutanol

TABLE C4.- FRAGMENTATION CHANGES WITH ELECTRON ENERGY - Continued

Oxygen Compounds

Alcohols (Cont'd)

2-methoxmethanol

2-methyl-2-butanol

2-Phenyl-2-Propanol

n-Propanol

2-Propanol

Isopropanol

2-Methyl-1-propanol

Vinylalcohol

Esters

Amylacetate

2-n-Butoxyethylacetate

2-(2-Butoxybutoxy)ethylacetate

2-Ethoxyethylacetate

2-(2-Ethoxyethoxy)ethylacetate

Ethylformate

Isopropylacetate

Methylacetate

Rhenyl acetate

n-Propylacetate

Isopropylacetate

Isopropylformate

(2-Butyrolactone)

Ketones

Acetophenone

Chloracetone

Diacetonealcohol

Mesityl oxide

Methylhexonone

Methylethylketone

Aldehydes

Benzaldehyde

Butyraldehyde

Isobutyraldehyde

2-Furalaldehyde

2-Methyl-2-Butanol

Propionaldehyde

Ethers

Diethylether, Ethylether

1,3-Dioxolane

Ethyleneoxide

Isopropyl ether

Methylisopropylketone

Methylisobutylketone

2-Methyl-4-Pentanone

4-Methyl-2-Pentanone

2-Pentanone

TABLE C4.- FRAGMENTATION CHANGES WITH ELECTRON ENERGY - Continued

Nitrogen Compounds

Acetonitrile
Cyanamide
Dimethylamine
Dimethylhydrazine
Indole
Methylhydrozine
N-Methylmorpholine
Nitrobenzene
Nitromethane
Skatole

Sulfur Compounds

Ethylsulfide
Ethylmercaptan
Methyl sulfide, Dimethylsulfide
Methylmercaptan

Hologenated Compounds

Carbon tetrachloride	Methyl chloroform
Chloracetone	Monochloroacetylene
Chlorobenzene	Proszene
Chloraform	Tetrafluoroethylene
1-Chlorapropane	Vinylidene chloride
2-Chlorapropane	
Dichloroacetylene	
Dichlorobenzene	
Ethyl chloride	
Freon-12	
Freon-22	
Freon-114	
Freon-125	
Methyl chloride	

TABLE C4.- FRAGMENTATION CHANGES WITH ELECTRON ENERGY - Concluded

Organic Silicon Compounds

Hexamethyltrisiloxane

Hexamethylcyclotrisiloxane

Trimethyl silanol

Inorganics

Chlorine

Hydrogen

Hydrogen Fluoride

Hydrogen Cyanide

Nitrogen Dioxide

Phosgene

APPENDIX D

NEW MAGNET DESIGN

Perkin-Elmer Aerospace System has developed a new high field intensity magnet for the Two Gas Sensor. This magnet is the third generation of the original Langley magnet. This new magnet differs from the two previous designs in increased uniformity and field strength. The three magnets have essentially the same weight. Magnets of generations one and two are made of Alnico V while generation three utilizes Alnico V-7. The dimensions of the three magnets are shown in Figures D1, D2 and D3. The new magnet design, third generation magnet, has a field strength of about 20% greater than the second generation magnet. This increase in field strength is accomplished with an accompanying increase in uniformity. Pole face maps demonstrating the increased uniformity are shown in Figures D4 through D7.

The new magnet allows two possible modifications. They are:

- (1) The size of magnetic material can be decreased in order to achieve the 4000 gauss field for which the Two Gas Sensor was designed.
- (2) The new magnet can be used with increased ion velocities in order to increase the sensitivity of the mass spectrometer.

Increasing the ion energy, increased (within limits) the ion density falling upon the collector slit. The number of ions lost due to thermal drift is decreased by increasing the ion energy. The sample equation for ions in a mass spectrometer is given by:

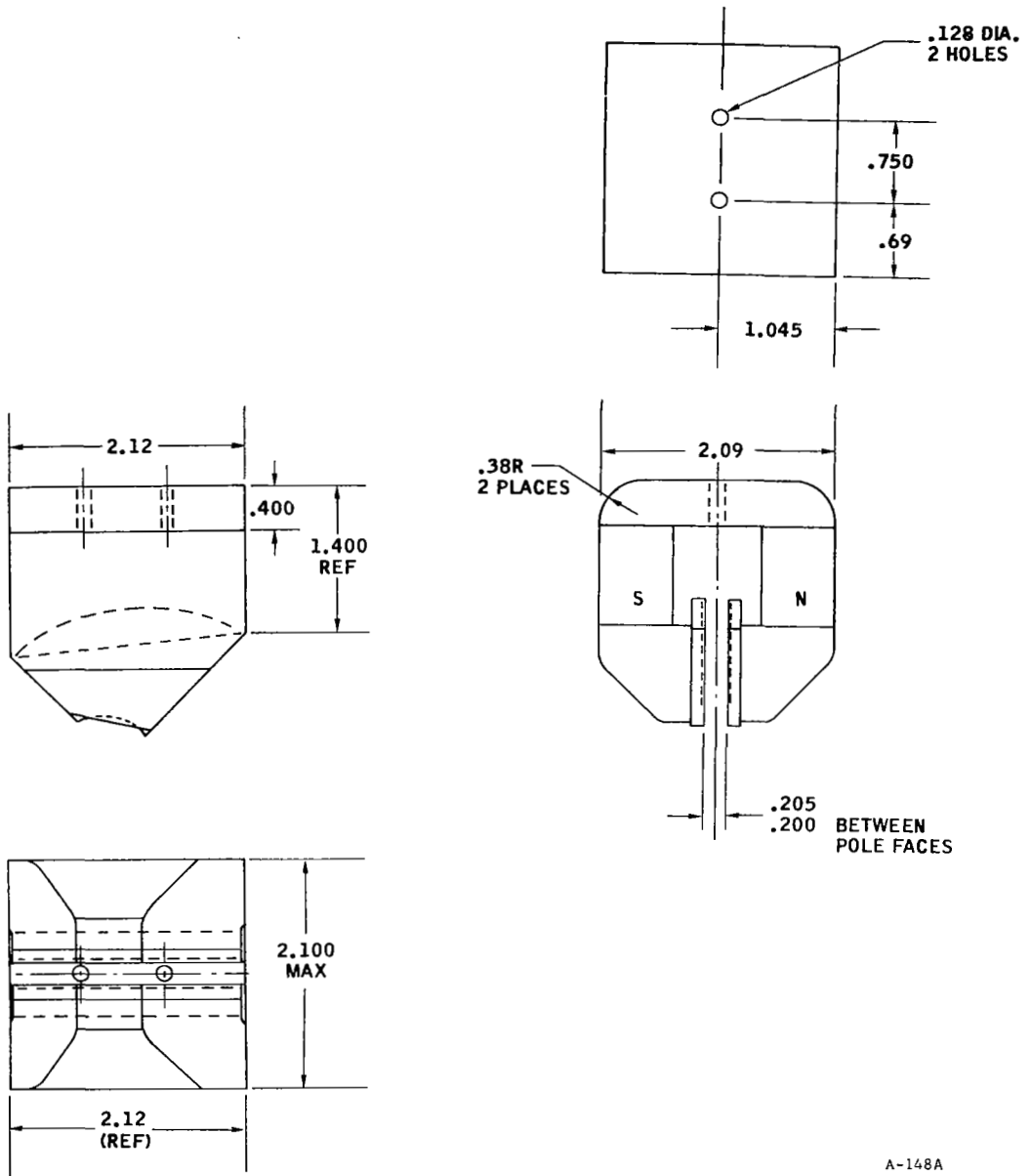
$$mV = \frac{B^2 r^2 q}{2}$$

where B is the magnetic field
 r is the radius of the path
 q is the ionic charge
 m is the mass of the ion
 V is the accelerating energy.

In order to have the same radius for a given mass once the ionic energy is increased the necessity to increase the strength of the magnetic field was noted.

The magnet has the same size and weight as the previous Langley magnets but produces a field greater by 20% when compared to the old design. Since the magnetic field appears to the second power in the equation, a 20% increase in B could compensate for a 44% change in V. Studies performed in the lab have shown that sensitivity increases almost linearly with increases in ion energy.

The new magnet design allows the choice of decreased weight or increased sensitivity.



A-148A

FIGURE D1
First Generation Magnet Design

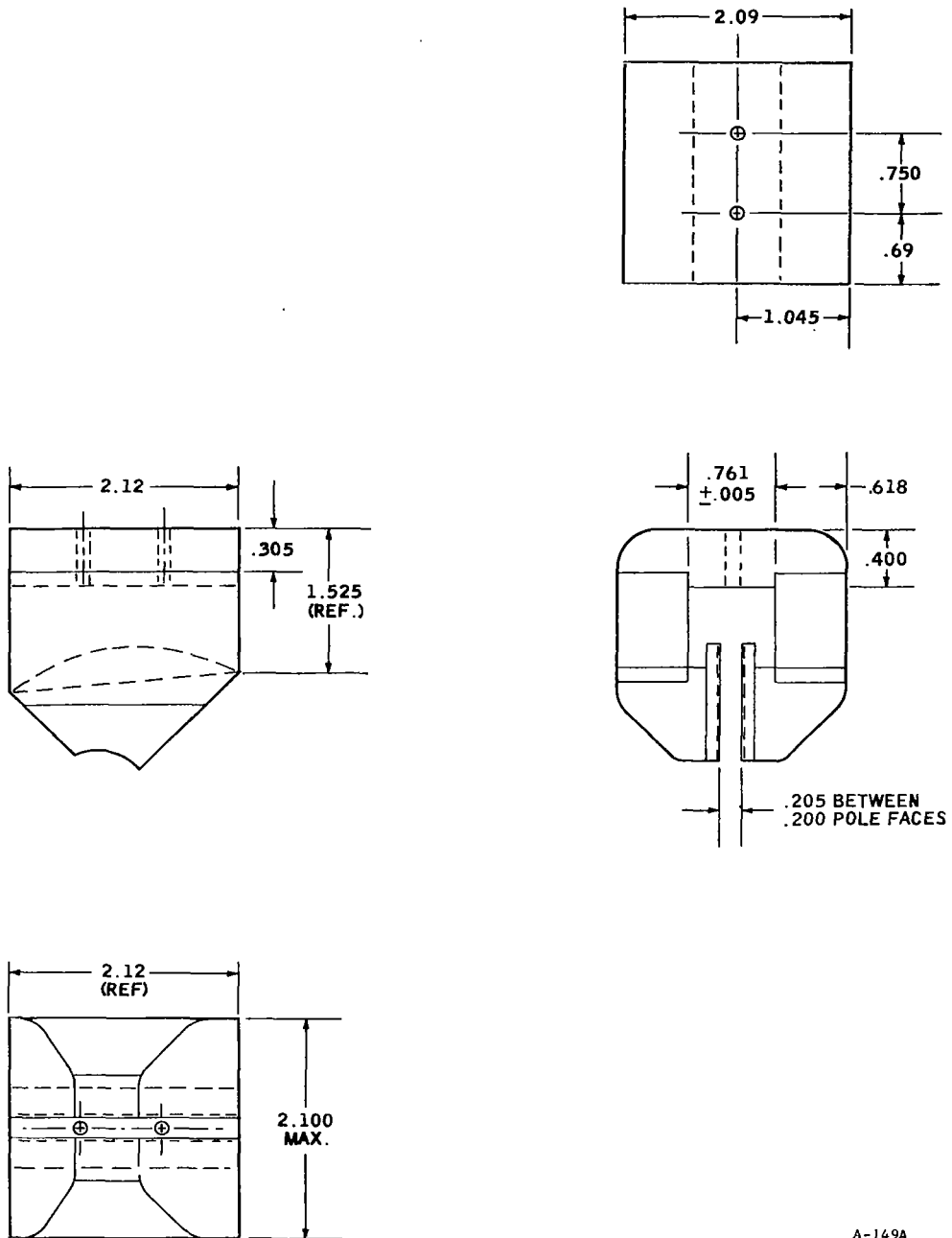
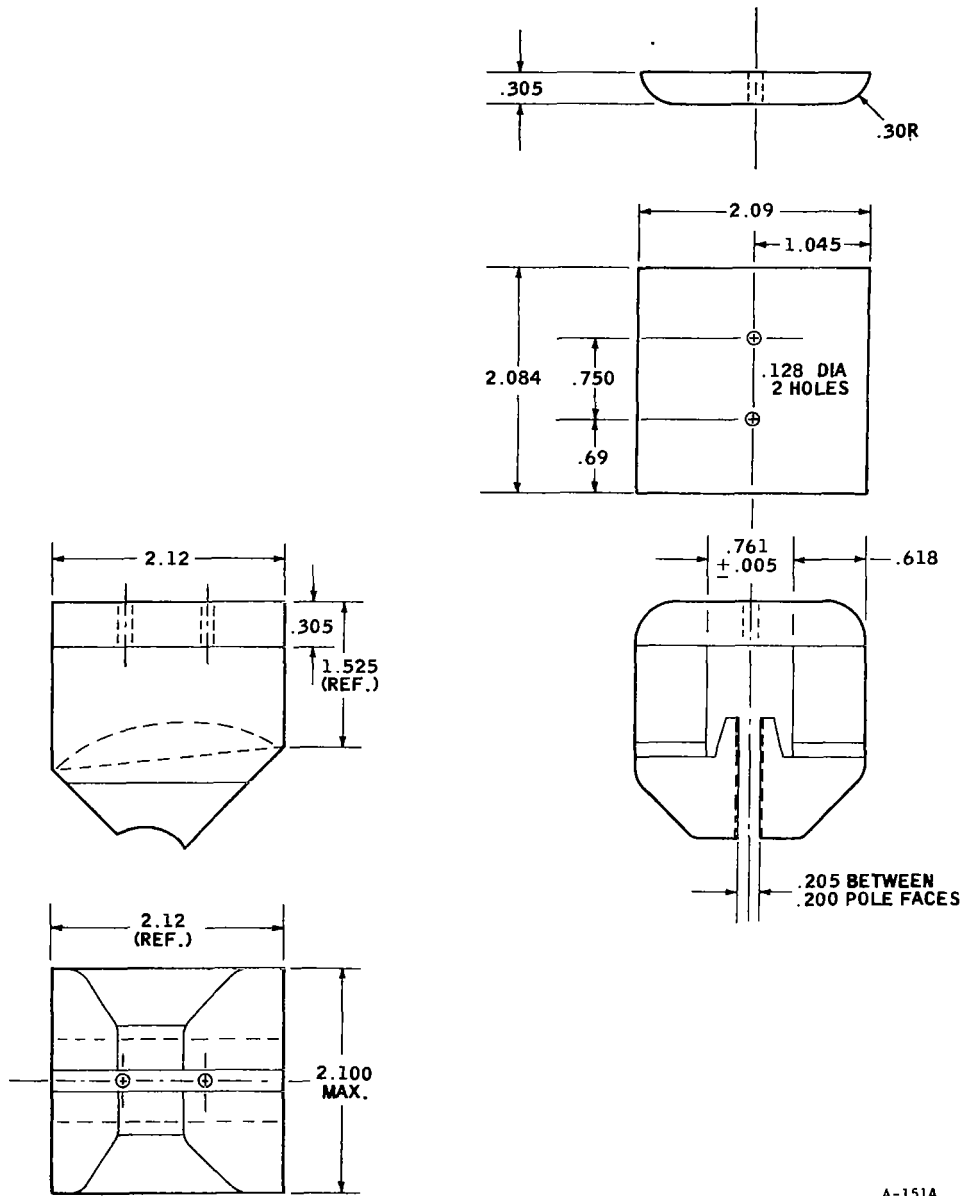


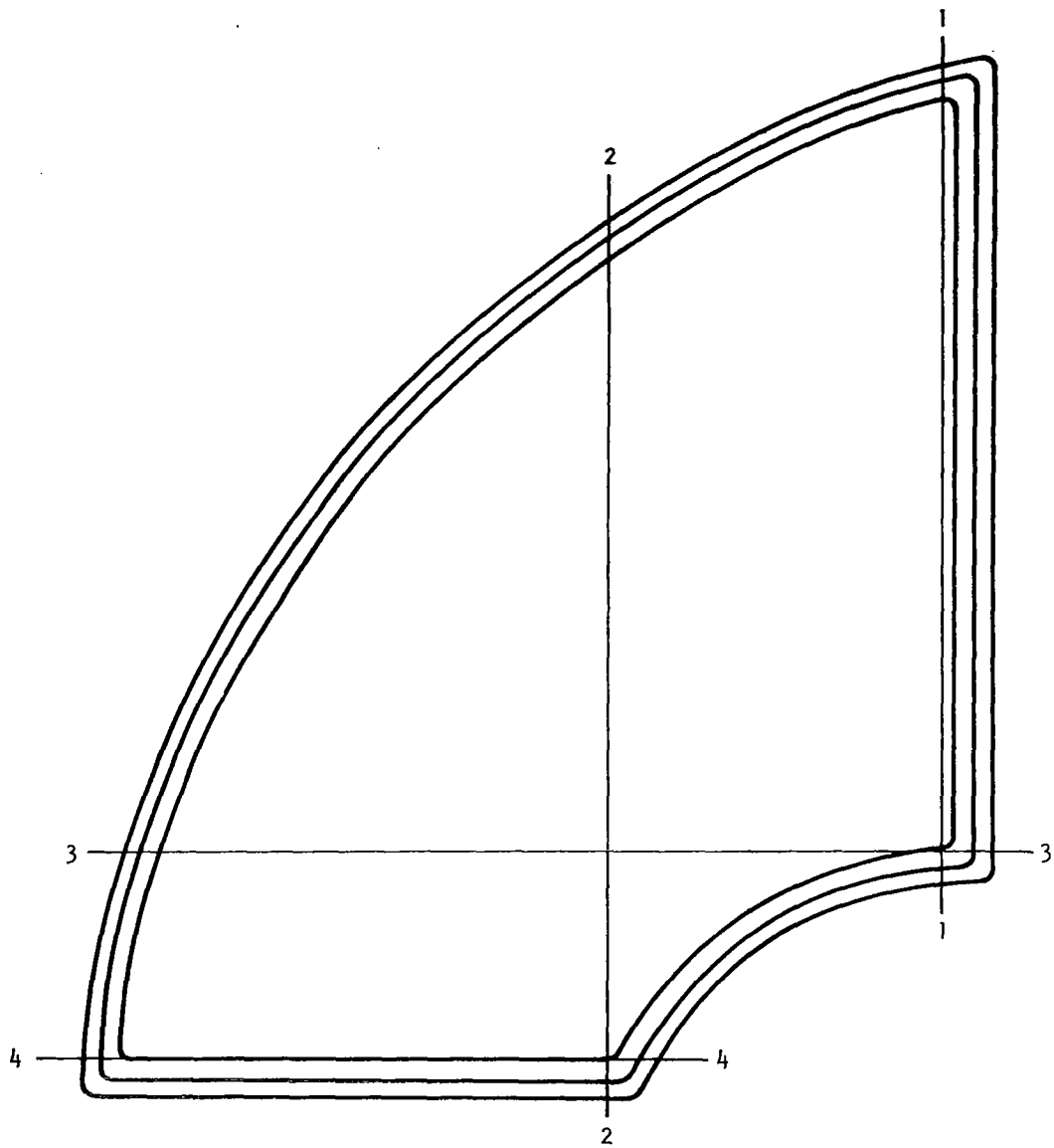
FIGURE D2
Second Generation Pole Pieces

A-149A



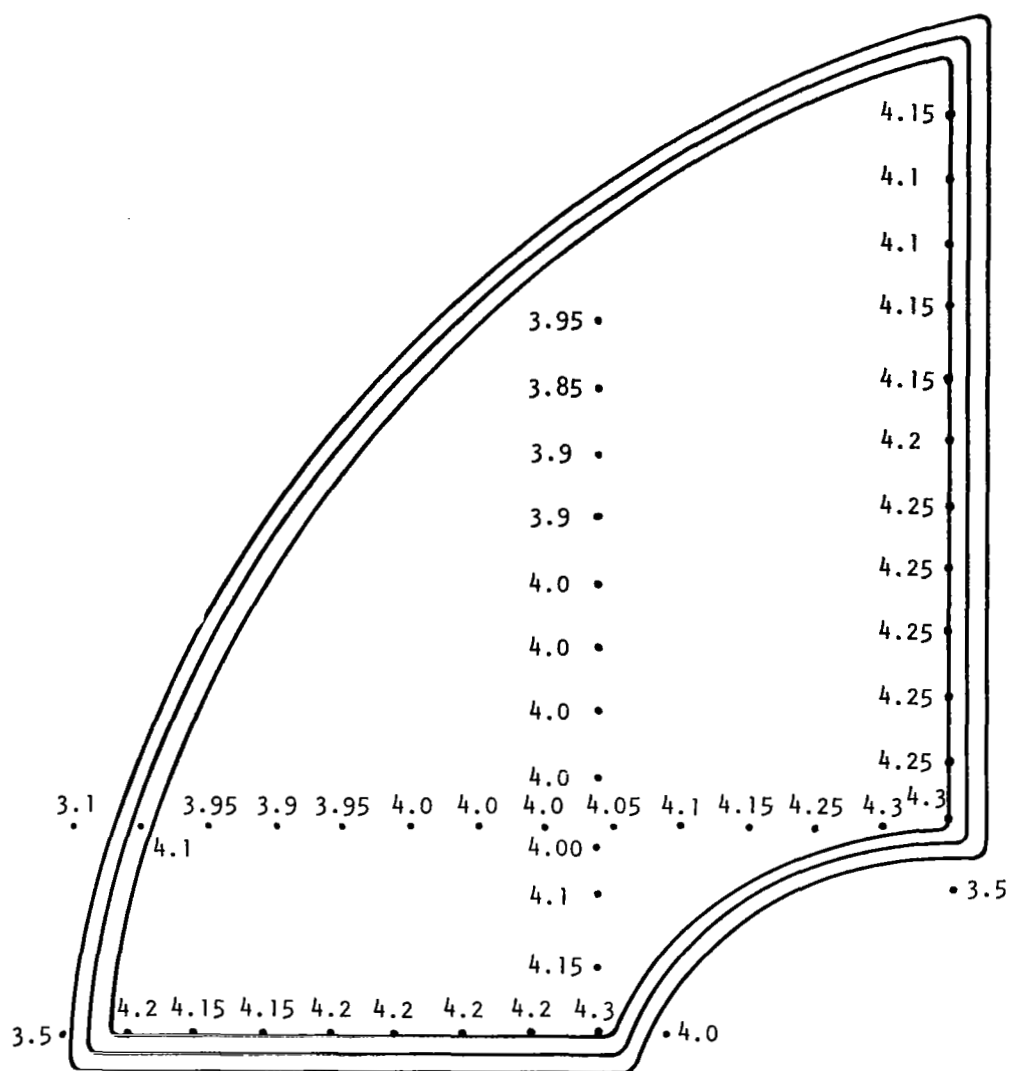
A-151A

FIGURE D3
Third Generation Pole Pieces



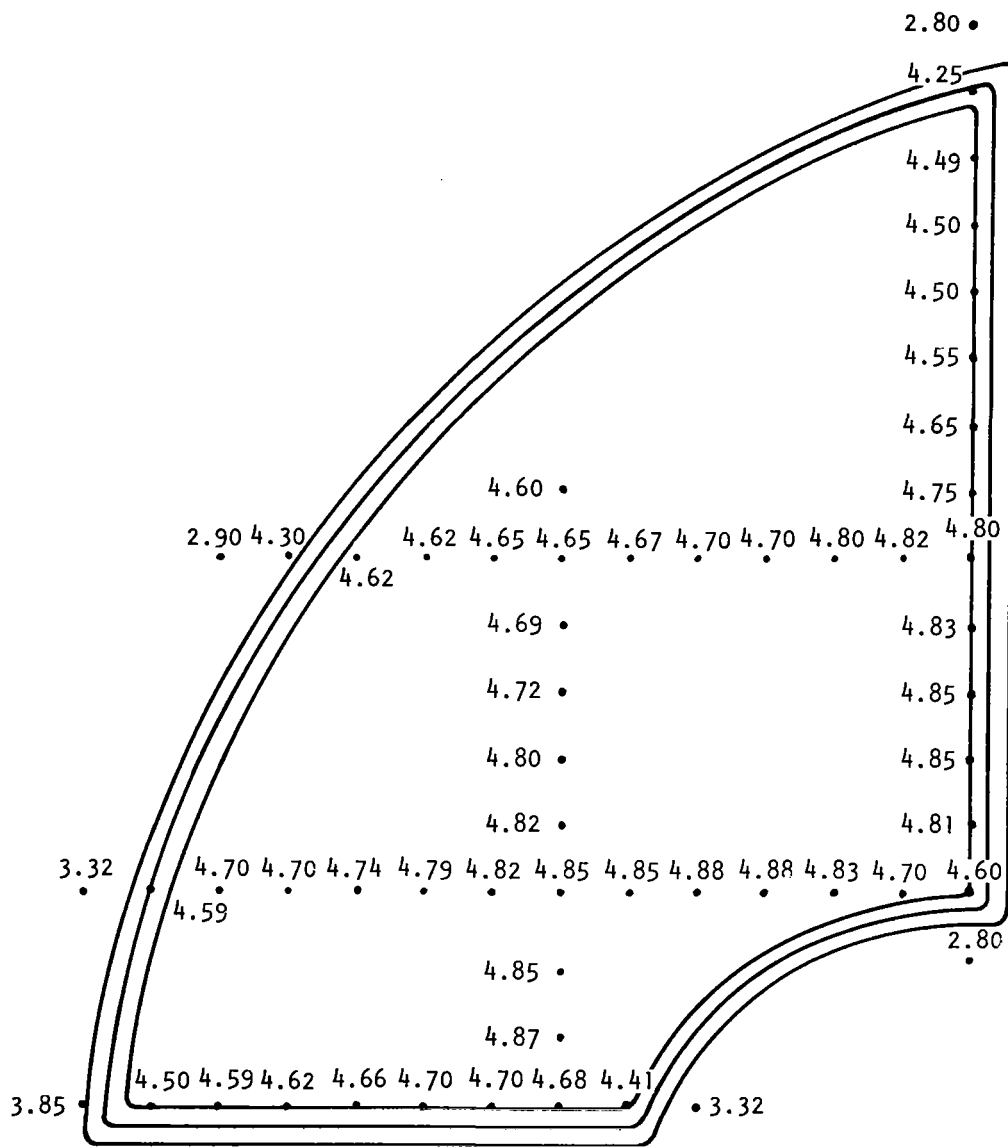
A-152C

FIGURE D4
Pole Face Map



A-154C

FIGURE D6
Second Generation Magnet Pole
Face Map (Field in Kilogauss)



A-155C

FIGURE D7
Third Generation Magnet Pole
Face Map (Field in Kilogauss)

With the event of the new magnet design, the problems previously encountered concerning charging and stabilization were solved. Charging and stabilization procedures, developed during the magnet stabilization study, produced magnets in which no measurable change in flux could be measured in a period of over 15 weeks.

APPENDIX E

ION SOURCE CONSTRUCTION MATERIALS

Materials used in ion source construction must meet a rather stringent set of conditions. In addition to the normal characteristics expected of construction materials such as adequate strength, stability and machineability, there are requirements of chemical and magnetic inertness which must be met by ion source materials. The material(s) used should be easily machineable to tolerances of 0.001" and to a finish of a few millionths of an inch. The materials should also be stable, with no tendency to warp at temperatures up to 400C. The above requirements practically exclude all materials, other than metals, from consideration. The exception to this is, of course, the dielectric material necessary for insulation of the various electrodes. The magnetic requirement is that the material have a permeability of 10 or less, which rules out any ferromagnetic substance. This will prevent additional distortion of the electron beam due to stray magnetic fields. The requirement of chemical inertness is the most critical and also the most difficult to satisfy.

Simply stated, the requirement is that the ion source materials should have no effect whatsoever on the chemical composition of the gases in the ion source. This means that the material should be nonreactive and should, in addition, contain no impurities which could cause spurious indications. This means also that metals that form protective oxide films in a normal atmosphere must be avoided, as must metals which corrode without protective oxide coats. Copper, aluminum, titanium, magnesium and beryllium are thus eliminated from consideration, although alloys or mixtures of the above are not ruled out.

Essentially, then, two types of metals are useful: iron-chromium-nickel-molybdenum alloys and precious metals. The ferrous group alloys, especially high nickel alloys, are quite inert, but often exceedingly difficult to fabricate. Austenitic stainless steels (300 series) are nonmagnetic, and fairly easy to machine, but may cause spurious readings from sulfur and carbon content. Also, the chromium oxide film formed on these steels may have some tendency towards contamination. Precious metals, especially iridium, rhodium, and gold, are quite inert enough for ion source applications, but present problems of softness and cost. Precious metal platings appear to be the most practical solution to the ion source material problem. Some objections to the plating approach have been raised because of possible migration of impurity atoms through the plating but these objections may be discounted because of the extremely low rates of diffusion in solids. A fairly thick layer of gold plating, with a final rhodium flash coating, should be a satisfactory surface and can be easily applied over almost any base metal.